博士学位論文

論文題目　A Study on Microwave Nondestructive Evaluation of Delamination in IC Package
（マイクロ波による電子パッケージ内のはく離の非破壊評価に関する研究）

提出者　東北大学大学院工学研究科
機械知能工学 専攻

学籍番号　8D6

氏名　巨陽（Ju Yang）

指導教官	坂 真澄 教授
審査委員 （○印は主査）	○ 坂 真澄 教授 1 庄子哲雄 教授　2 高木敏行 教授 3 教授　4 教授

備考(1) 外国人留学生は、国籍を記入すること。

(2) 履歴事項は、大学入学から年次にしたがって記入すること。

(3) 博士課程の修了年月日は、学位記授与式年月日を記入すること。

(1)

A Study on Microwave Nondestructive Evaluation of Delamination in IC Package

Yang Ju

CONTENTS

1 INTRODUCTION **1**

1.1 Reliability of IC Package **1**

1.2 Delamination in IC Package **2**

1.3 Conventional Nondestructive Evaluation Techniques **2**

1.3.1 Radiographic Inspection 2

1.3.2 Ultrasonic Inspection 7

1.4 Microwave Nondestructive Evaluation Technique **10**

1.4.1 Background and History 10

1.4.2 Rectangular Waveguide 14

1.4.3 Open-Ended Coaxial Line Sensor 15

1.5 Summary **17**

References **20**

2 FUNDAMENTAL EXPERIMENT **24**

2.1 Introduction **24**

2.2 Coaxial Line Sensor **25**

2.3 Experimental Procedure **29**

2.4 Results and Discussion **31**

2.5 Conclusions **39**

References **41**

3 EVALUATION OF DELAMINATION BASED ON MAGNITUDE MEASUREMENT 43

3.1 Introduction 43

3.2 Approach 44

3.3 Experimental Procedure 45

3.4 Results and Discussion 48

3.5 Conclusions 59

References 59

4 EVALUATION OF DELAMINATION BASED ON PHASE MEASUREMENT 61

4.1 Introduction 61

4.2 Approach 62

4.3 Experimental Procedure 62

4.4 Results and Discussion 64

4.5 Conclusions 81

Reference 81

5 THEORETICAL CONSIDERATIONS 84

5.1 Introduction 84

5.2 Theoretical Model 84

5.3 Evaluation 91

5.4 Comparison with Experimental Results 92

5.5 Conclusions 92

References 97

6 MICROWAVE IMAGING 98

6.1 Introduction 98

6.2 Imaging System and Sample Description 98

6.3 Measured Results and Discussion 99

6.4 Conclusions 103

References 107

7 CONCLUSIONS 108

ACKNOWLEDGMENTS 111

1

INTRODUCTION

1.1 RELIABILITY OF IC PACKAGE

With the development of integrated circuit (IC) technology, the increasing complexity of ICs has moved most of the functionality of electronics system inside the chip package. This trend has increased the demand for packages with superior performance including greater heat dissipation, more leads, denser internal interconnection, smaller dimensions and greater reliability.

The main concerns in the reliability analysis are the failure mechanisms and the life expectancy under application conditions. The current prediction theories and models use thermal-mechanical strain and stress as parameters of estimating damages and failures, which require the analytical and experimental capabilities of structural mechanics analysis. As electronic technology advance, more novel materials are used in packages. Electronic components usually consist of multi-materials and their interfaces with highly compact and integrated features. Determinations of thermal strain/stress and predictions of failure and reliability become more and more difficult. Knowledge in many technical disciplines and specialized experimental methods and tools are required for the package design and reliability analysis. Recently, a variety of advanced experimental techniques have been adopted from other technical areas for applying to packages and at the same time new experimental tools have been developed.

1.2 DELAMINATION IN IC PACKAGE

The size of IC chip has been enlarged to raise the level of integration and, simultaneously, the package has been made thinner and smaller to increase the density of surface mount. Therefore, the reliability of packages has become more and more an important issue in the design of packages. During the soldering process by infrared reflow, IC package is heated above the melting temperature of solder, which is typically in the region of 215 ℃. High stresses are caused within the package as a result of enhanced thermal mismatch between the dissimilar materials of the package. At the same time, the evaporation of the moisture absorbed from the ambient by the plastic package causes a pressure between the chip pad and the packaging resin. These two sources of stress and pressure can cause delamination in IC package. It has been reported that the package cracking is initiated from the delamination, and which mostly takes place at the interface between the chip pad and the resin[1-4]. As shown in Fig. 1.1, once a delamination of the chip pad is initiated in the package, the delamination will grow and propagate until the bottom pad interface is substantially or fully delaminated, thereby cracks occur at the sides of the chip pad. Figure 1.2 shows a delamination and crack observed by microscope. The delamination depends on the chip size, the relative thickness of the resin on the chip and under the chip pad, the material properties of the components, the adhesion strength of the interfaces, the moisture content absorbed in the package and the soldering temperature. Therefore, an inspection technique to detect and evaluate the delamination in IC package has become an urgent need for increasing the reliability of IC package. The inspection technique is wished to be able to investigate the mechanism of the delamination under the application condition, thereby it is possible to predict the condition of delamination and crack occurrence.

1.3 CONVENTIONAL NONDESTRUCTIVE EVALUATION TECHNIQUES

1.3.1 Radiographic Inspection

Radiographic inspection[5-7] is one of the oldest nondestructive evaluation (NDE)

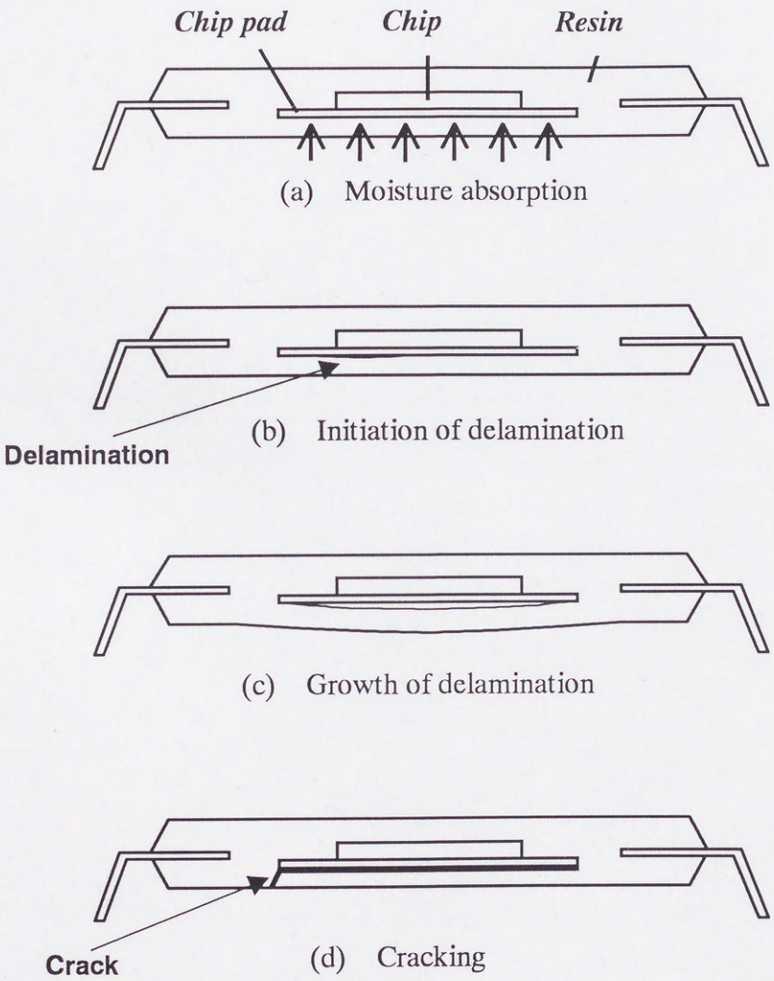

Fig. 1.1 Mechanism of package cracking

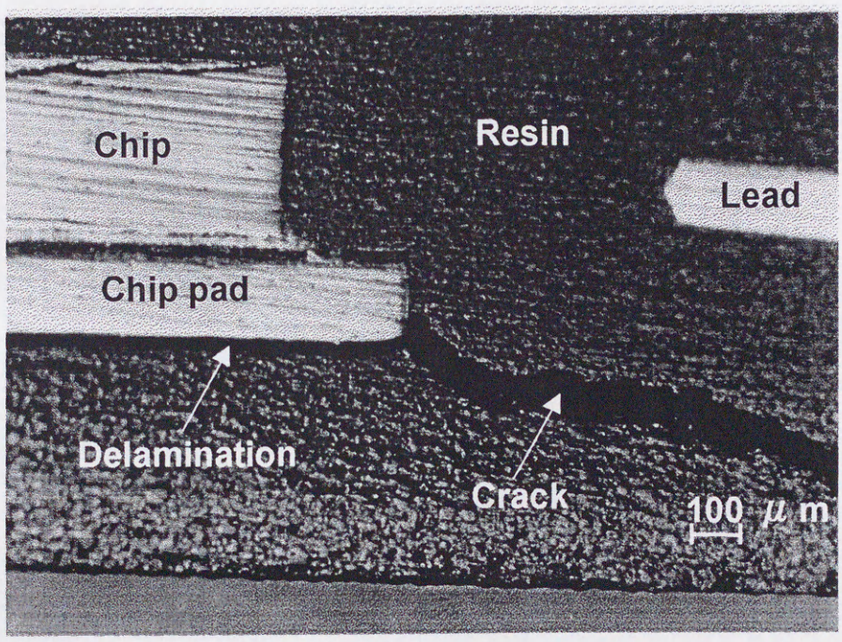

Fig. 1.2 Actual delamination and crack observed by microscope

inspection methods. Its primary advantage is that it can detect the existence of defects in the volume as well as some surface defects. However, it is much less effective in detecting planar-type defects unless careful attention is paid to the orientation of the x-ray beam relative to the defect orientation. A traditional advantage of the radiographic method is that it produces a permanent record for reference at a later time. This advantage has become less unique as other NDE methods become implemented in computer-aided formats capable of storing inspection data.

Figure 1.3 shows a schematic of the arrangement in a typical x-ray environment, where the source has a finite size and a geometric unsharpness is produced on the film because of the size and the spacing of the film and object. X-ray sources have finite size because of the necessity of cooling the target, since most of the energy generated by the electron beam is thermal. The amount of geometric unsharpness can be calculated simply from geometric relationships. Unsharpness is equal to the source size times the ratio of the object-film distance to the source-object distance. It is clear that the geometric unsharpness can be reduced by increasing the source-object distance. However, an additional concern factor is that x-ray sources allow an inverse-square radiation law; increasing the source-object distance by 2 will cause an increase in the exposure by a factor of 4.

Gamma-ray sources are also used in radiography. The advantages of gamma-ray sources are their simplicity, compactness, and easy transportability. They are regularly used to radiography thick sections and components not easily transported to a primary source. In contrast to x-ray tubes, the energy of gamma-ray sources is quantized at fixed energy levels associated with the disintegration of radioactive atoms. The intensity of the source depends on the amount of radioactive material in the source. Because of the decay, the amount of radiation is continually reduced.

Thermal neutrons are also used in radiography. Neutrons and x-rays obey different absorption rules; and, in general, neutron absorption does not depend on density; unlike x-ray absorption, moreover, it does not generally increase with atomic number. Neutron radiography is commonly used to detect changes or the presence of materials with low-atomic-number. This type of evaluation can be done in the presence of materials with higher-atomic-number such as steel because of the low absorption capacity. The detection of corrosion products is one important use for neutron radiography.

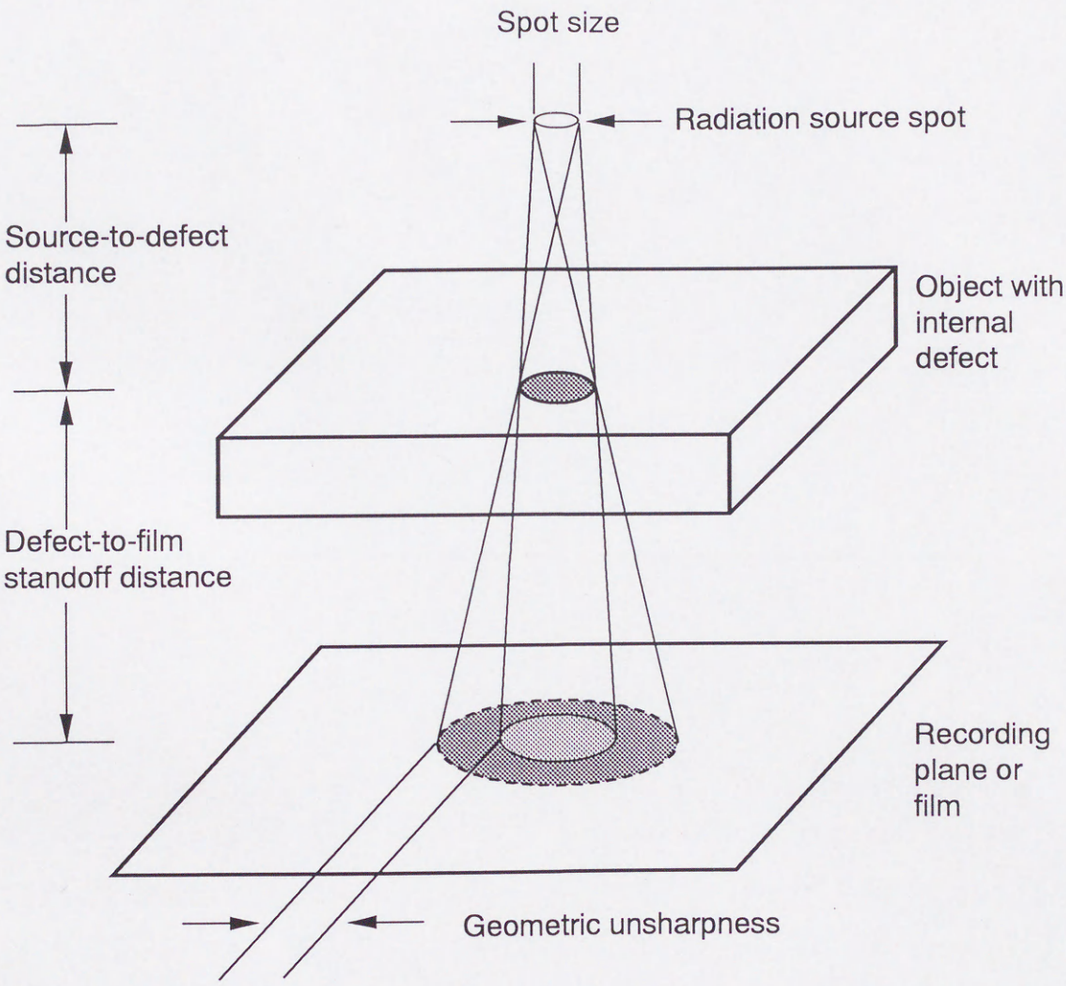

Fig. 1.3 Schematic of typical x-ray setup. Geometric unsharpness exists because of finite source spot size

Radiographys are less used for inspection of IC package since their absorption in the dielectric materials is so small that the contrast of radiograph for the defects is extremely low.

1.3.2 Ultrasonic Inspection

Ultrasonic inspection is one of the more widely used nondestructive testing (NDT) methods. Originally, it was established to provide volumetric inspection of defects in forgings and castings. It has since become an important method for inspecting welds and has been extended to detect surface defects such as cracks[8].

The primary advantages of ultrasonic testing are the ability to penetrate solid objects and to detect defects deep within the part. In many cases, ultrasonic inspection has greater sensitivity than radiographic inspection to volumetric defects. Additional advantages over radiography are that ultrasonics can be used to determine the depth, or distance, to the defect and to detect cracklike defects. Another important advantage is the ability to conduct a nonhazardous inspection. Ultrasonic inspection can be applied almost immediately after the welding for repair or fabrication.

The disadvantages of the ultrasonic method are related mostly to limited sensitivity produced by material and physical properties such as grain size and surface roughness. Because ultrasonic inspection is performed using beams, some component geometries limit accessibility to defects in some locations. Another disadvantage is the requirement of coupling medium such as water, because ultrasonic wave cannot propagate in air. It makes ultrasonic cannot be used for high temperature inspection, on-line testing, etc.

The ultrasonic method depends on the interaction of ultrasonic waves with defects. These defects can have different configurations, but in all cases they must constitute impedance discontinuities to be able to interact with the waves. An impedance discontinuity is a change in either local density or elastic properties. The processes of interaction include those most often encountered in wave-propagation situations: refraction, scattering, defraction, reflection, and absorption.

Ultrasound propagates as bulk, surface, and plate waves. Bulk waves propagate in a three-dimensional medium, which is essentially infinite in extent. Surface waves propagate along the surface between high-and low-acoustic-impedance materials and at

a velocity close to the longitudinal wave velocity in the bulk material. Plate or lamb waves are often encountered in ultrasonic inspections. The many complex plate-wave mode shapes are similar to the modes of vibration of a drum or a large sheet.

Practical ultrasonic testing methods are concerned with the way that ultrasonic beams propagate through test materials and the methods by which the ultrasonic information is displayed. The two primary methods for controlling ultrasonic beams propagating through media are pulse echo and through transmission. The pulse-echo method is a single-sided approach whereby the transmitted and received signals occur on the same side and are produced and received by the same transducer. This method is reminiscent of radar, or sonar, where items of interest or interfaces are detected by the presence of echoes at a given range. In a through-transmission mode, the object to be inspected is located between the transmitter and the receiver. Objects of interest usually appear as shadows or an increase in loss of beam transmission. This method is good for inspecting laminates and other multilayer structures for interface defects. A variance of the through-transmission is performed by using a single transducer on one side. In this method, a signal reflected from an interface beyond the object of interest is monitored, and defects are indicated as shadows or variations in the amplitude.

The common displays for ultrasonic information are the A-, B-, C-scans (see Fig. 1.4). The A-scan is simply an amplitude-versus-time representation of the received information. The display can be scaled in distance so that defect depth can be read directly. The B-scan is a collection of A-scans that shows all defects in a cross section. The C-scan is a plan view of returned signals from a given range thickness. Conventionally, the C-scan is a binary display, where the information above a certain threshold is shown in a contrasting black or white shade. A C-scan can have graduated shade scale, and it is now a common feature with computer-aided systems for both B- and C-scans to be displayed in color graphic modes.

Since the 1980s, considerable effort has been directed at evolving ultrasonic schemes to image internal volumes of material. One of these receiving considerable attention is scanning acoustic tomography[9]. Scanning acoustic tomography (SAT), which is in some case called scanning acoustic microscope (SAM), is recognized as a powerful tool for nondestructive detection of the defects in IC package. It uses a pulse-echo transducer with typical frequency in the range of 10 to 15 MHz scanning over the

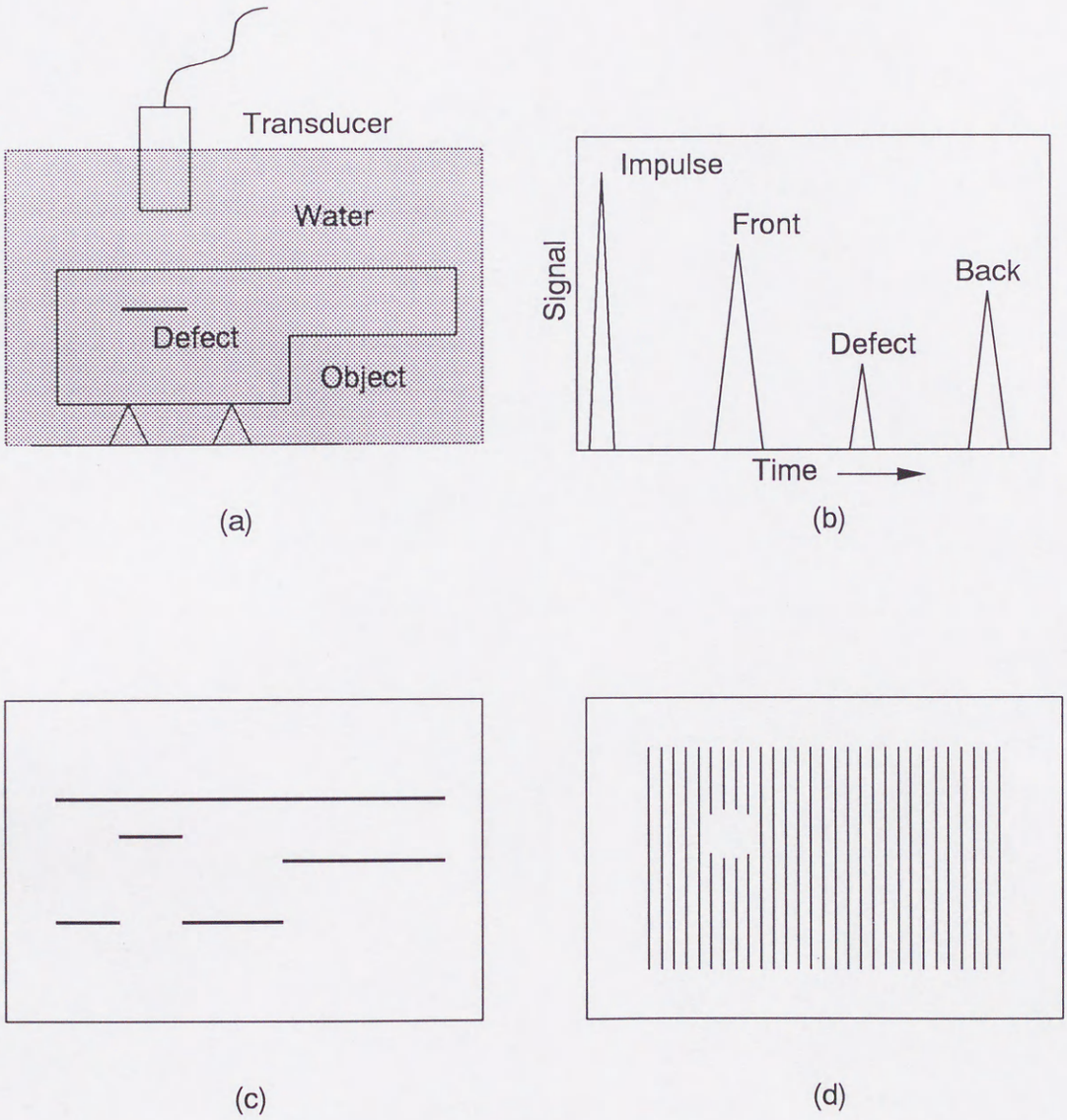

Fig. 1.4 Common ultrasonic data displays: (a) object to be inspected; (b) A-scan (one-dimensional) fixed transducer; (c) B-scan (one-dimensional) cross section; (d) C-scan (two-dimensional) plan view

sample mechanically. The ultrasound is focused into the sample to a certain depth and reflected at the interfaces of materials. The intensity and the polarity of the reflected signal depend on the difference of acoustic impedance of the two materials. The intensity variation and polarity change are then used to make an image. This technique can be employed to characterize internal defects such as voids, delamination, inclusions, porosity and cracks in packages.

1.4 MICROWAVE NONDESTRUCTIVE EVALUATION TECHNIQUE

1.4.1 Background and History

The spectrum of electromagnetic radiation may be divided into two parts that differ primarily in the principal methods for the detection of the radiation. The first of these regions, which is the optical region, extends from the shortest γ-ray, up through the ultraviolet and visual wavelengths, to some indefinite wavelength in the far infrared. In this region the elementary processes are discontinuous and must be described by the quantum theory. The methods of detection involve quantum effects—the photoelectric effect or photochemical processes in the human eye or in a photographic plate. In the second region, the phenomena are more directly associated with electrical effects. Radiation is detected by the transformation of the radiant energy into some mechanical motion—the deflection of a meter, the sound from a loudspeaker, or the motion of an electron beam that falls upon the screen of a cathode-tube. It is the short-wavelength end of this electrical region of the spectrum, which is the region of microwaves, that is the concern of this volume. The microwave region extends from about 1 GHz to about 300 GHz. The range of wavelengths, which is from 1 to 300 mm, is identical with the range of dimensions of most experimental apparatus, and it is this circumstance that leads to a separation of the microwave region from the region of longer wavelength.

Microwave inspection is also an old nondestructive testing technique, although it was not produced so much impact in the field of NDT such as x-ray and ultrasonic. In recent years, according to the occurrence of new materials such as polymeric and ceramic composite materials, microwave inspection has become more and more an

important technique. Since traditional methods for NDT have been developed for metals, they are not readily applicable to dielectric materials, which differ from metals in their physical properties: Ultrasonic inspection is limited by high attenuation in the material while absorption for x-ray is too low for defects. As a consequence, an insufficient signal-to-noise ratio in the case of ultrasonic inspection and insufficient contrast between good and defective areas in x-ray inspection are resulted. Microwaves have also a low absorption in dielectric materials, but they still interact strongly with structures and defects inside the dielectric materials. The special advantage of microwave NDT over other techniques is that the inspection result is not based on density but dielectric property. In the microwave frequency region, the variation of dielectric permittivity for dielectric materials is significantly larger than the contrast of density; that is why microwave inspection is more sensitive than the other techniques for dielectric material testing. In addition, since the inspection result depends on dielectric property of materials, much additional information associated with that of the detected objects may be obtained.

The disadvantage of microwave NDT is on the divergent property of microwave. Microwave cannot propagate along a straight line, and is difficult to be focused. Thus a narrow microwave beam is so difficult to be obtained that the resolution of microwave inspection is relatively lower.

Microwave nondestructive testing can be separated into two approaches, which are time domain and frequency domain methods. Radar inspection, which has widely been used in many applications, is the example of time domain method. It employs the method of time domain analysis to measure the reflected pulse from detected objects. This technique is generally used to detect large and far objects such as bridge decks and concrete etc.[10-12]. Another approach is frequency domain method. In this case, sample is placed in the near field of the electromagnetic probe; a continuous wave (CW) is used as the incident wave and the frequency domain measurement is carried out. It is commonly used to detect the small defects with a small distance from the probe. Since the sixties, some researchers[13-14] have used this technique to measure the depth of thin slits and cracks in metals. Recently, It has been used for testing voids, delamination, disbond, and porosity etc. in a variety of dielectric materials, including polymers, ceramics, plastics, polymeric and ceramic composites, wood, and nonmetal-over-metal

type coatings[15-17]. Microwave NDT techniques have demonstrated tremendous potential in such applications.

Microwave NDT techniques are sensitive to geometrical and dimensional variations of a medium or a defect. Measurements can be conducted in a contact or noncontact fashion while operating on one side of a material or using both of its sides (reflection or transmission techniques). It is not necessarily true that because microwave signals have wavelengths in the centimeter range, the resolution obtained using these signals cannot be better than a large fraction of the operating wavelength. For instance, in monitoring thickness variation in dielectric slabs and coatings, if resolution is considered to be the smallest thickness variation that is possible to be detected, then microwave NDT techniques have shown measurement resolutions of a few microns at 10 GHz (wavelength of 3 cm in free space)[18]. If, in a given application, resolution is considered to be the smallest spatial distance between two defects, so that they can be detected individually, then near-field microwave and millimeter-wave techniques have provided resolutions of better than one-tenth of a wavelength. In addition, spatial resolution is a function of the microwave sensor used (e. g., open-ended waveguides, oped-ended coaxial lines, cavity resonators, etc.). Changes in the reflection coefficient properties for a given microwave sensor and defect are very different in the near-field compared to the far-field.

Hardware systems for microwave NDT applications need not be expensive. It is true that if laboratory test equipment is used to conduct measurements, the cost will be high. However, hardware for a specific application can be developed and built to be relatively inexpensive, simple in design, hard-held, battery-operated, operator friendly, and operate on an on-line basis. The capability of providing real-time information makes these techniques suitable for on-line industrial applications. The operator need not be a microwave expert to conduct microwave NDT measurements once a system has become operational. Since the required operating power for most NDT applications (excluding ground probing radars and microwave heating sources) are in the few milliwatts range, and the majority of these techniques are conducted in the near-field with a high degree of frequency selectivity (narrow band CW measurements), they do not cause any electromagnetic interference (EMI) and are not affected by EMI. There are no environmentally hazardous or undesirable byproducts associated with these

techniques.

Large scan areas can be accommodated with an array of sensors. Microwave signals do not penetrate inside conductors and graphite composites. However, this is not always a limitation, since surface features such as cracks on metal surfaces and impact damage on graphite composites can be inspected along with the properties of dielectric coatings (thickness and material composition) on top of metals and graphite composites. One of the most attractive aspects of microwave NDT techniques is the availability of many different probes/sensors. Some of these may render better results than the others for a specific application. In addition, optimization of system parameters for obtaining more sensitive results makes microwave NDT techniques very powerful.

Areas that may (some already even have) benefit from using microwave NDT techniques are[18]:

- Accurate thickness measurement of coatings, single dielectric slabs, layered dielectric composites made of plastics, ceramics, and any other types of dielectric materials.
- Minute thickness variation of each layer in these dielectric media.
- Disbond, delamination, void detection, and thickness evaluation in stratified media.
- Inspection of thick plastics and glass-reinforced composites for the detection of interior flaws, fiber bundle orientation and breakage, moisture content, etc.
- Detection and estimation of porosity in dielectrics.
- Impact damage detection and evaluation in reinforced composite structures including graphite composites.
- Accurate material/constituent characterization in dielectric mixtures.
- Detection and evaluation of curing in chemically reactive media.
- Relating electrical properties of materials, such as dielectric characteristics, to physical and mechanical properties, such as compressive strength of concrete members.
- Detection of surface cracks (stress and fatigue) in metals, including sizing of the three dimensions of a crack. This feature extends to filled cracks and cracks covered with various dielectric coatings. As a matter of fact, which allows for crack detection

under various coatings without the need for coating removal prior to testing.

- Optimization capability for all of these measurements to obtain higher measurement sensitivity.
- Production of defect images.
- Using microwaves as heat sources in thermography.
- And, finally, new applications are continuously being discovered.

The time is right for renewed vigor in applying microwave NDT techniques to new inspection problems. A fresh sustained effort in this area should be very fruitful. Many investigators believe that, given the same level of effort enjoyed by other NDT techniques during their development, microwave NDT will find a prominent place in a wide realm of applications. In some cases it will prove to be the technique of choice. In other cases it will prove to be a useful complement when used in conjunction with other methods.

1.4.2 Rectangular Waveguide

Open-ended rectangular waveguide is the mostly used probe for microwave nondestructive testing and has been proved to be a powerful tool for the evaluation of dielectric materials[19-21]. However, for detecting small defects, waveguide presents some frequency limitations. Waveguide supports transverse electric (TE) and/or transverse magnetic (TM) waves, which are characterized by the presence of longitudinal magnetic and electric field components, respectively. The TE and TM modes of a waveguide have cutoff frequencies below which propagation is not possible[22]. Since the higher order modes begin at the upper frequencies, in order to remain only the dominant mode propagating in the waveguide, the operation frequency should be higher than the cutoff frequency of the dominant mode and lower than that of the higher order mode, respectively. As the operation frequency depends on the dimensions of waveguide, the size of waveguide aperture cannot be made too small in order that the operation frequency is not cut off. It means that the spatial resolution is limited by the size of

waveguide aperture (see Fig. 1.5). When defects are smaller relative to the dimensions of waveguide aperture, the details of those defects cannot be detected, because the ratio of the areas of the defect to the probe-aperture is small. In other words, the capability for distinguishing smaller defects is poor.

The advantage of rectangular waveguide is that the effective standoff distance is larger. Since the intensity of electric and magnetic fields, in the near field of the waveguide, are directly proportional to the area of the probe aperture, the relatively larger dimensions of probe aperture make the defect that has a larger distance from the probe detectable effectively.

1.4.3 Open-Ended Coaxial Line Sensor

Open-ended coaxial line technique has been used to measure the constitutive parameters of dielectric materials previously[23-27]. In those studies, as the technique was not used for detecting defects, the resolution was not required to be considered. Therefore the size of sensors was relatively large. In contrast to the conventional microwave NDT methods, a new technique by using open-ended coaxial line sensor was developed in this study. Here, the open-ended coaxial line sensor was first used to detect defects and the spatial resolution was improved effectively[28]. The implementation of this advanced technique has produced a significant impact on microwave NDT.

Coaxial line that consists of two conductors may support transverse electromagnetic (TEM) waves, which are characterized by the lack of longitudinal field components. Hence there is no cutoff frequency for the fundamental TEM mode and also, the operation frequency band can be on a broad range. It is thus possible to decrease the size of coaxial line aperture for increasing the spatial resolution. Since the size of the sensor aperture can be made smaller (not limited by frequency), the area of incident beam is smaller. Thereby the ratio of defect-area to the beam-area is relatively large; therefore, smaller defects can be detected effectively.

It should be noted that because of the near field used in the measurement, the smaller size of the sensor aperture will lead to the decrease of effective standoff distance.

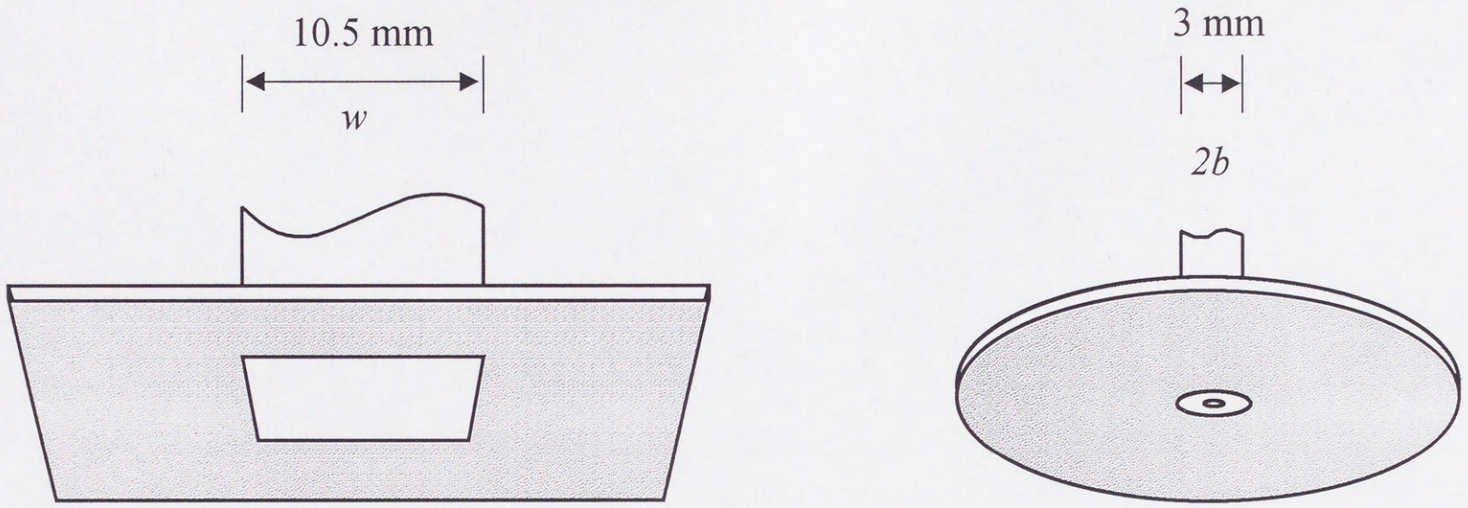

(a) Open-ended waveguide probe

(b) Open-ended coaxial line sensor

Fig. 1.5 Comparison of the dimensions of microwave sensors at the frequency of 20 GHz

1.5 Summary

The features of x-ray, ultrasonic and microwave inspection are summarized in Table 1.1. Since the disadvantages of x-ray and ultrasonic for detection of defects in dielectric materials and the larger lateral area of the delamination in IC package, microwave is recognized to be a powerful tool to detect the delamination in IC package. For increasing the spatial resolution, an open-ended coaxial line sensor is employed to detect delamination in IC package. The features of it compared with the open-ended rectangular waveguide probe are shown in Table 1.2.

In case of x-ray inspection, as the thickness of delamination is very thin, the absorption for x-ray due to the delamination is very small; in other words, the contrast of density for delamination is very small, so the delamination cannot be detected. Although scanning acoustic tomography (SAT) technique has been used for inspection of delamination in IC package[1], the limitation of the requirement of a coupling medium makes it impossible to observe the mechanism of delamination under the similar conditions of soldering. In addition, when the package is very thin, it is difficult to separate the echoes from the surface of the package and the delamination. Therefore, a new technique of microwave NDT has been developed in an attempt to evaluate the interfaces of IC package[29]. Microwave imaging of IC package was also demonstrated for observing the area of delamination which is one of the most important reliability concerns for IC package[30]. The sensitivity to the change in dielectric properties of materials, the ability to penetrate deeply inside dielectric materials, and the characteristic to reflect completely from the metal surface make microwave inspection highly sensitive to detect such delamination. On the other hand, since the detected result is not based on density but dielectric property, the properties of package concerning the moisture and temperature are also possible to be estimated.

In Chapter 2, development of an open-ended coaxial line sensor for detection of small defects in dielectric materials is described. The study employs swept-frequency technique to measure the magnitude of transmission coefficient in discontinuous coaxial line, and analyzes its first abrupt transition with some epoxy composite samples

Table 1.1 Comparison of microwave NDT with other NDT techniques for detection of defects in dielectric materials

	X-ray	Ultrasonic	Microwave
Resolution	Very high	High	Low
Sensitivity	Very low	Low	High
Coupling medium	No	Necessary	No
Safety	Low	High	High
Cost	Very high	Not high	Low

Table 1.2 Comparison of open-ended coaxial line sensor with waveguide probe

	Coaxial line sensor	Waveguide probe
Resolution	High	Low
Sensitivity	High	High
Standoff distance	Small	Large
Frequency range	Wide	Narrow
Field distribution	Complex	Simple

containing artificial defects. In Chapter 3, in an attempt to detect delamination effectively in IC package, the magnitude of effective reflection coefficient is measured by using the open-ended coaxial line sensor. The phenomenon of coherent resonance is realized to increase the sensitivity of the measurement. In Chapter 4, we pay attention to improve the inspection technique; consequently, phase measurement is introduced because of the fact that it is less affected by the scattering of the microwave. Delamination in IC package is detected at a relatively lower frequency and, more importantly, the optimization of the parameters, namely, the frequency and standoff distance, is not need required to be carried out in advance. The phase difference of the measured sample from the reference one is calculated for eliminating the influence of the lack of spatial resolution. In Chapter 5, a new theoretical model of microwave interaction with IC package is built up, by which the experiment can be optimized and the reference sample can be replaced. Also the experiment is verified by the theoretical calculation. In Chapter 6, for investigating the shape and the size of the delamination in IC package, microwave imaging is realized by recording the phase of effective reflection coefficient continuously, corresponding to scanning position. Finally, conclusions are summarized in Chapter 7.

REFERENCES

1 Omi, S., Fujita, K., Tsuda, T. and Maeda, T., 'Causes of Cracks in SMD and Type Specific Remedies', *IEEE Transactions on Components, Hybrids, and Manufacturing Technology*, Vol. 14, No. 4, 1991, pp. 818-823.

2 Kawamura, N., Kawakami, T., Matsumoto, K., Sawada, K. and Taguchi, H., 'Structural Integrity Evaluation for a Plastic Package During the Soldering Process', *Advances in Electronic Packaging, Vol. 1, Structural Analysis, Materials and Processes, Design, Reliability, ASME,* EEP-Vol. 4-1, 1993, pp. 91-95.

3 Tay, A. A. O., Tan, G. L. and Lim, T. B., 'Predicting Delamination in Plastic IC Packages and Determining Suitable Mold Compound Properties', *IEEE Transactions on Components, Packaging, and Manufacturing Technology-Part B: Advanced Packaging*, Vol. 17, No. 2, 1994, pp. 201-208.

4 Lee, H. and Earmme, Y. Y., 'A Fracture Mechanics Analysis of the Effects of Material Properties and Geometries of Components on Various Types of Package Cracks', *IEEE Transactions on Components, Packaging, and Manufacturing Technology-Part A*, Vol. 19, No. 2, 1996, pp. 168-178.

5 *Nondestructive Testing Handbook*, 2nd ed., American Society for Nondestructive Testing, Columbus, OH.

6 Quinn, R. A. and Sigl, C. C. (Eds.), *Radiography in Modern Industry*, 4th ed., Eastman Kodak Company, Rochester, NY, 1980.

7 Kobayashi, A. S. (Ed), *Handbook on Experimental Mechanics*, 2nd rev. ed., Society for Experimental Mechanics, Inc., 1993.

8 Krautkrammer, J., *Ultrasonic Testing of Materials*, Springer-Verlag, Berlin, 1969.

9 Ahmed, M., Want, K. Y. and Metherell, A. F., 'Holography and Its Application to Acoustic Imaging', *Proc. IEEE, 67*, No. 4, 1979.

10 Chen, H. L. R., Halabe, U. B., Sami, Z. and Bhandarkar, V., 'Impulse Radar Reflection Waveforms of Simulated Reinforced Concrete Bridge Decks', *Materials Evaluation*, Vol. 52, No. 12, 1994, pp. 1382-1388.

11 Halabe, U. B., Sotoodehnia, A., Maser, K. R. and Kausel, E. A., 'Modeling the Electromagnetic Properties of Concrete', American Concrete Institute (ACI) *Materials Journal*, Vol. 90, No. 6, 1993, pp. 552-563.

12 Maser, K. R. and Roddis, W. M. K., 'Principles of Thermography and Radar for Bridge Deck Assessment', *Journal of Transportation Engineering*, Vol. 116, No. 5, 1990, pp. 583-601.

13 Hruby, R. J. and Feinstein, L., 'A Novel Nondestructive Noncontacting Method of Measuring the Depth of Thin Slits and Cracks in Metals', *The Review of Scientific Instruments*, Vol. 41, No. 5, 1997, pp. 679-683.

14 Yeh, C. Y., Ranu, E. and Zoughi, R., 'A Novel Microwave Method for Surface Crack Detection Using Higher Order Waveguide Modes' *Materials Evaluation*, Vol. 52, No. 6, 1994, pp. 676-681.

15 Gray, S., Ganchev, S., Qaddoumi, N., Beauregard, G., Radford, D. and Zoughi, R., 'Porosity Level Estimation in Polymer Composites Using Microwaves', *Materials Evaluation*, Vol. 53, No. 3, 1995, pp. 404-408.

16 Gopalsami, N., Bakhtiari, S., Dieckman, S. L., Raptis, A. C. and Lepper, M. J.,

'Millimeter-Wave Imaging for Nondestructive Evaluation of Materials', *Materials Evaluation*, Vol. 52, No. 3, 1994, pp. 412-415.

17 Ambrosio, G.d', Migliore, M.D., Ciliberto, A. and Sabatino, C., 'Microwave Defect Detection on Low-Loss Composites', *Materials Evaluation*, Vol. 51, No. 2, 1993, pp. 285-289.

18 Zoughi, R., 'Microwave and Millimeter Wave Nondestructive Testing: A Succinct Introduction', *Research in Nondestructive Evaluation*, Vol. 7, No. 2, 1995, pp. 71-74.

19 Zoughi, R. and Bakhtiari, S., 'Microwave Nondestructive Detection and Evaluation of Disbonding and Delamination in Layered-Dielectric-Slabs', *IEEE Transactions on Instrumentation and Measurement*, Vol. 39, No. 6, 1990, pp. 1059-1063.

20 Qaddoumi, N., Carriveau, G., Ganchev, S. and Zoughi, R., 'Microwave Imaging of Thick Composite with Defects', *Materials Evaluation*, Vol. 53, No. 8, 1995, pp. 926-929.

21 Diener, L., 'Microwave Near-Field Imaging with Open-Eeded Waveguide — Comparison with Other Techniques of Nondestructive Testing', *Research in Nondestructive Evaluation*, Vol. 7, No. 3, 1995, pp. 137-152.

22 Pozar, D. M., Microwave Engineering, ch. 4, 1990. Addison Wesley, New York, NY.

23 Scott, W. R. Jr., 'A New Technique for Measuring the Constitutive Parameters of Planar Materials', *IEEE Transactions on Instrumentation and Measurement*, Vol. 41, No. 5, 1992, pp. 639-645.

24 Belhadj-tahar, N.-E., Fourrier-lamer, A. and Chanterac, H., 'Broad-Band Simultaneous Measurement of Complex Permittvity and permeability Using a Coaxial Discontinuity', *IEEE Transactions on microwave theory and techniques*, Vol. 38, No. 1, 1990, pp. 1-7.

25 Stuchly, M. A. and Stuchly, S. S., 'Coaxial Line Reflection Methods for Measuring Dielectric Properties of Biological Substances at Radio and Microwave Frequency-A Review', *IEEE Transactions on Instrumentation and Measurement*, Vol. IM-29, No. 3, 1980, pp. 176-183.

26 Mosig, J. R., Besson, J. E., Gex-fabry, M. and Gardiol, F. E., 'Reflection of an Open-Ended Coaxial Line and Application to Nondestructive Measurement of Materials', *IEEE Transactions on Instrumentation and Measurement*, Vol. IM-30,

No. 1, 1981, pp. 46-51.

27 Grant, J. P., Clarke, R. N., Symm, G. T. and Spyrou, N. M., 'A Critical Study of the Open-Ended Coaxial Line Sensor Technique for RF and Microwave Complex Permittivity Measurements', *Journal of Physics E: Scientific Instruments*, Vol. 22, No. 9, 1989, pp. 757-770.

28 Ju, Y., Saka, M. and Abé, H., 'A Method for Nondestructive Testing of Defects in Dielectric Material Utilizing Coaxial Line Sensor Technique', *Proc. International Conference on Materials and Mechanics '97*, JSME, Tokyo, 1997, pp. 401-404.

29 Ju, Y., Saka, M. and Abé, H., 'Microwave Nondestructive Detection of Delamination in IC Packages Utilizing Open-Ended Coaxial Line Sensor', *NDT & E International,* 1999, in press.

30 Ju, Y., Saka, M. and Abé, H., 'Microwave Imaging for Nondestructive Inspection of Delamination in IC Packages by Open-Ended Coaxial Line Sensor', *Proc. of the Workshop on Mechanical Reliability of Polymeric Materials & Plastic Packages of IC Devices*, ASME/IEEE-CPMT/IMAPS, Paris, EEP-Vol. 25, 1998, pp 265-270.

2

FUNDAMENTAL EXPERIMENT

2.1 INTRODUCTION

The study on NDE of the delamination in IC packages has begun at the research for evaluating defects in packaging materials nondestructively. As defect size is very small, a coaxial line sensor was first used for NDE of defects in order to increase the spatial resolution.

IC packaging material, which is a kind of epoxy filled silica composite, has been studied over a long time. Much improvement has been made, but a problem that, the size of some silica powder is in some cases larger than the requirement (e. g., diameter should be smaller than 0.2mm in our case), still cannot be avoided in the manufacturing process. It directly affects the production cost. Therefore, nondestructive testing technique is desired to detect those defects in order to reject them in the following process. The dielectric properties of the packaging material are related to those of epoxy and silica and also to their quantity. Thus, it is possible to determine the volume of silica powder, if the spatial resolution of the inspection is high enough, and if the dielectric properties of silica and the mixture are known. The sensitivity to the change in dielectric properties of materials and the ability to penetrate deeply inside dielectric materials make microwave technique very attractive for testing such materials.

Microwave technique has been used for testing voids, delaminations, porosity etc. in a variety of dielectric materials[1-5]. However, for detecting small defects, waveguide that was used in the above researches presents some frequency limitations. The

existence of cutoff frequency does not allow to make the waveguide aperture small enough, thereby the spatial resolution was limited by the aperture size of waveguide. In contrast with the conventional microwave methods, here, a coaxial line sensor is proposed to be used for increasing the spatial resolution. Coaxial line technique has been used to measure the constitutive parameters of dielectric materials[6-10], but has not yet been used for NDE of defects. The primary advantages of coaxial line sensor are that it can work on a wide frequency range (radio frequency and microwave), and the aperture, which is independent of working wavelength, can be made in very small dimensions for increasing the spatial resolution. This study employs swept-frequency technique to measure the magnitude of transmission coefficient in discontinuous coaxial line, and analyzes its first abrupt transition with some epoxy composite samples containing artificial defects[11]. The results indicate that the present technique is very effective and convenient for testing such material.

2.2 COAXIAL LINE SENSOR

The measurement system configuration is shown in Fig. 2.1; the configuration of measurement fixture consisting of coaxial line sensors and sample is shown in Fig. 2.2, where a and b are radii of the inner and outer conductors of the coaxial line, and c the outer radius of the flange. Because of the relatively lower operation frequency, for simplicity, the method of calculating the transmission coefficient is based on a model of the discontinuity of the coaxial line as an equivalent lumped circuit. As shown in Fig. 2.3, the capacitor C_s models the capacity coupling between the center conductors, and the admittance Y_t models the radial component between the flanges. When the sample is placed in the measurement fixture, the admittance, Y_s, of the capacitor can be approximated as

$$Y_s = j\omega C_s \approx j\omega\tilde{\varepsilon}_r C_0 \tag{2.1}$$

where $\tilde{\varepsilon}_r$ is the complex relative permittivity of the sample and C_0 the value of C_s

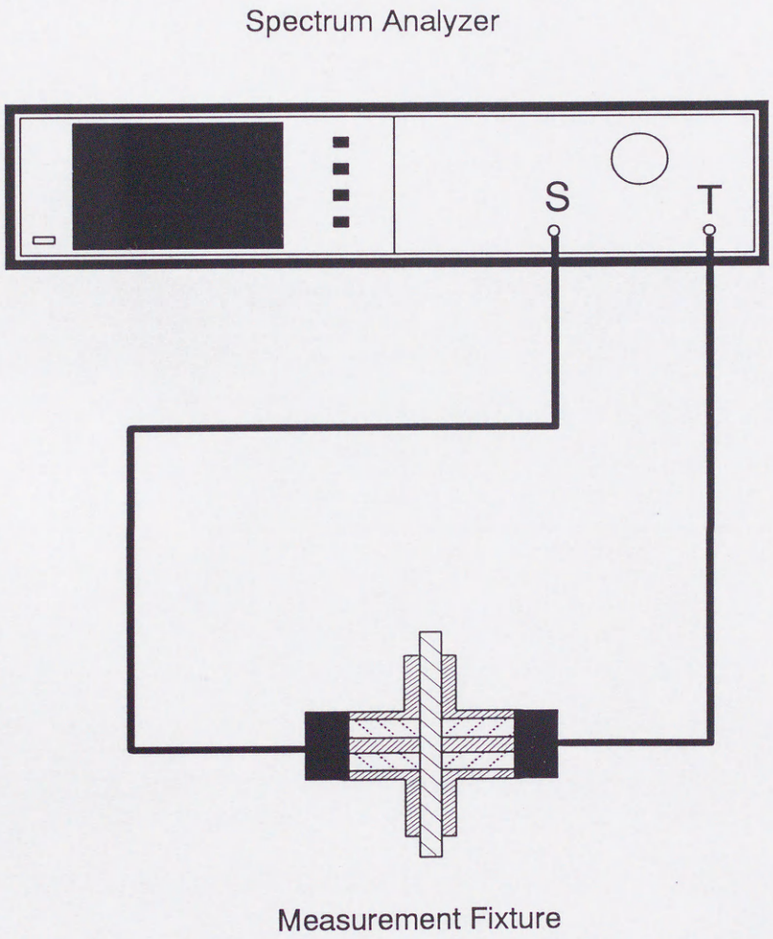

Fig. 2.1 Measurement system configuration

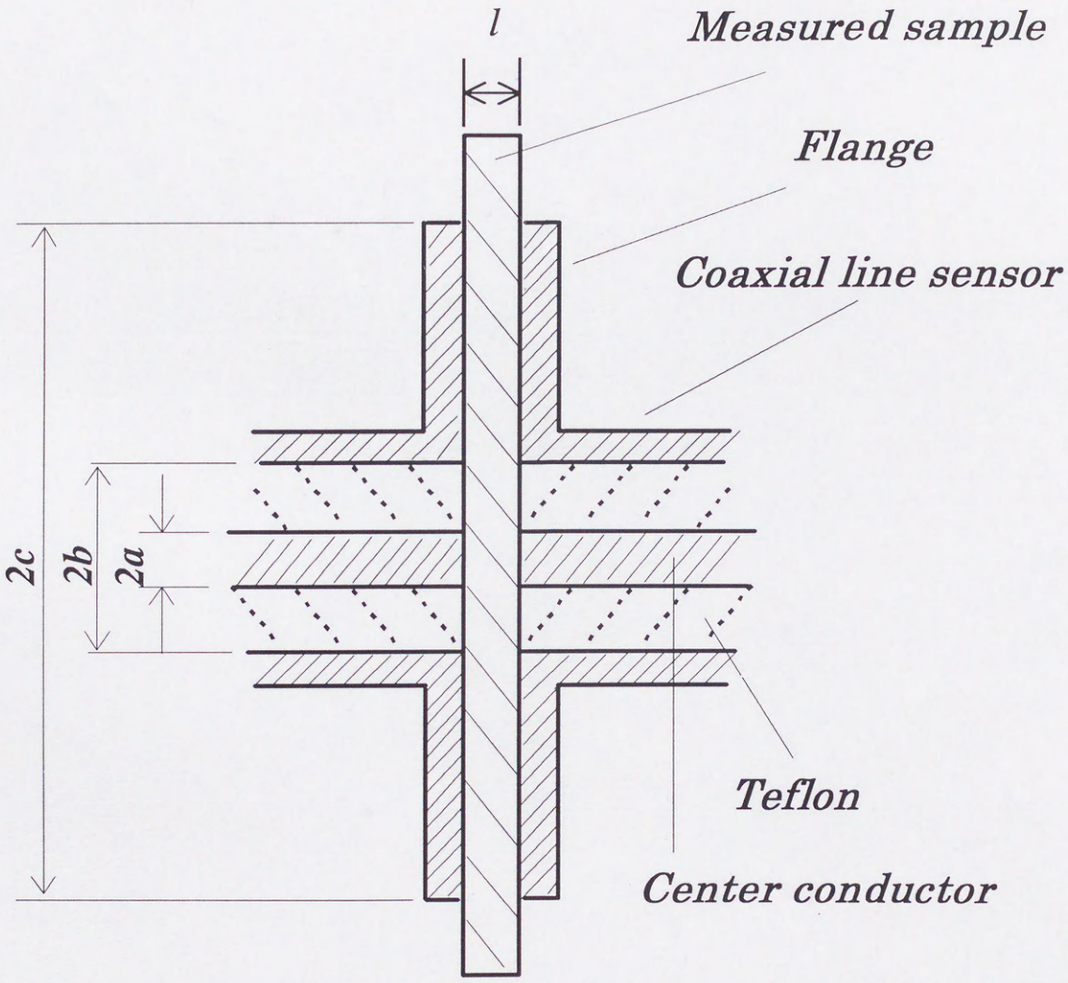

Fig. 2.2 Configuration of coaxial line sensor

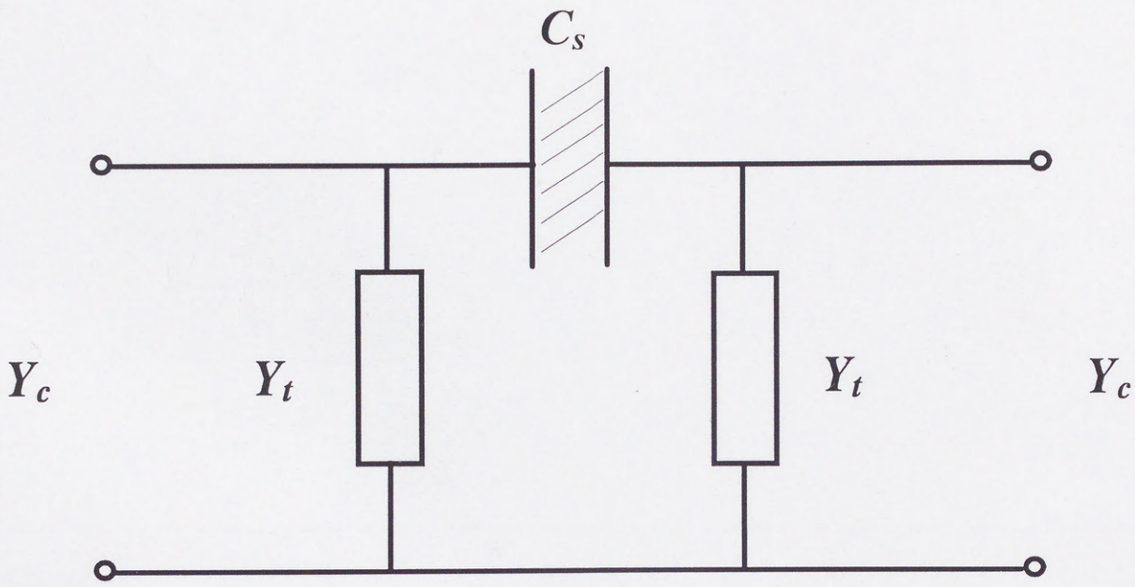

Fig. 2.3 Fixture modeled by a lumped equivalent circuit

when sensors are filled with free space. The angular frequency is denoted by ω and $j = \sqrt{-1}$. The approximation is due to the fact that the flange size of the sensors is not infinitely large so that a portion of the fringe fields is not in the capacitor.

In terms of the equivalent circuit model, the transmission coefficient, T, is given by

$$T = \frac{Y_s}{Y_s + Y_t + Y_c} \tag{2.2}$$

where Y_c is the characteristic admittance of the coaxial line. The transmission coefficient T of the measurement fixture is primarily determined from the capacitance between the center conductors when the inequality

$$\frac{|Y_s|}{|Y_t|} >> 1 \tag{2.3}$$

is satisfied. The value of Y_t depends on the shape and position of the sensors. Increasing the radius c of flange will increase the ratio $|Y_s|/|Y_t|$. When c/b=10, Eq. (2.3) can be satisfied approximately. The equivalent circuit parameter Y_t can be inferred from the measurement on a known dielectric sample as reference.

2.3 EXPERIMENTAL PROCEDURE

To conduct the experimental study, the coaxial line sensor was made by a coaxial line connector (a =1.5, b =2.5 mm) machined to a flat surface and fitted with a 20 mm diameter flange. Two composite plates making from the actual packaging material with thickness of 2 mm were used as samples. Several artificial defects were introduced in the samples with different dimensions. One sample is shown in Fig. 2.4, where the area scanned on the sample has four flat bottom holes filled with silica, having the depth of 1 mm and diameters of 2, 1, 0.5 and 0.3 mm respectively. For analyzing the influence of

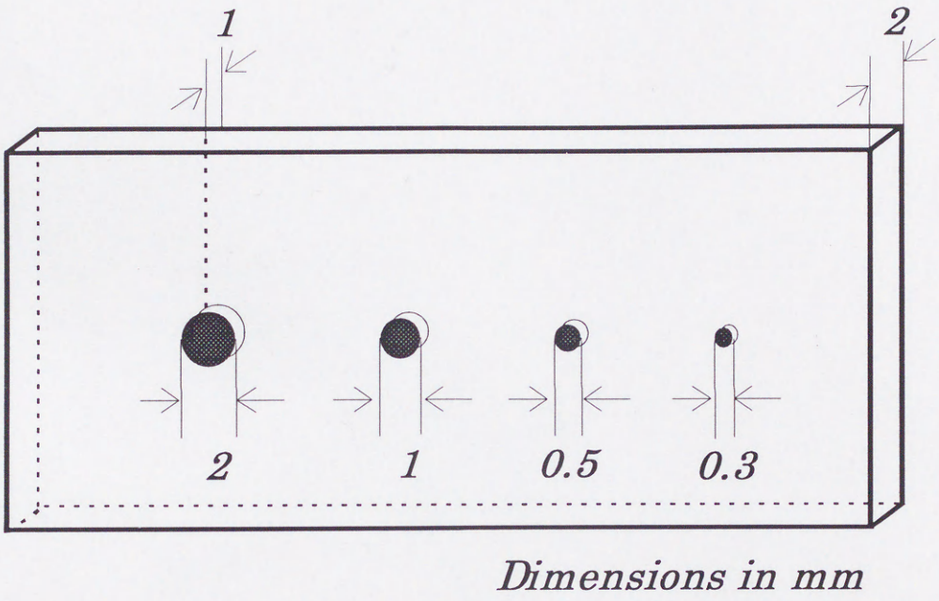

Fig. 2.4 Descriptive geometry of a composite plate with four flat bottom holes having the depth of 1 mm, filled with silica (Sample 1)

defect thickness, another sample containing four flat bottom holes filled with silica, having the depth of 0.5mm and same diameters as the previous one was also measured; the descriptive geometry of the epoxy composite plate sample with defects in different size is shown in Fig. 2.5. The spectrum analyzer was used for determining the relationship between the magnitude of transmission coefficient and the frequency.

The transmission coefficient varied with the sample thickness d, permittivity $\tilde{\varepsilon}_r$ and the operation frequency $f\ (=\omega/2\pi)$. In the measurement, d took a fixed value, and $\tilde{\varepsilon}_r$ and f were varied. The magnitude of transmission coefficient, $|T|$, was thus measured as

$$|T| = |T|(\tilde{\varepsilon}_r, f) \tag{2.4}$$

First, the magnitude of transmission coefficient, $|T_0|$, in case of no defect ($\tilde{\varepsilon}_r = \tilde{\varepsilon}_{r0}$), was measured as a function of $\tilde{\varepsilon}_{r0}$ and f to be used as the reference. Then, for a given defect, $\tilde{\varepsilon}_r = \tilde{\varepsilon}_{ri}$, the magnitude of transmission coefficient, $|T_i|\left[=|T|(\tilde{\varepsilon}_{ri}, f)\right]$, was measured. Here, $\tilde{\varepsilon}_{ri}$ is the mixture permittivity corresponding to different defects.

2.4 RESULTS AND DISCUSSION

In the experiment, when the frequency was swept, a series of small magnitude resonances of the transmission coefficient were generated at the different frequencies periodically. Figure 2.6 shows two abrupt transitions of the magnitude of transmission coefficient at low frequency range. The phenomenon is due to the interaction of the reflection with the transmission wave thereby leading to the phase variation of the transmission coefficient, because the impedance of the discontinuity of the coaxial line does not match with the characteristic impedance of the coaxial line. For increasing the measurement sensitivity, the higher magnitude resolution of the spectrum analyzer was used, and the first abrupt transition of the magnitude of transmission coefficient was

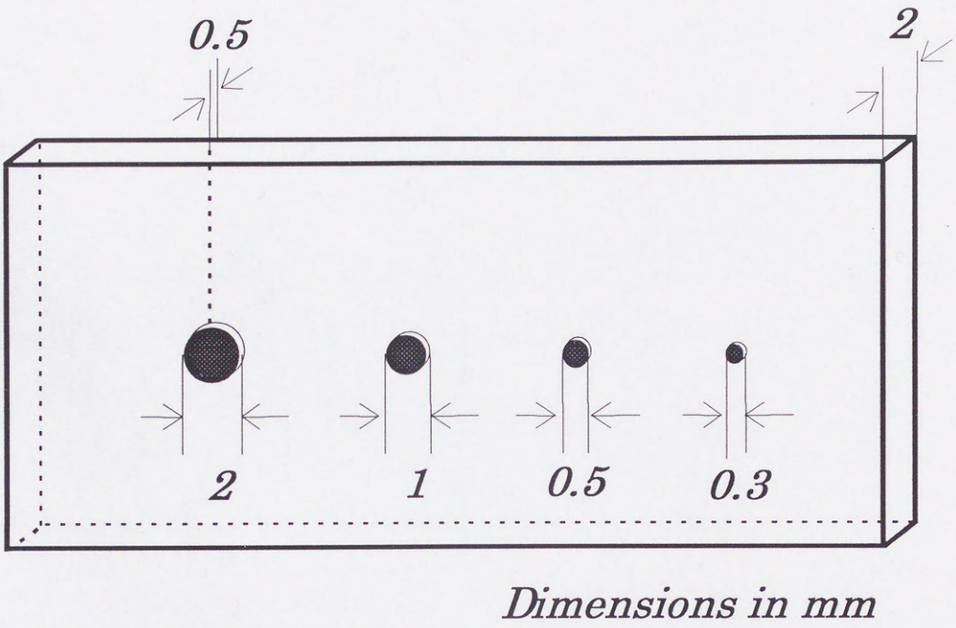

Fig. 2.5 Descriptive geometry of a composite plate with four flat bottom holes having the depth of 0.5 mm, filled with silica (Sample 2)

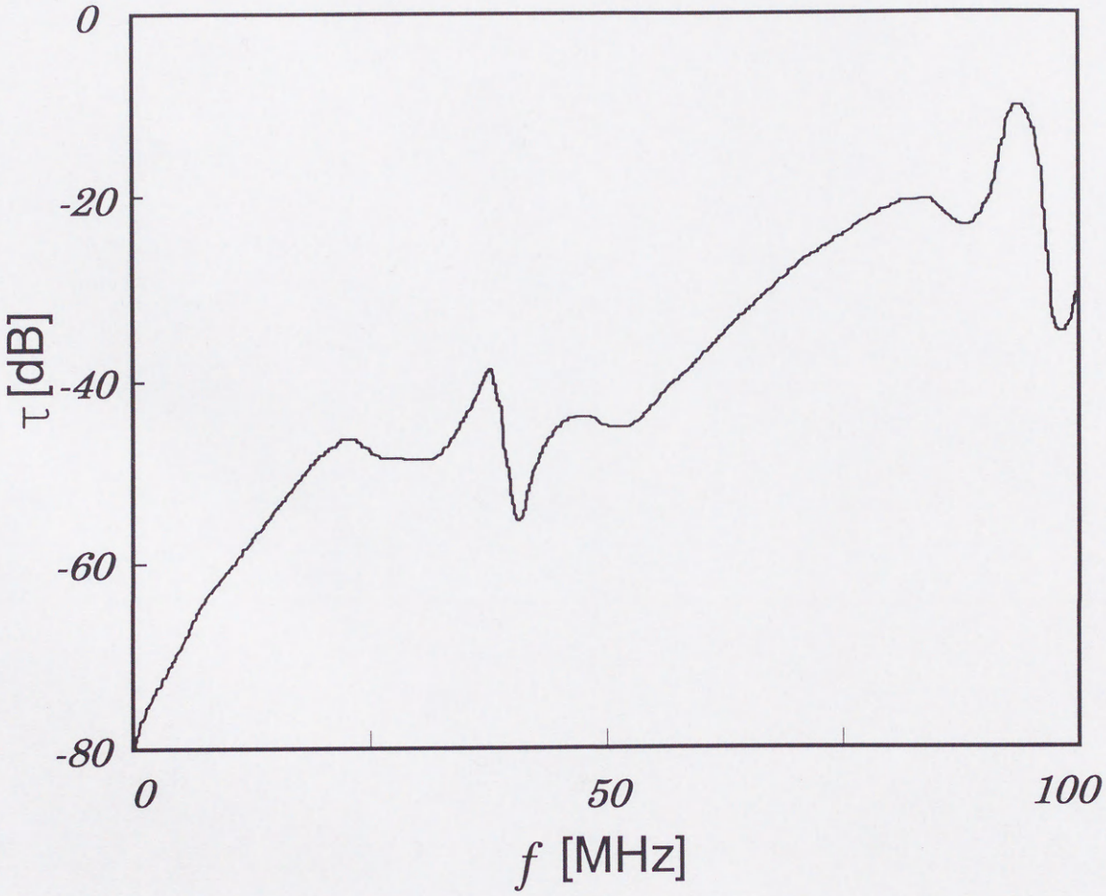

Fig. 2.6 Measured abrupt transitions of the magnitude of transmission coefficient as a function of frequency

measured in detail.

The measured first abrupt transition of the magnitude of transmission coefficient for Sample 1 is shown in Fig. 2.7, where ϕ is the diameter of the defects. With the increase of defect size, the mixture permittivity is decreased because the permittivity of silica is smaller than that of composite; thus the magnitude of transmission coefficient is decreased. While, a little change in both the position and shape of the first abrupt transition are also observed. The first abrupt transition of the magnitude of transmission coefficient measured for Sample 2 is shown in Fig. 2.8. It shows that when the defect diameter is larger than 0.5 mm, the difference in magnitude of the transmission coefficients between with and without defect is also evident. When the defect diameter is smaller than 0.3 mm, the defect cannot be distinguished, thus the higher magnitude resolution of the spectrum analyzer is required. In Fig. 2.9, a part of the positive peak is shown in detail with the smaller scale of the spectrum analyzer. The difference in magnitude of the transmission coefficients in cases of no defect and 0.3 mm diameter defect is observed clearly.

For further analysis of the relationship between the defects and the measurement results, the difference of the positive peak value of the first abrupt transition between with and without defects, D, was calculated as follows;

$$D(\tilde{\varepsilon}_{ri}, f_i) = \tau(\tilde{\varepsilon}_{r0}, f_0) - \tau(\tilde{\varepsilon}_{ri}, f_i) \tag{2.5}$$

where f_i indicates the positive peak of the first abrupt transition taking place at different frequency corresponding to different defects and f_0 the value of f_i in the case of no defect. Figure 2.10 shows the calculated results of D versus defect diameters. It shows that the sensitivity is decreased according to the decrease of the defect diameter, and D is approximately proportional to the square of the defect diameter. The sensitivity is also decreased when the thickness of defect is decreased, and the relationship of D with the defect thickness is approximately linear. Consequently, D is approximately proportional to the volume of the defect. It is possible to classify defects with different size by selecting suitable threshold of D. For example, for classifying the defects with diameter larger than 1mm, the threshold D_1,

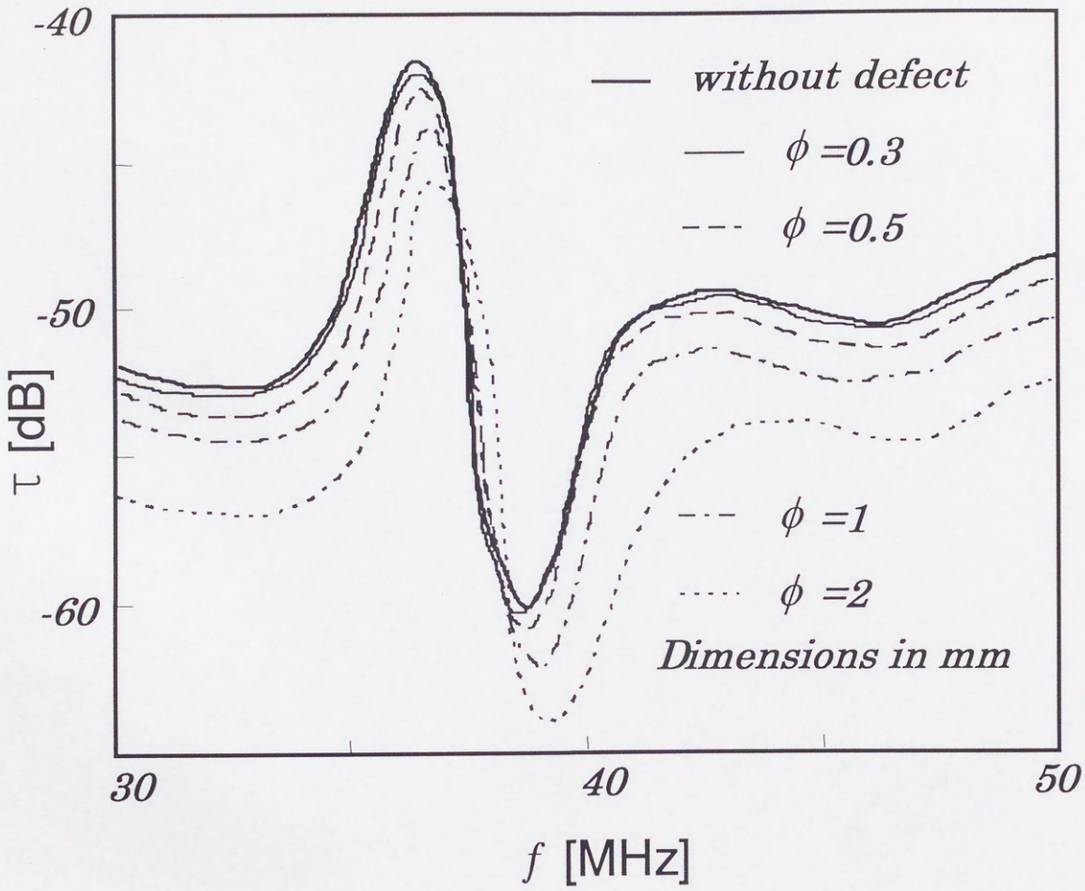

Fig. 2.7 The first abrupt transition of the magnitude of transmission coefficient for Sample 1

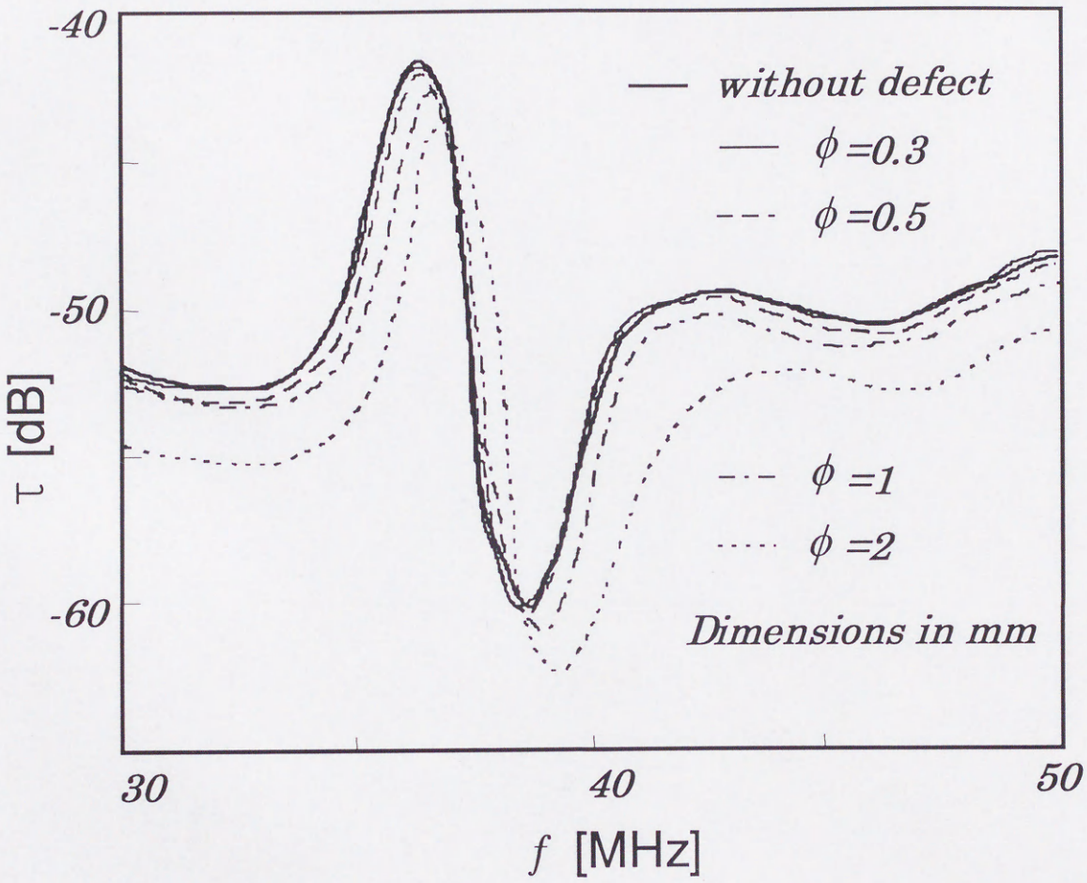

Fig. 2.8 The first abrupt transition of the magnitude of transmission coefficient for Sample 2

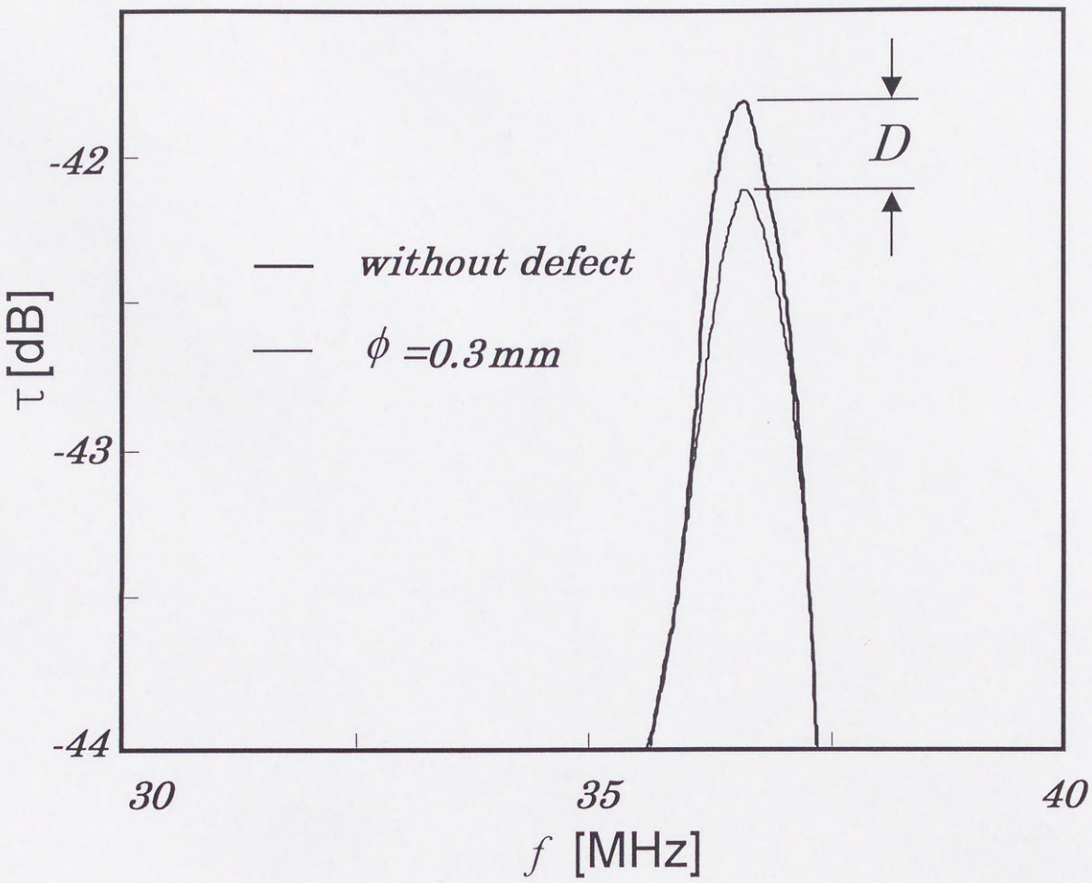

Fig. 2.9 A part of the positive peak in Fig. 2.8 measured with the smaller scale of the spectrum analyzer

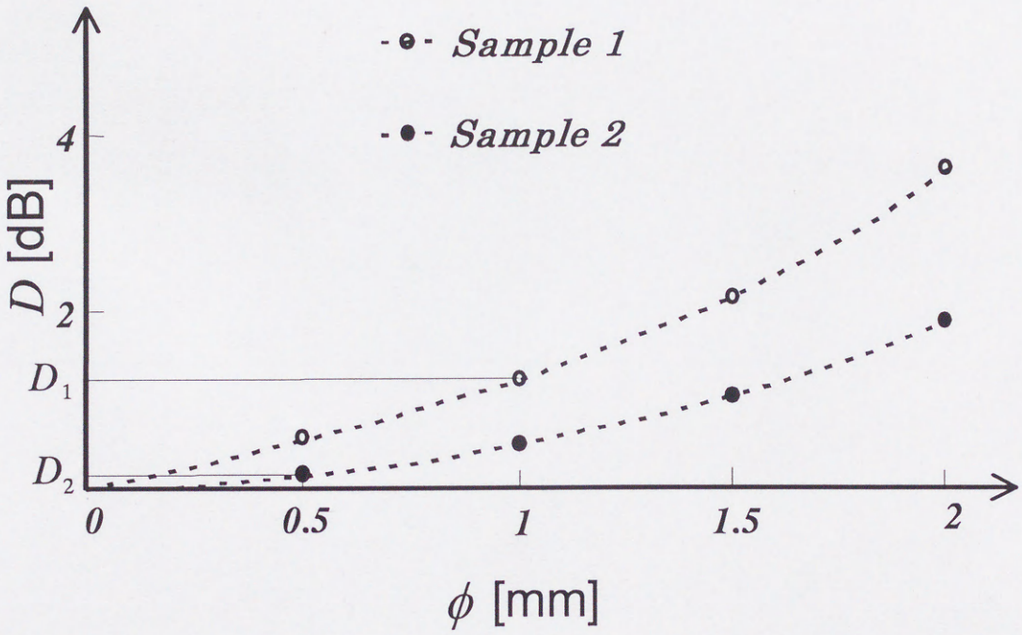

Fig. 2.10 Relationship between D and ϕ for two samples

as shown in Fig. 2.10, should be selected. If the defects with diameter larger than 0.5 mm are required to be detected, the threshold D_2 should be selected. For on-line testing the packaging material, it is possible to determine the threshold of 0.2 mm diameter defect by measuring a known sample. When the composite plate is scanned, if D is larger than the threshold, a defect will be marked.

In the above measurements, the measurement fixture was in contact with the sample. It means the distance between the coaxial line sensors is same as the thickness of sample. In case of noncontact measurement, the sample is required to be fixed in the center of the measurement fixture. Measurements were also done for change the distance, l, between the sensors. Figure 2.11 shows the measurement results with the normal epoxy composite plate of 2mm thickness. It indicates that along with the increase of l, the amplitude of first abrupt transition increases largely but the magnitude of transmission coefficient decreases significantly, thus the sensitivity to detect the defects is decreased. The change in the shape of first abrupt transition indicates the change in phase of the transmission coefficient. It means that the phase of transmission coefficient is sensitive to change in thickness of sample, which can be used for detecting the defects based on the thickness difference, such as delaminations etc., in homogeneous dielectric materials.

For increasing measurement resolution, the use of sensors with smaller dimensions is emphasized. It is important to note that the aperture of coaxial line sensor can be made in very small dimension without a limitation of operation frequency. That is the special advantage over the waveguide testing technique of which the aperture size is determined by operation frequency.

2.5 CONCLUSIONS

Coaxial line sensor technique was confirmed to be a powerful tool for detecting defects in dielectric materials. The magnitude of transmission coefficient was found to be sensitive to the change in dielectric properties of materials. The first abrupt transition phenomenon was found to be very effective for detecting defects due to the difference of permittivity. The phase of transmission coefficient is sensitive to the change in

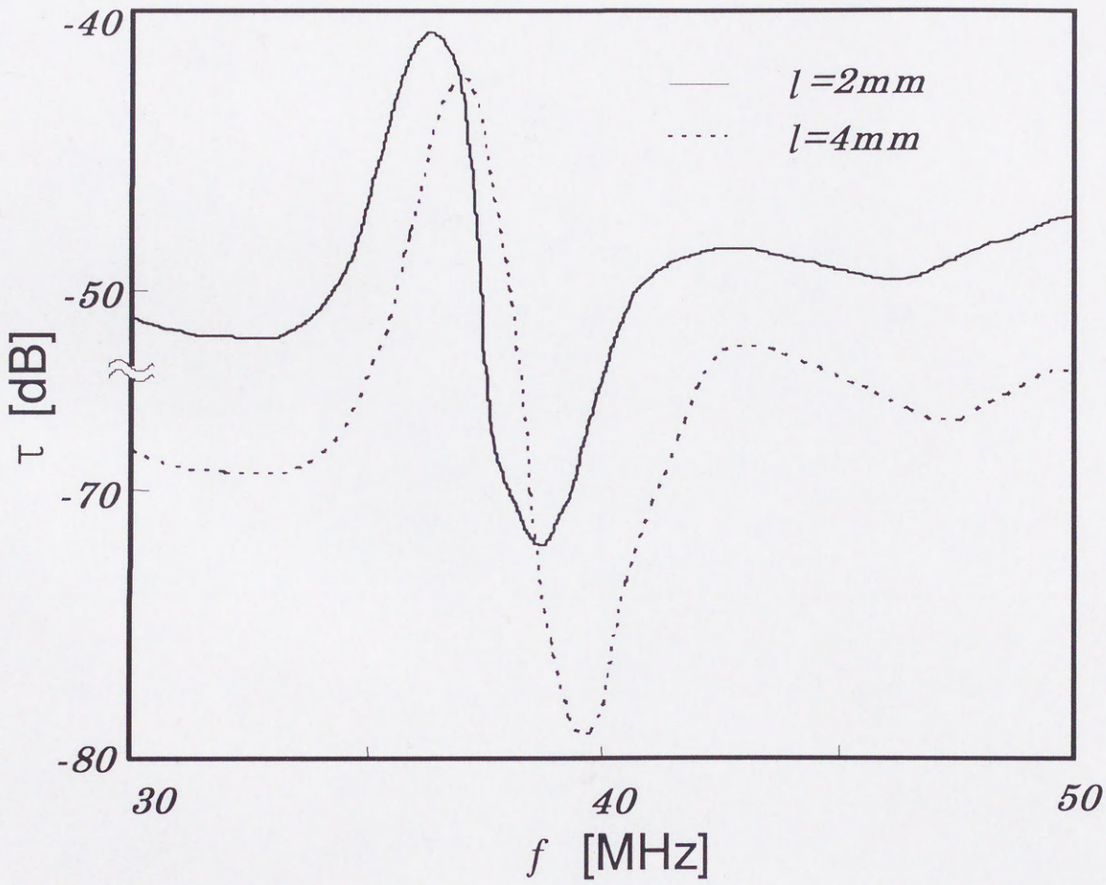

Fig. 2.11 The magnitude of transmission coefficient with different distance between sensors

thickness of sample that also can be used for detecting the defects based on the thickness difference in dielectric materials.

REFERENCES

1 Zoughi, R. and Bakhtiari, S., 'Microwave Nondestructive Detection and Evaluation of Disbonding and Delamination in Layered-Dielectric-Slabs', *IEEE Transactions on Instrumentation and Measurement*, Vol. 39, No. 6, 1990, pp. 1059-1063.

2 Gopalsami, N., Bakhtiari, S., Dieckman, S. L., Raptis, A. C. and Lepper, M. J., 'Millimeter-Wave Imaging for Nondestructive Evaluation of Materials', *Materials Evaluation*, Vol. 52, No. 3, 1994, pp. 412-415.

3 Gray, S., Ganchev, S., Qaddoumi, N., Beauregard, G., Radford, D. and Zoughi, R., 'Porosity Level Estimation in Polymer Composites Using Microwaves', *Materials Evaluation*, Vol. 53, No. 3, 1995, pp. 404-408.

4 Qaddoumi, N., Carriveau, G., Ganchev, S. and Zoughi, R., 'Microwave Imaging of Thick Composite with Defects', *Materials Evaluation*, Vol. 53, No. 8, 1995, pp. 926-929.

5 Ambrosio, G.d', Migliore, M.D., Ciliberto, A. and Sabatino, C., 'Microwave Defect Detection on Low-Loss Composites', *Materials Evaluation*, Vol. 51, No. 2, 1993, pp. 285-289.

6 Scott, W.R.Jr., 'A New Technique for Measuring the Constitutive Parameters of Planar Materials', *IEEE Transactions on Instrumentation and Measurement*, Vol. 41, No. 5, 1992, pp. 639-645.

7 Belhadj-tahar, N.-E., Fourrier-lamer, A. and Chanterac, H., 'Broad-Band Simultaneous Measurement of Complex Permittvity and Permeability Using a Coaxial Discontinuity', *IEEE Transactions on Microwave Theory and Techniques*, Vol. 38, No. 1, 1990, pp. 1-7.

8 Stuchly, M. A. and Stuchly, S. S., 'Coaxial Line Reflection Methods for Measuring Dielectric Properties of Biological Substances at Radio and Microwave Frequency-A Review', *IEEE Transactions on Instrumentation and Measurement*, Vol. IM-29, No. 3, 1980, pp. 176-183.

9 Mosig, J. R., Besson, J. E., Gex-fabry, M. and Gardiol, F. E., 'Reflection of an Open-Ended Coaxial Line and Application to Nondestructive Measurement of Materials', *IEEE Transactions on Instrumentation and Measurement*, Vol. IM-30, No. 1, 1981, pp. 46-51.

10 Grant, J. P., Clarke, R. N., Symm, G. T. and Spyrou, N. M., 'A Critical Study of the Open-Ended Coaxial Line Sensor Technique for RF and Microwave Complex Permittivity Measurements', *Journal of Physics E: Scientific Instruments*, Vol. 22, No. 9, 1989, pp. 757-770.

11 Ju, Y., Saka, M. and Abé, H., 'A Method for Nondestructive Testing of Defects in Dielectric Material Utilizing Coaxial Line Sensor Technique', *Proc. International Conference on Materials and Mechanics '97*, JSME, Tokyo, 1997, pp. 401-404.

3

EVALUATION OF DELAMINATION BASED ON MAGNITUDE MEASUREMENT

3.1 INTRODUCTION

Based on the study described in Chapter 2, the methods of microwave nondestructive evaluation of delamination in IC package are discussed in details.

Package cracking problems have been studied by many researchers[1-5], and most of the mechanical analyses of packages have been carried out concerning stress. These studies provide a lot of insight into the analysis of cracking and condition prediction, but an effective experimental tool to inspect the delamination in IC packages is still lack.

Scanning acoustic tomography (SAT) technique can be used to observe such delamination, but the requirement of a coupling medium such as water makes it very difficult to realize on-line testing, and the observation of the full mechanism of delamination under some simulated conditions is also impossible. In this study, a new technique of microwave nondestructive testing (NDT) is developed to inspect the delamination in IC packages.

Microwave technique has been successfully used for NDT by some researchers[6-9]. The sensor might not essentially be in contact with the sample under testing, which makes it possible to realize on–line testing conveniently. A special advantage of microwave NDT over other techniques is that the inspection result is not based on density but dielectric property, by which much additional information of the detected objects may be obtained. Thereby the moisture and temperature properties of IC

package may also be estimated. In addition, in the microwave frequency region, dielectric permittivity variation for dielectric materials is significantly larger than the contrast range of density; that is why microwave inspection is more sensitive than the other techniques for dielectric material testing.

In this Chapter, a kind of novel open-ended coaxial line sensor improved from the sensor that has been used in Chapter 2 is employed to detect the delamination in IC package. In case of detecting delamination in IC package, the incident wave will be reflected completely at the surface of the chip pad (conducting sheet), thus the reflection measurement is introduced in the study. Although the transmission technique has been confirmed to be a powerful tool to detect small defects in dielectric materials. An open-ended coaxial line technique has been used to measure the constitutive parameters of dielectric materials previously, see Mosig et al.[10] and Grant et al.[11]. Since the techniques were not used for detecting defects in those studies, the resolution was not needed to be considered and the size of sensors was relatively large. In addition, the measured material was set in contact with the sensor and its dimensions must be sufficiently large to make the field decayed to a negligible amplitude on the far sides. In other words, only the discontinuity of coaxial line was used; the reflection from the inside of measured material was assumed to be zero. Differing from these studies, here the near-field reflection from the inside of the detected objects carrying the information of defects is used to inspect the delamination. That is the reason why higher resolution in the transmitting direction can be obtained.

The purpose of this study is to develop a new microwave NDT method for increasing the resolution, by which some new applications of the detection of small defects are expected to be carried out, consequently, the reliability estimation of IC package is done by detecting its delamination nondestructively[12]. The foundation of this work covers the research of the detection of defects in dielectric materials as described in Chapter 2.

3.2 APPROACH

The principle of this technique is based on the interaction of electromagnetic wave with IC package. The coaxial line aperture acts as a source of microwave that transmits into the package; the same aperture also acts as the receiver of the signal reflected by the chip pad. In fact, due to the discontinuity of mediums, reflections will take place at all the interfaces between different mediums. The total reflection emerging at the coaxial line aperture will be the sum of the components reflected from different interfaces of mediums. Because the phases of reflected components are difference, an interference phenomenon will occur; the magnitude of the total reflection changes periodically according to the sum of the phases of those reflected components. The phase associated with the component reflected at the surface of chip pad varies with the thickness and also dielectric constant of the delamination layer. When it is, especially, opposite to the sum of the phases of other reflected components, the magnitude of the total reflection will have an abrupt decrease and show an extremely small value, around where a little change in thickness of delamination will generate a great change in the magnitude of the total reflection. In other words, the magnitude of effective reflection coefficient is highly sensitive to the change in the thickness of delamination. Once the dielectric constant of the delamination medium is known, the thickness of delamination will also be evaluated.

3.3 EXPERIMENTAL PROCEDURE

The configuration of the measurement system is shown in Fig. 3.1. A network analyzer (HP8510) is used to generate a continuous wave signal fed to the coaxial line sensor and measure the magnitude of effective reflection coefficient at the coaxial line aperture. A computer is employed to process the data output from the network analyzer and control the stage translation in the x- and y-directions. The open-ended coaxial line sensor transmits and receives the test signal that interacts with samples. As shown in Fig. 3.2, the sensor having an inner and outer radii, $a = 0.46$ and $b = 1.50$ mm, respectively, is terminated into a flat metallic flange with radius $c = 14.50$ mm. The flange of the sensor was made about ten times large than the aperture of the sensor, so the fringe field

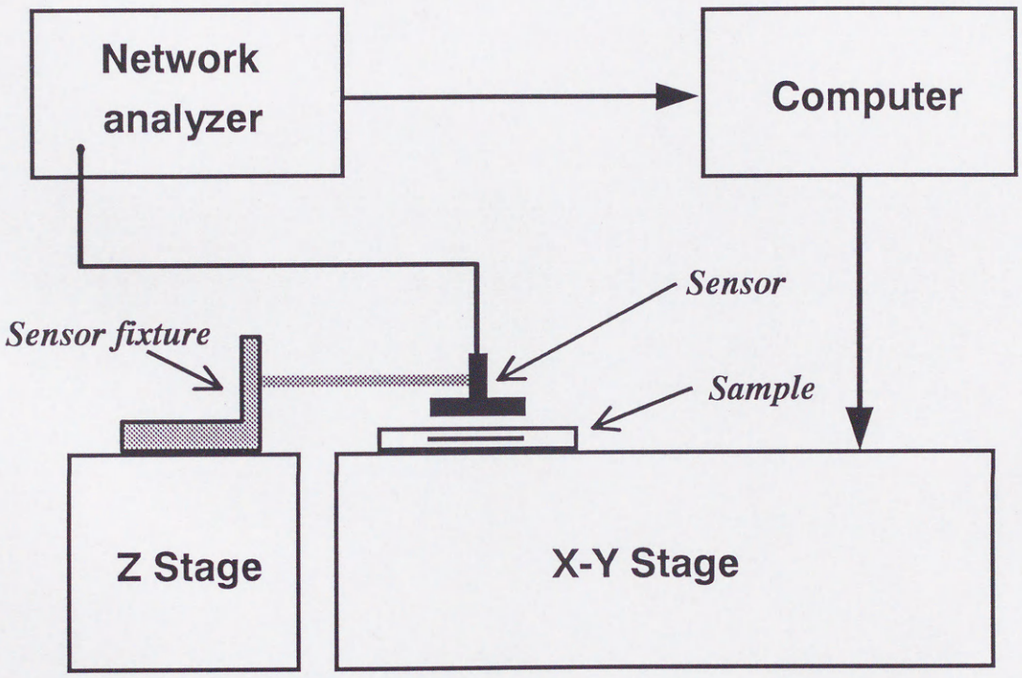

Fig. 3.1 Configuration of the measurement system

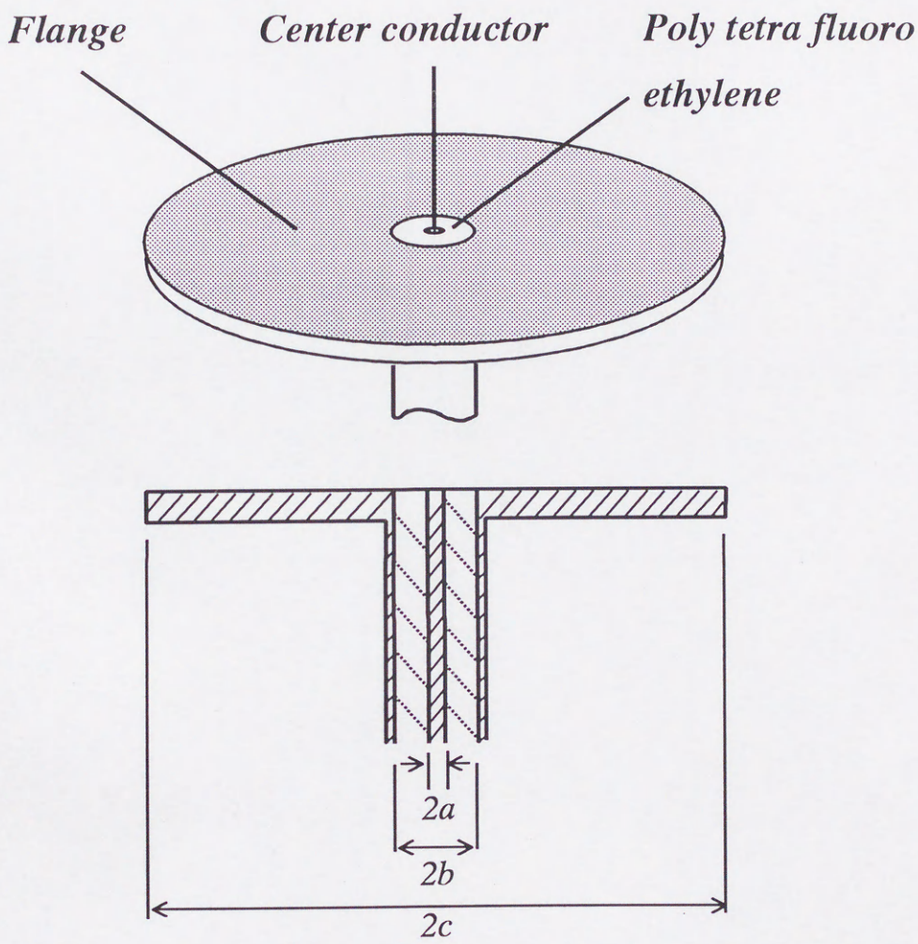

Fig. 3.2 Configuration of the open-ended coaxial line sensor

under the flange can be neglected. Figure 3.3 shows an actual open-ended coaxial line sensor used in the experiment.

To conduct the experimental study, four IC packages were used as samples. Two of them (S114-2, S114-3) are free from delamination, and the others (S113-2, S113-3) contain artificially introduced delamination that has been confirmed by the SAT testing. The thickness of the delaminations introduced here is around 20 μm. In most of the cases, the lateral area of the delaminations encountered in practice is same as the area of the chip pad (fully delaminated) and the associated thickness of the same is normally in the range of 10 to 50 μ m. The dimensions of the sample are shown in Fig. 3.4. The package resin is assumed to be homogeneous, isotropic, and nonmagnetic. An actual package used in the experiment is shown in Fig. 3.5.

Because the effective reflection coefficient is not only relative to the properties of the samples, but also dependent on the operation frequency and the standoff distance (distance between the sensor and the sample), it is very important to select the operation frequency and standoff distance for optimizing the experiment. First, frequency is swept with a fixed standoff distance. The frequency, on which the difference of the magnitudes measured between the two category packages with and without delamination takes the biggest value, is selected as the operation frequency. After determining the operation frequency, the influence of the standoff distance to the magnitude of effective reflection coefficient is investigated. The standoff distance that is sensitive to the magnitude difference between the two category packages is fixed for later measurement. Finally, the magnitude of effective reflection coefficient is measured by scanning the samples in the x- and y-directions with the selected operation frequency and standoff distance.

3.4 RESULTS AND DISCUSSION

Figure 3.6 illustrates the relationship between measured magnitude of effective reflection coefficient, $|\tau|$, versus swept frequency, f, for Samples S113-3 and S114-3 at $x = y = 0$, where the frequency range is 48.40 to 48.60 GHz and the standoff distance d is 0.25 mm. It is clear that, on the frequency of 48.50 GHz, the magnitudes show the

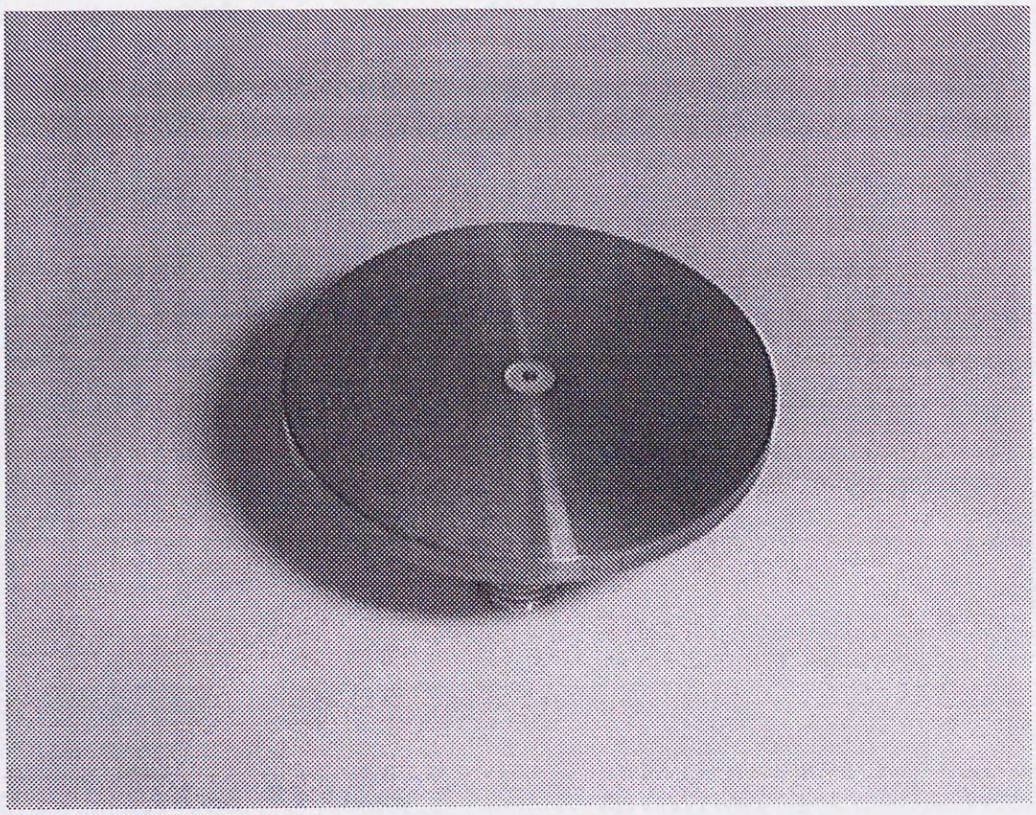

Fig. 3.3 An open-ended coaxial line sensor used in the experiment

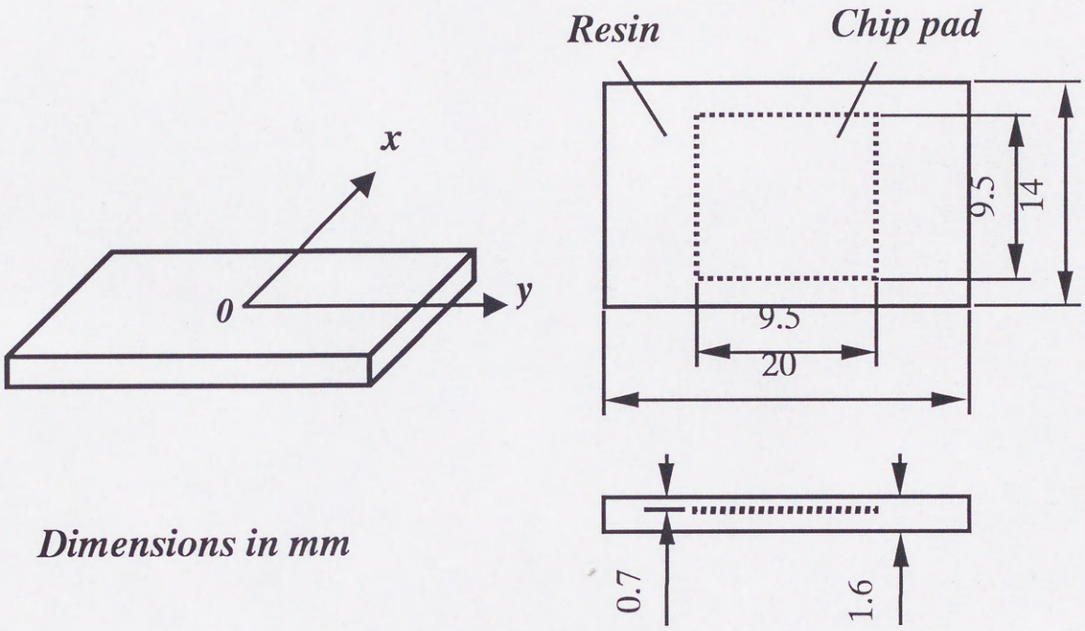

Fig. 3.4 Descriptive geometry of sample

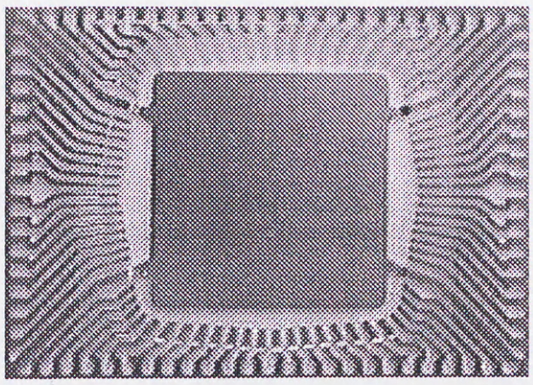

(a) Lead frame

(b) Package

Fig. 3.5 A package used in the experiment

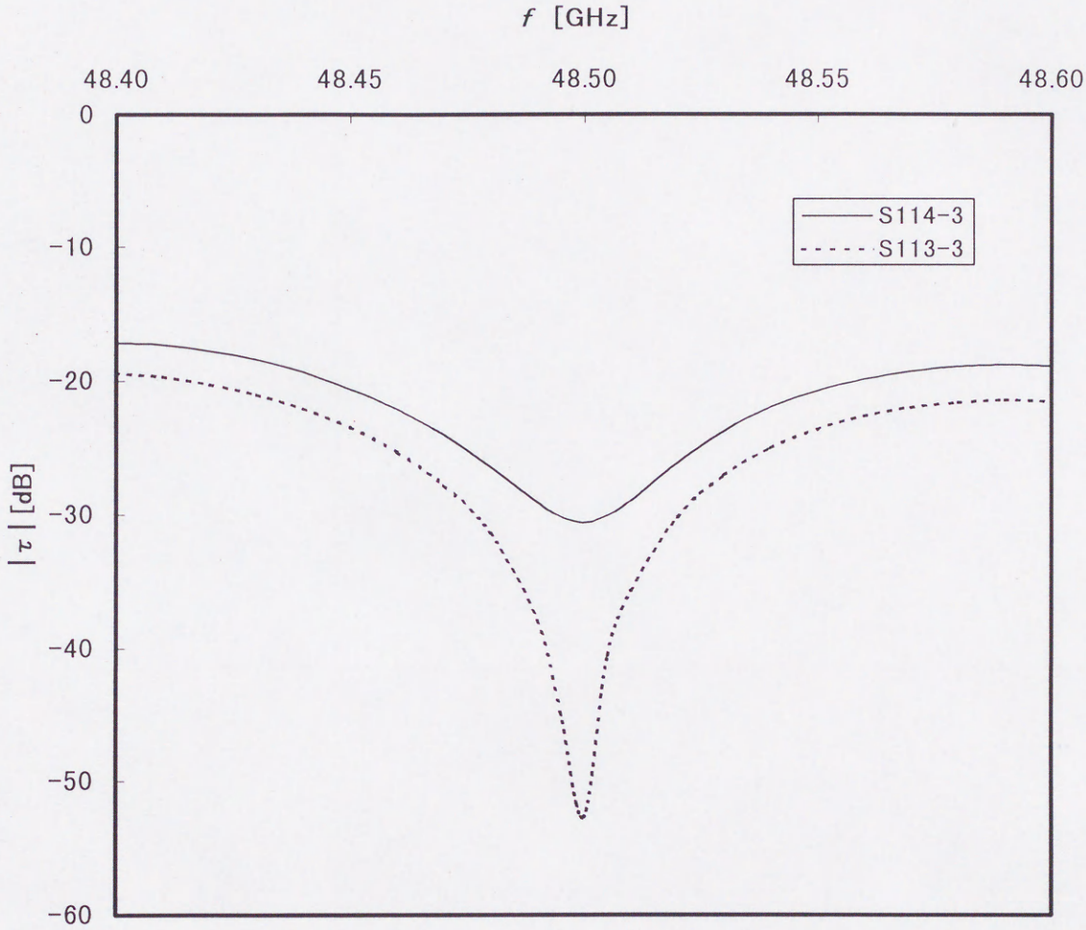

Fig. 3.6 Magnitude of effective reflection coefficient versus swept frequency for Samples S113-3 with and S114-3 without delamination measured by the standoff distance of 0.25 mm

largest difference between S113-3 with and S114-3 without delamination since a coherent resonance of magnitude takes place for S113-3 on this frequency.

The magnitudes of effective reflection coefficient versus standoff distance were measured on the frequency of 48.50 GHz, for S113-3 and S114-3 at $x = y = 0$, as shown in Fig. 3.7. It indicates that, for some special standoff distances, the magnitudes of effective reflection coefficient have a great decrease due to the coherent resonance of magnitude. As the resonance phenomenon takes place at different standoff distances for S113-3 and S114-3, the standoff distance of 0.24 mm corresponding to the largest magnitude difference was adopted to increase the measurement sensitivity.

The measurements were carried out for all the samples under the conditions of $f = 48.50$ GHz and $d = 0.24$ mm, and the scanning was performed in the x- and y-directions with a pitch of 0.5 mm. The measured results along the x- and y-axes are shown in Figs. 3.8 and 3.9, respectively. The difference between the two category packages with and without delamination can be observed clearly. The curves of the magnitude of effective reflection coefficient versus measurement position are smooth and show smaller decrease for packages without delamination, but fluctuating and larger decrease for packages containing delamination. The fluctuating phenomenon may be due to the roughness of the delaminated surface.

In case of on-line detection, when IC packages are passed through under the sensor in the x- or y-direction, a series of magnitudes of effective reflection coefficient can be measured and the average values corresponding to the region of chip pad are calculated for each package. By comparing with the reference value, packages containing delamination can easily be distinguished at once. If the scanning speed is high enough, microwave imaging may realize highly qualitative on-line evaluation of the delamination in IC packages.

It is worthy to note that the horizontal resolution of the coaxial line sensor used in this experiment is about 3 mm (the diameter of its aperture) that is a bit higher than the case of waveguide, 4.33 mm (the wide side of the waveguide aperture, $w \approx 0.7v / f$, where v is light speed and $f = 48.50\,GHz$). In contrast with the waveguide technique, the resolution of coaxial line sensor is independent of the cutoff frequency; therefore it can be further enhanced as the requirement.

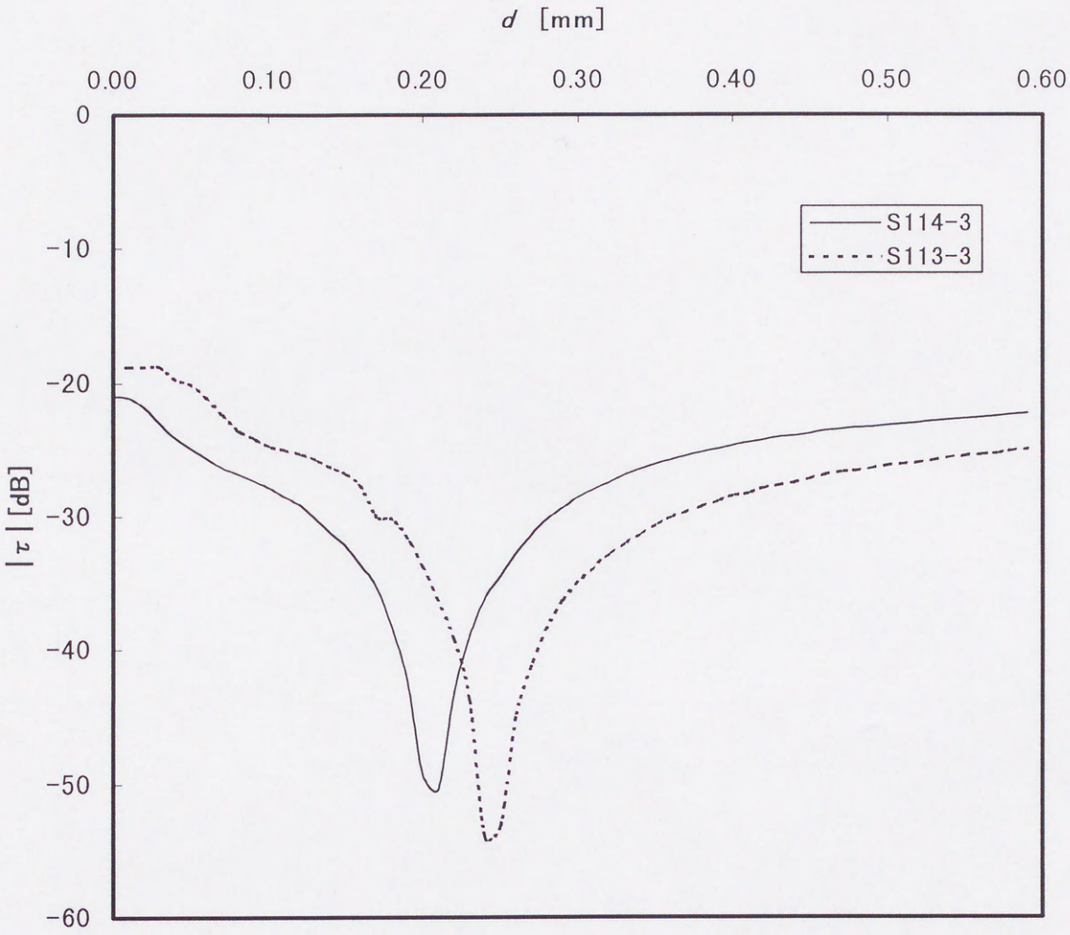

Fig. 3.7 Magnitude of effective reflection coefficient versus standoff distance for Samples S113-3 with and S114-3 without delamination measured on the frequency of 48.50 GHz

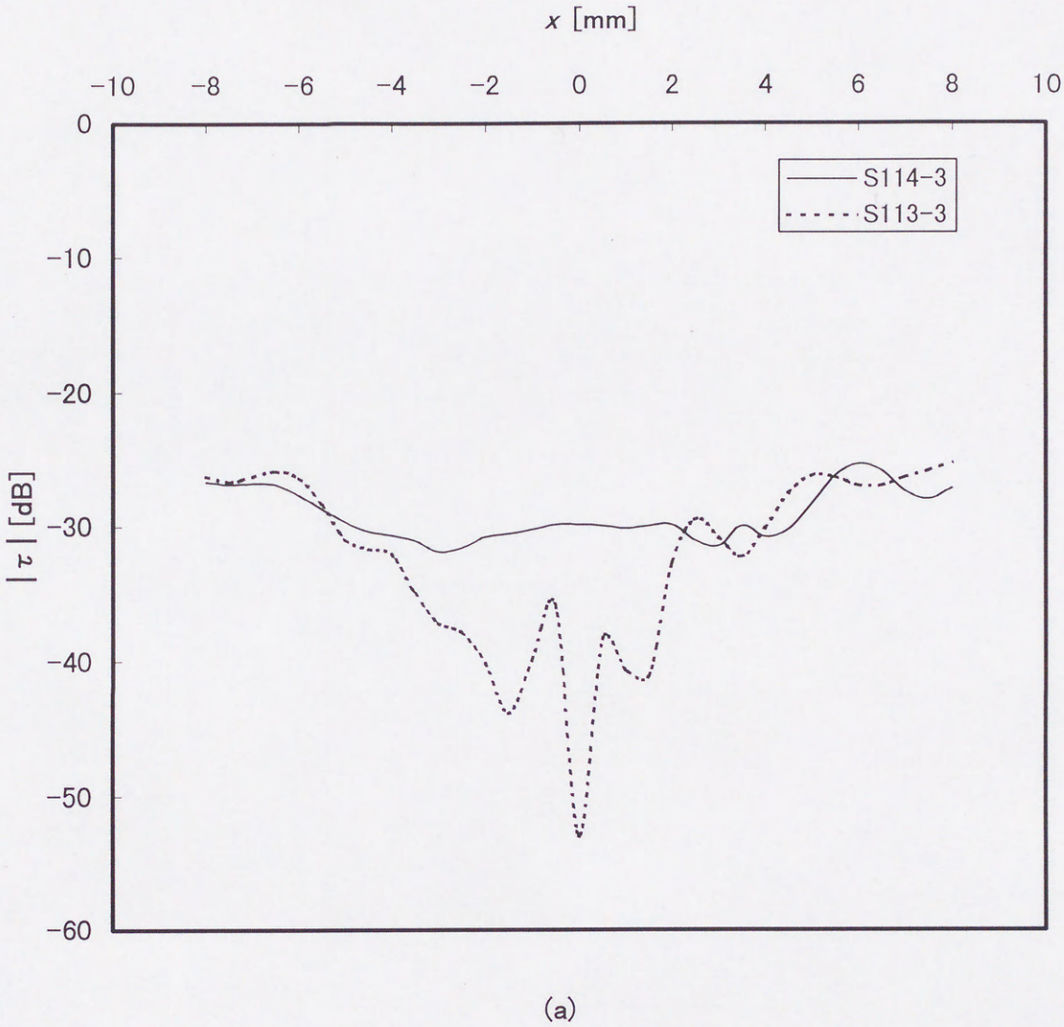

Fig. 3.8 Measured magnitude of effective reflection coefficient versus measurement position in the x-direction, frequecy 48.50 GHz, and standoff distance 0.24 mm: (a) comparison between S113-3 with and S114-3 without delamination

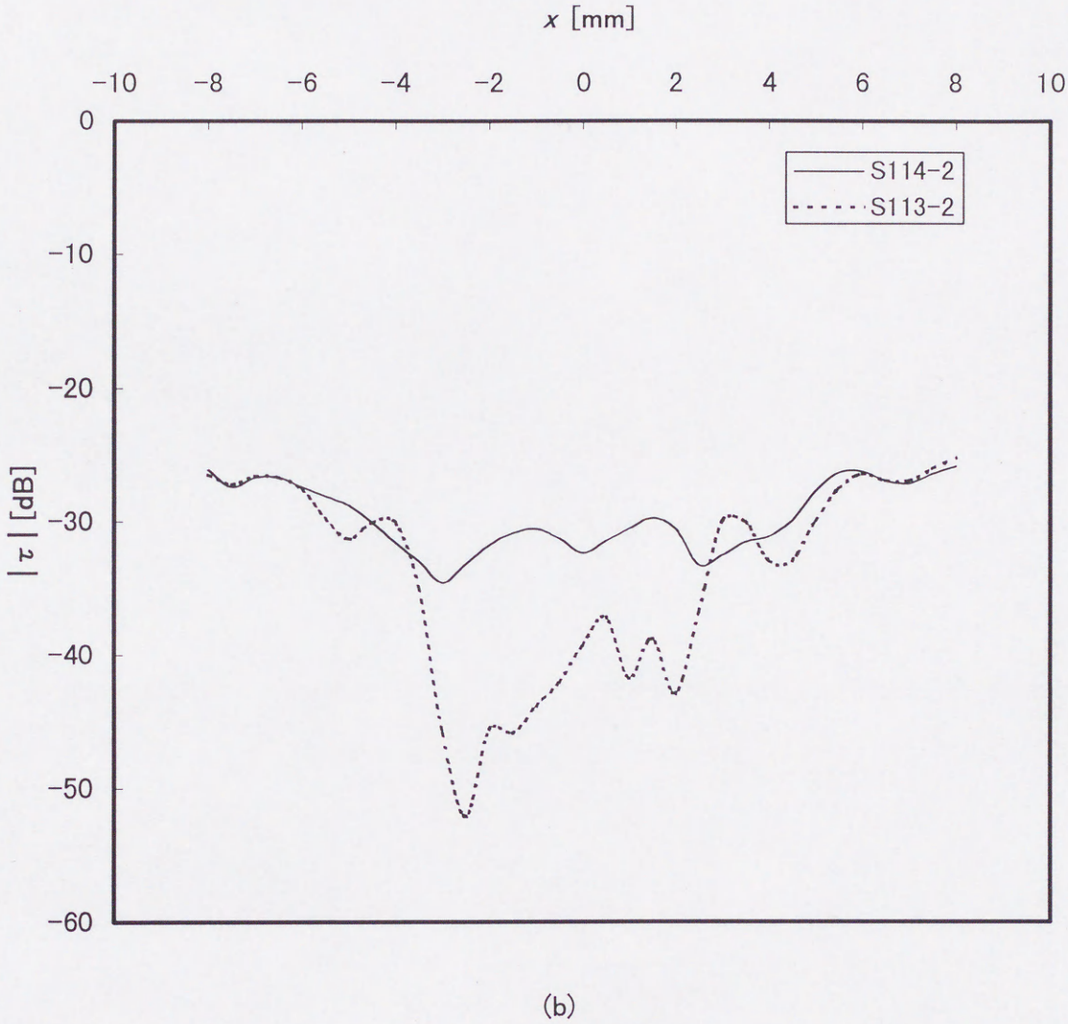

Fig. 3.8 Measured magnitude of effective reflection coefficient versus measurement position in the x-direction, frequecy 48.50 GHz, and standoff distance 0.24 mm: (b) comparison between S113-2 with and S114-2 without delamination

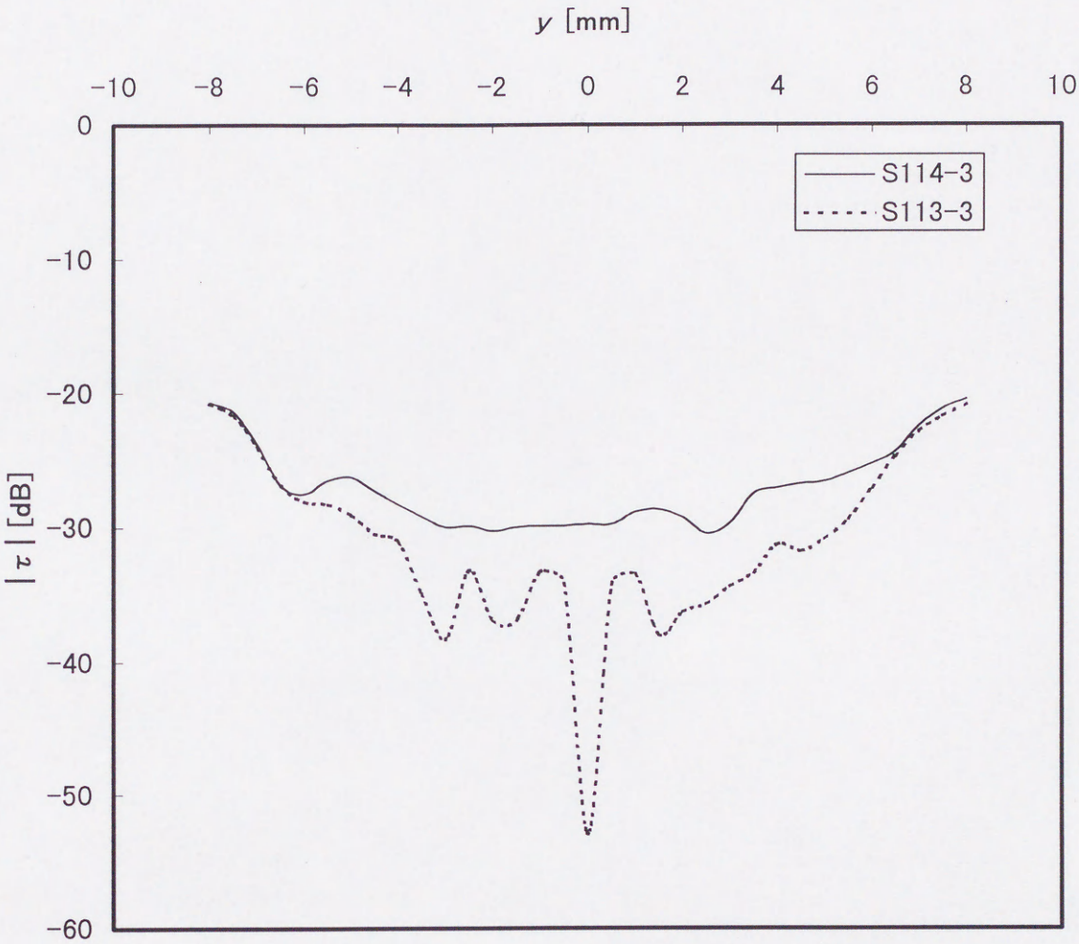

(a)

Fig. 3.9 Measured magnitude of effective reflection coefficient versus measurement position in the y-direction, frequency 48.50 GHz, and standoff distance 0.24 mm: (a) comparison between S113-3 with and S114-3 without delamination

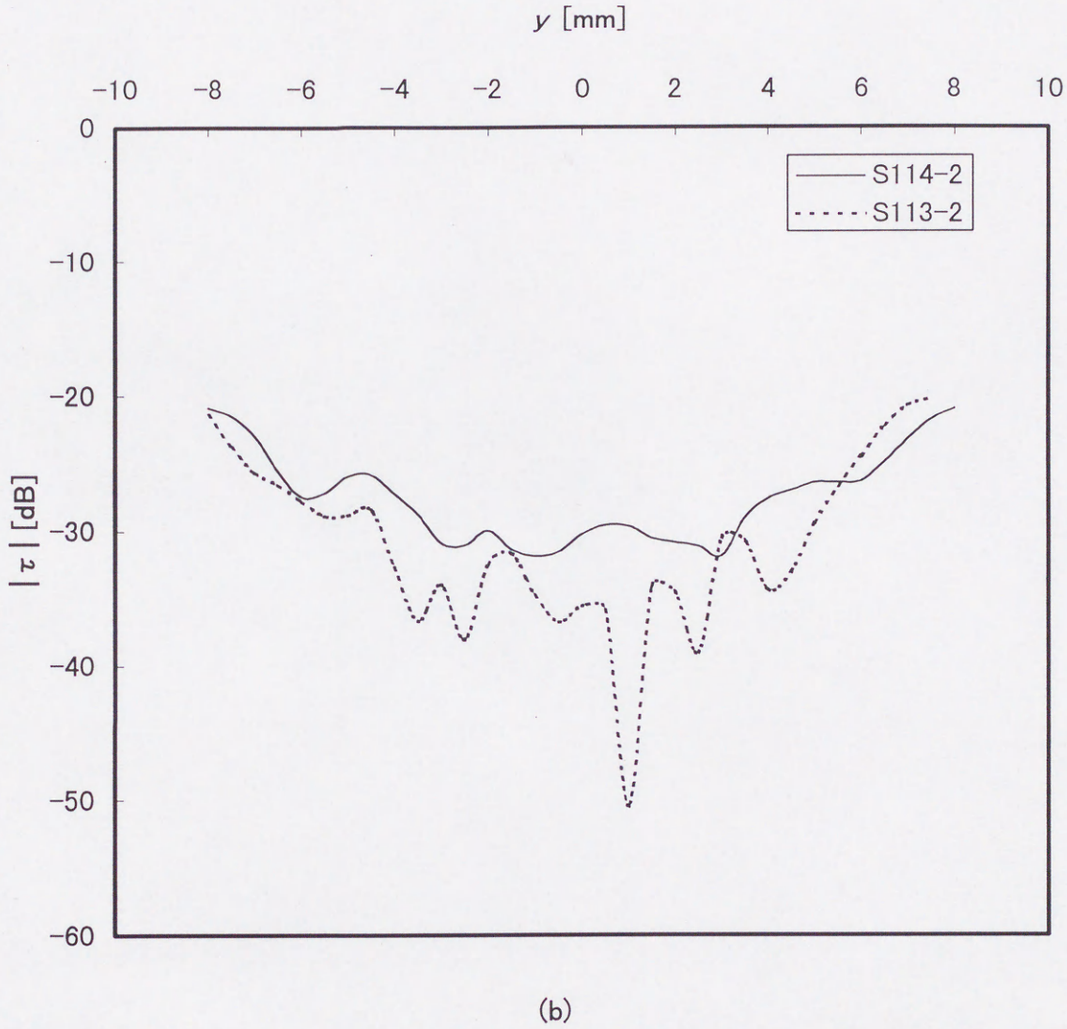

Fig. 3.9 Measured magnitude of effective reflection coefficient versus measurement position in the y-direction, frequency 48.50 GHz, and standoff distance 0.24 mm: (b) comparison between S113-2 with and S114-2 without delamination

3.5 CONCLUSIONS

The potential of improving the resolution of microwave nondestructive testing by the open-ended coaxial line sensor has been confirmed in the study. The delamination in IC package was detected successfully, and hence it was possible to estimate the reliability of package by evaluating its delamination. The magnitude of effective reflection coefficient and its coherent resonance are very sensitive to the delamination of IC package. Good resolution and high sensitivity of the open-ended coaxial line sensor make it possible to detect defects in small dimensions, thereby providing a potential use for nondestructive evaluation of dielectric materials.

REFERENCES

1 Kitano, M., Kawai, S., Nishimura, A. and Nishi, K., 'A Study of Package Cracking During the Reflow Soldering Process', *Transactions of the JSME (A)*, Vol. 55, No. 510, 1989, pp. 356-363 (in Japanese).

2 Omi, S., Fujita, K., Tsuda, T. and Maeda, T., 'Causes of Cracks in SMD and Type Specific Remedies', *IEEE Transactions on Components, Hybrids, and Manufacturing Technology*, Vol. 14, No. 4, 1991, pp. 818-823.

3 Kawamura, N., Kawakami, T., Matsumoto, K., Sawada, K. and Taguchi, H., 'Structural Integrity Evaluation for a Plastic Package During the Soldering Process', *Advances in Electronic Packaging, Vol. 1, Structural Analysis, Materials and Processes, Design, Reliability, ASME,* EEP-Vol. Vol. 4-1, 1993, pp. 91-95.

4 Tay, A. A. O., Tan, G. L. and Lim, T. B., 'Predicting Delamination in Plastic IC Packages and Determining Suitable Mold Compound Properties', *IEEE Transactions on Components, Packaging, and Manufacturing Technology-Part B: Advanced Packaging*, Vol. 17, No. 2, 1994, pp. 201-208.

5 Lee, H. and Earmme, Y. Y., 'A Fracture Mechanics Analysis of the Effects of Material Properties and Geometries of Components on Various Types of Package

Cracks', *IEEE Transactions on Components, Packaging, and Manufacturing Technology-Part A*, Vol. 19, No. 2, 1996, pp. 168-178.

6 Zoughi, R. and Bakhtiari, S., 'Microwave Nondestructive Detection and Evaluation of Disbonding and Delamination in Layered-Dielectric-Slabs', *IEEE Transactions on Instrumentation and Measurement*, Vol. 39, No. 6, 1990, pp. 1059-1063.

7 Gopalsami, N., Bakhtiari, S., Dieckman, S. L., Raptis, A. C. and Lepper, M. J., 'Millimeter-Wave Imaging for Nondestructive Evaluation of Materials', *Materials Evaluation*, Vol. 52, No. 3, 1994, pp. 412-415.

8 Gray, S., Ganchev, S., Qaddoumi, N., Beauregard, G., Radford, D. and Zoughi, R., 'Porosity Level Estimation in Polymer Composites Using Microwaves', *Materials Evaluation*, Vol. 53, No. 3, 1995, pp. 404-408.

9 Qaddoumi, N., Carriveau, G., Ganchev, S. and Zoughi, R., 'Microwave Imaging of Thick Composite with Defects', *Materials Evaluation*, Vol. 53, No. 5, 1995, pp. 926-929.

10 Mosig, J. R., Besson, J. E., Gex-fabry, M. and Gardiol, F. E., 'Reflection of an Open-Ended Coaxial Line and Application to Nondestructive Measurement of Materials', *IEEE Transactions on Instrumentation and Measurement*, Vol. IM-30, No. 1, 1981, pp. 46-51.

11 Grant, J. P., Clarke, R. N., Symm, G. T. and Spyrou, N. M., 'A Critical Study of the Open-Ended Coaxial Line Sensor Technique for RF and Microwave Complex Permittivity Measurements', *Journal of Physics E: Scientific Instruments*, Vol. 22, No. 9, 1989, pp. 757-770.

12 Ju, Y., Saka, M. and Abé, H., 'Microwave Nondestructive Detection of Delamination in IC Packages Utilizing Open-Ended Coaxial Line Sensor', *NDT&E International,* 1999, in press.

4

EVALUATION OF DELAMINATION BASED ON PHASE MEASUREMENT

4.1 INTRODUCTION

Delamination in IC package has been detected by measuring the magnitude of effective reflection coefficient of the microwave at the aperture of the open-ended coaxial line sensor, as described in Chapter 3[1]. The magnitude measurement is so sensitive to the thickness of delamination layer that even the delamination with very thin thickness can be detected. However, since the measurement sensitivity is affected by the operation frequency and the standoff distance, the suitable selection of those for optimizing the experiment is required. It increases the complexity of the experiment. In addition, the measured magnitude difference in cases of with and without delamination is not linear with the thickness of delamination that makes the quantitative evaluation of the delamination difficult.

For detection and evaluation of the delamination automatically, phase measurement is introduced in the experiment since it is less affected by the scatter of microwave in comparison with the case of magnitude measurement. The frequency of the phase measurement can work on the relatively lower region. The experimental results show that the sensitivity of the measurement is almost independent of the operation frequency and linear with the standoff distance in their effective ranges. It means that the operation frequency and the standoff distance are not required to optimize in advance. Another merit of the phase measurement is that the measured phase difference in cases of with and without delamination changes almost linearly with the thickness of delamination,

thereby the delamination can be evaluated correctly without any special processing.

4.2 APPROACH

The principle of this technique is based on the interaction of electromagnetic wave with IC package. The coaxial line sensor acts as a source of the microwave that is transmitted into the package, and also acts as the receiver of the signal reflected from the package. Due to the discontinuity of medium, reflection will take place at all the interfaces of different mediums. The total reflection emerging at the coaxial line aperture will be the sum of the components reflected from different interfaces of mediums. The dominant reflection is the component reflected at the surface of the chip pad (perfect conductor), which carries the information of delamination. The phase of the effective reflection coefficient at the aperture of the open-ended coaxial line sensor, associated with the component reflected at the surface of the chip pad and varying with the thickness and also dielectric constant of the delamination layer, was measured as a characteristic signal to detect the delamination. The phase difference in cases of package with and without delamination was also calculated to evaluate the delamination and crack.

4.3 EXPERIMEMTAL PROCEDURE

The configuration of the measurement system is shown in Fig. 3.1. A network analyzer (HP8510) was used to generate a continuous wave signal fed to the coaxial line sensor and measure the phase of effective reflection coefficient at the aperture of the coaxial line sensor. A computer was employed to record the data output from the network analyzer and synchronize the stage translation in the x- and y-directions. The open-ended coaxial line sensor transmitted the test signal into the package and also received it reflected from the package. As shown in Figs. 3.2 and 3.3, the same sensor that has been described in Chapter 3 was used for the phase measurement.

To evaluate the influence of the epoxy resin on the delamination, package samples were formed by four kinds of epoxy resin with different silica powder. Table 4.1 shows

Table 4.1 Samples formed by different epoxy resins

Sample Series	Quantity of Filled Silica Powder wt%	Maximum Silica Diameter μm
1	70	74
2	80.75	74
3	70	120
4	80.75	120

the difference of the silica powder in size and quantity, respectively. All of them were hardened for 2 hours in 175 ℃ and exposed to the post cure for 8 hours in 175 ℃. Each kind of packages (series 1 to 4) contained four samples, and those were separated into two categories as shown in Table 4.2. Two of them (S1 and S2), were treated for introducing delamination by moisture absorption for 168 hours in 85 ℃ and 85% RH, and then treated by infrared reflow for 10 seconds in 240 ℃. The others (S3 and S4) are free from delamination. The dimensions of the used sample are the same as shown in Fig. 3.4; the size of chip pad is 9.5×9.5 mm and the thickness of the resin above the chip pad is 0.7 mm. The package resin is assumed to be homogeneous, isotropic, and nonmagnetic.

The phase of effective reflection coefficient is a function of the operation frequency, the dielectric constant of medium, and the distance from the sensor aperture to the interface of mediums. In the experiment, the operation frequency was 20 GHz that is significantly lower than the case of magnitude measurement. Higher frequency can increase the spatial resolution, however the cost will also be increased. Therefore, as low as possible frequency was used to detect delamination in this study. The standoff distance from the sensor aperture to the sample surface was fixed to be 0.2 mm. Thus, the measured phase was just as a function of the thickness and dielectric constant of the delamination layer. The operation frequency and standoff distance do not have significant influence on the measurement sensitivity, while the spatial resolution can be improved by increasing the operation frequency or decreasing the standoff distance. The experiment was performed by scanning the sample along the y direction with a 0.5 mm pitch at the center of package. The phase of effective reflection coefficient versus the scanning position was measured for each sample. In order to show the delamination clearly, for each series of samples, a sample (S4) which is free from delamination was used as a reference; the phase difference, $\phi_4 - \phi_i$, between the reference sample (ϕ_4) and other samples (ϕ_i; i=1,2,3) was measured corresponding to the scanning position.

4.4 RESULTS AND DISCUSSION

The relationship between measured phase of effective reflection coefficient and

Table 4.2 Two category samples with and without delamination

Sample Number	Moisture Absorption and Infrared Reflow
S1, S2	Processed
S3, S4	Unprocessed

measurement position for series 1 samples is shown in Fig. 4.1 (a) and (b), respectively. In Fig. 4.1 (a), the measured phase for Sample S1 with delamination is significantly smaller than that for Sample S3 without delamination. The shape of the measured curves indicates total influence of wave beam, lead frame, crack and the edge of the package. The central part between y=-4.5 and +4.5 mm, which is corresponding to the chip pad, expresses the information of delamination; the different phase values in that part for Samples S1 and S3 indicate the existence of delamination. The curved shape is due to a lack of the spatial resolution. The almost same shape of the measured curves for S2 with and S4 without delamination shown in Fig. 4.1 (b) illustrates a good reappearance property of this inspection technique. Same measurements were also carried out for series 2 samples as shown in Fig. 4.2 (a) and (b), respectively. The measured phase difference between the samples with and without delamination was observed almost same as that of series 1 samples at the part corresponding to the chip pad, but it was observed significantly larger than the case of series 1 samples at the part outside the chip pad. It means cracks extended in large amount in the series 2 samples. The measured results for series 3 samples, shown in Fig. 4.3 (a) and (b), illustrate that delamination level will be increased when the diameter of the filled silica powder is larger than some value. Figure 4.4 (a) and (b) show the significantly large delamination contained in the series 4 samples due to over-quantity of the silica powder filled in the epoxy package.

For eliminating the influence of the lack of the spatial resolution and observing the measurement results clearly, the phase difference was calculated and shown in Fig. 4.5 (a) to (d), respectively, where the measurement position was limited same as the size of chip pad approximately. In Fig. 4.5 (a), the phase difference of Sample 1-S3 from the reference sample 1-S4, ($\phi_4 - \phi_3$), is approximately zero. It means Sample 1-S3 does not contain delamination and also indicates a good repeatability of the experiment. On the other hand, for Samples 1-S1 and 1-S2, the phase differences from 1-S4 ($\phi_4 - \phi_1$ and $\phi_4 - \phi_2$) illustrate the existence of delaminations and the shape of the curves reflects the distribution of delamination. It is worthy to note that the curve $\phi_4 - \phi_2$ in Fig. 4.5 (a) tends to zero nearby y=-5 mm. This observation shows that delamination tends to disappear at the edge of chip pad, thereby indicating no existence of extended crack there. At another edge of chip pad, the existence of delamination indicates an extended

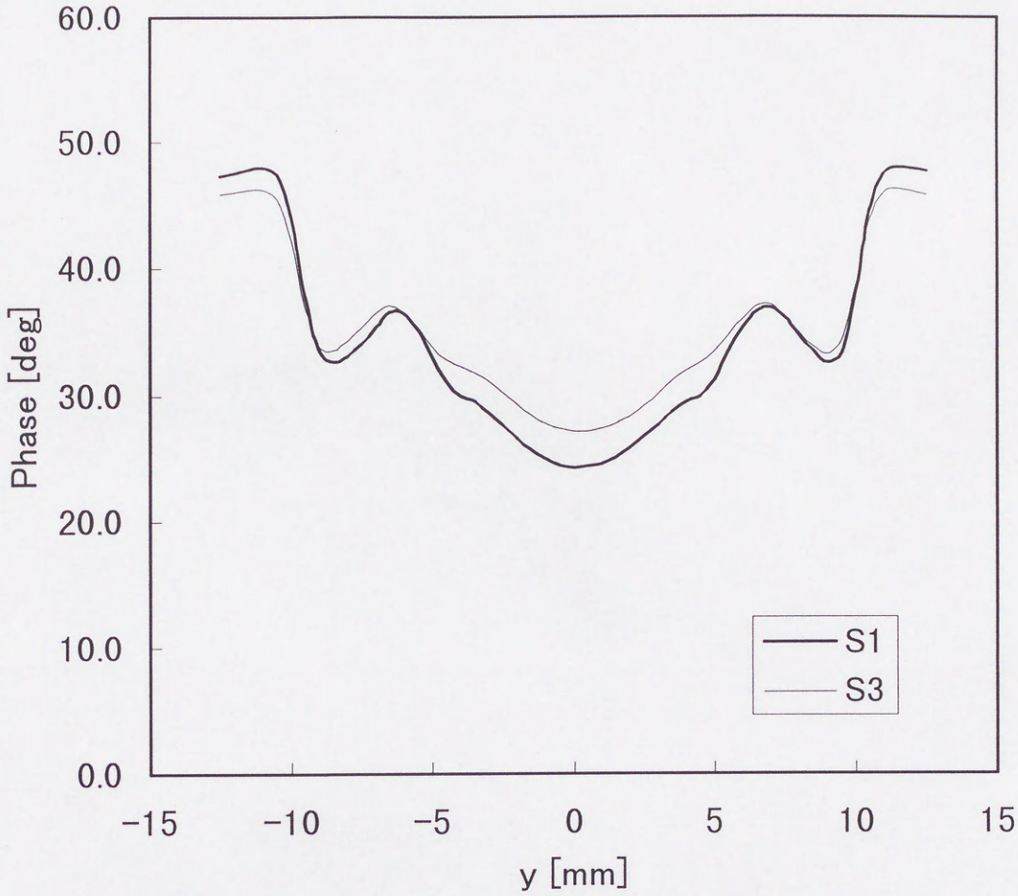

(a)

Fig. 4.1 Measured phase of effective reflection coefficient versus measurement position in the *y*-direction for series 1 samples: (a) comparison between S1 with and S3 without delamination

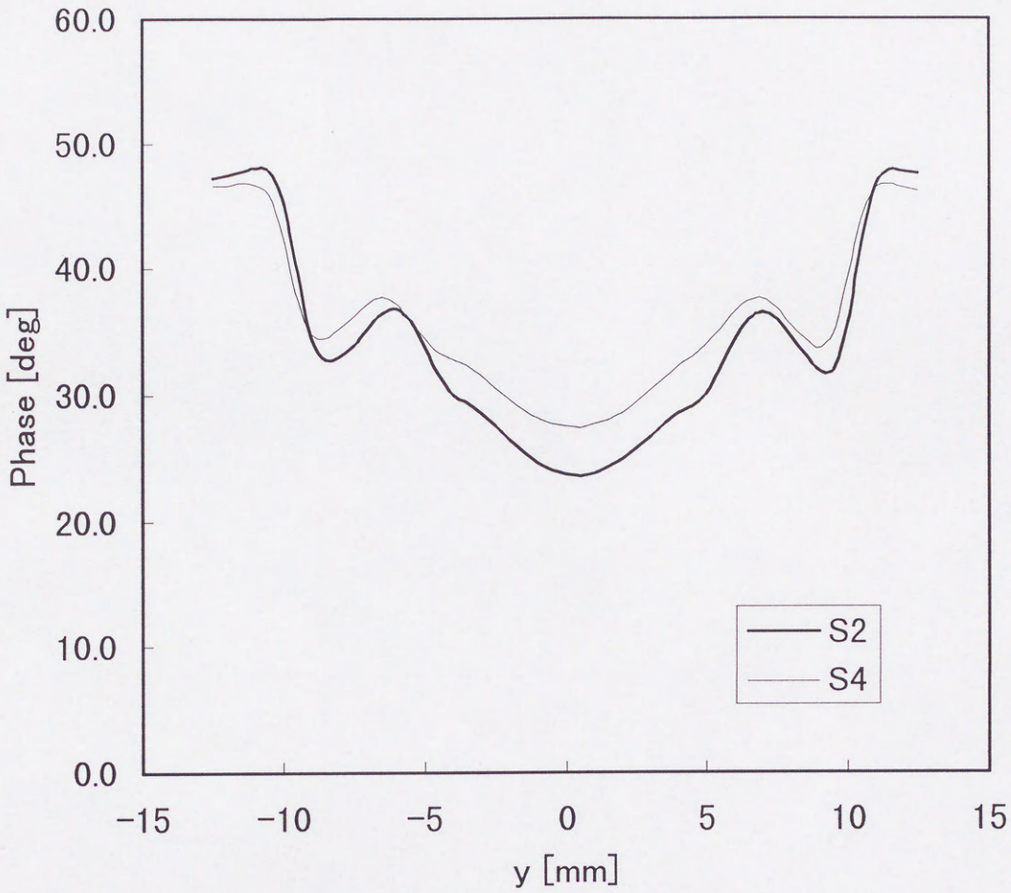

(b)

Fig. 4.1 Measured phase of effective reflection coefficient versus measurement position in the *y*-direction for series 1 samples: (b) comparison between S2 with and S4 without delamination

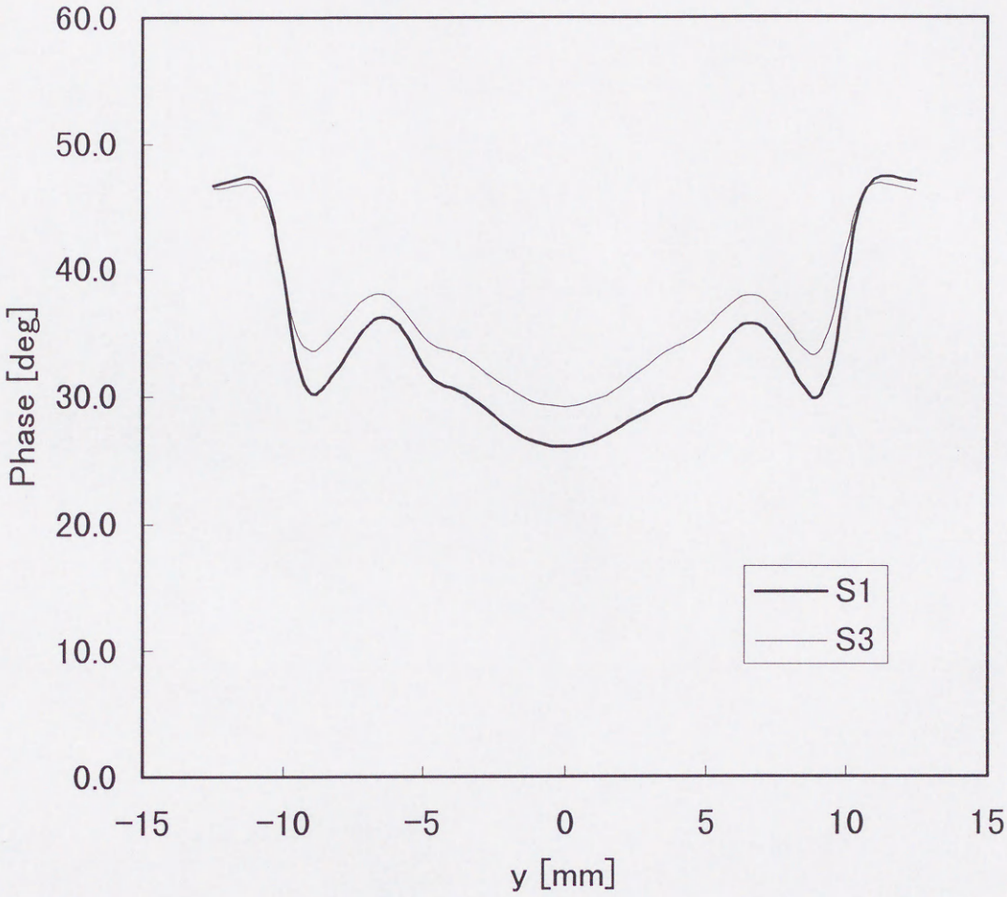

(a)

Fig. 4.2 Measured phase of effective reflection coefficient versus measurement position in the y-direction for series 2 samples: (a) comparison between S1 with and S3 without delamination

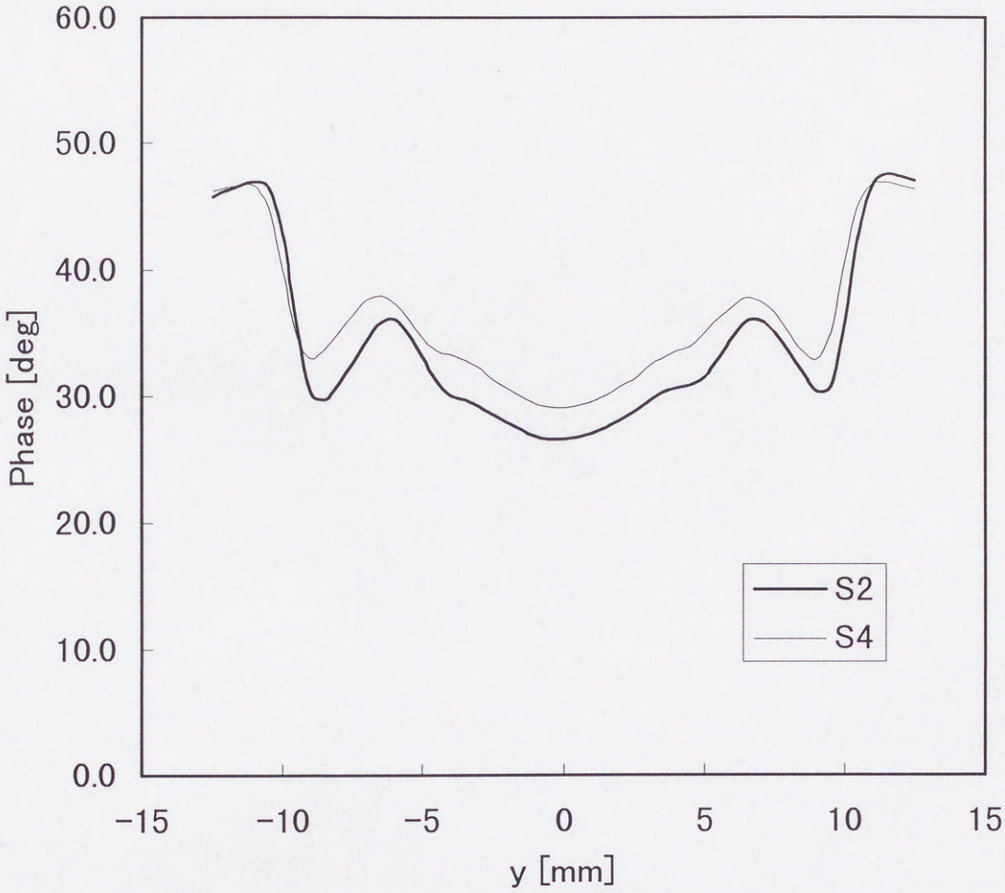

(b)

Fig. 4.2 Measured phase of effective reflection coefficient versus measurement position in the *y*-direction for series 2 samples: (b) comparison between S2 with and S4 without delamination

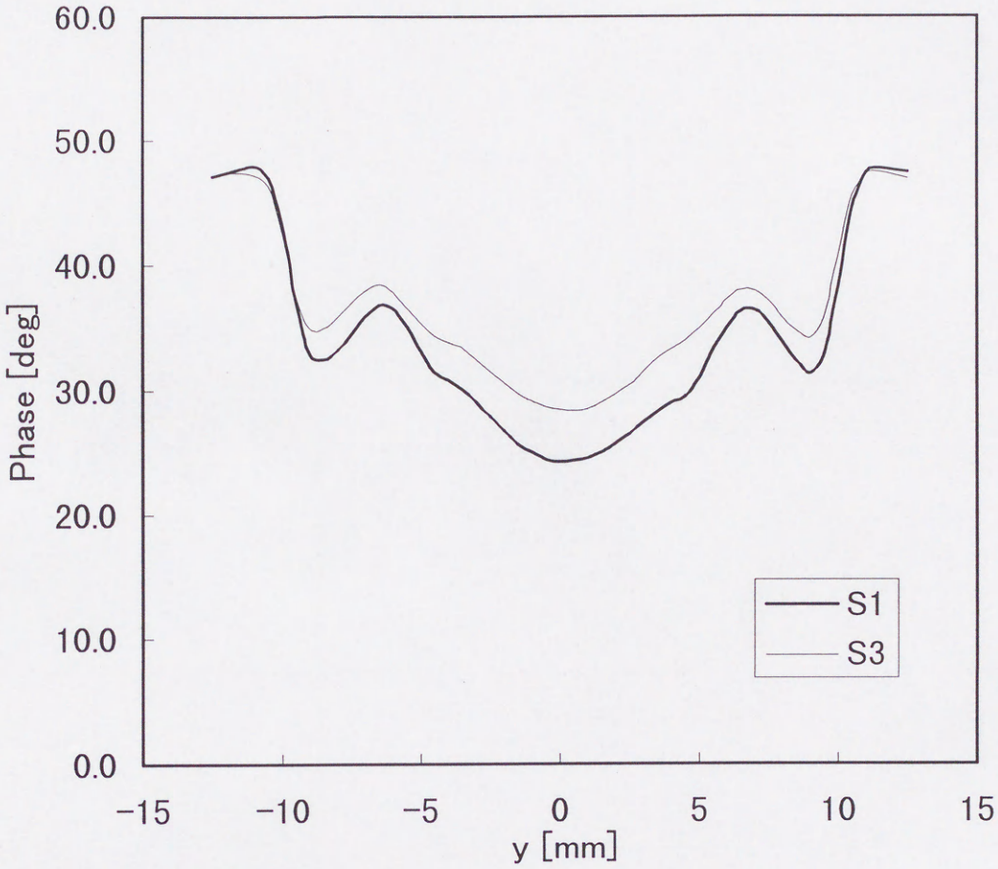

(a)

Fig. 4.3 Measured phase of effective reflection coefficient versus measurement position in the y-direction for series 3 samples: (a) comparison between S1 with and S3 without delamination

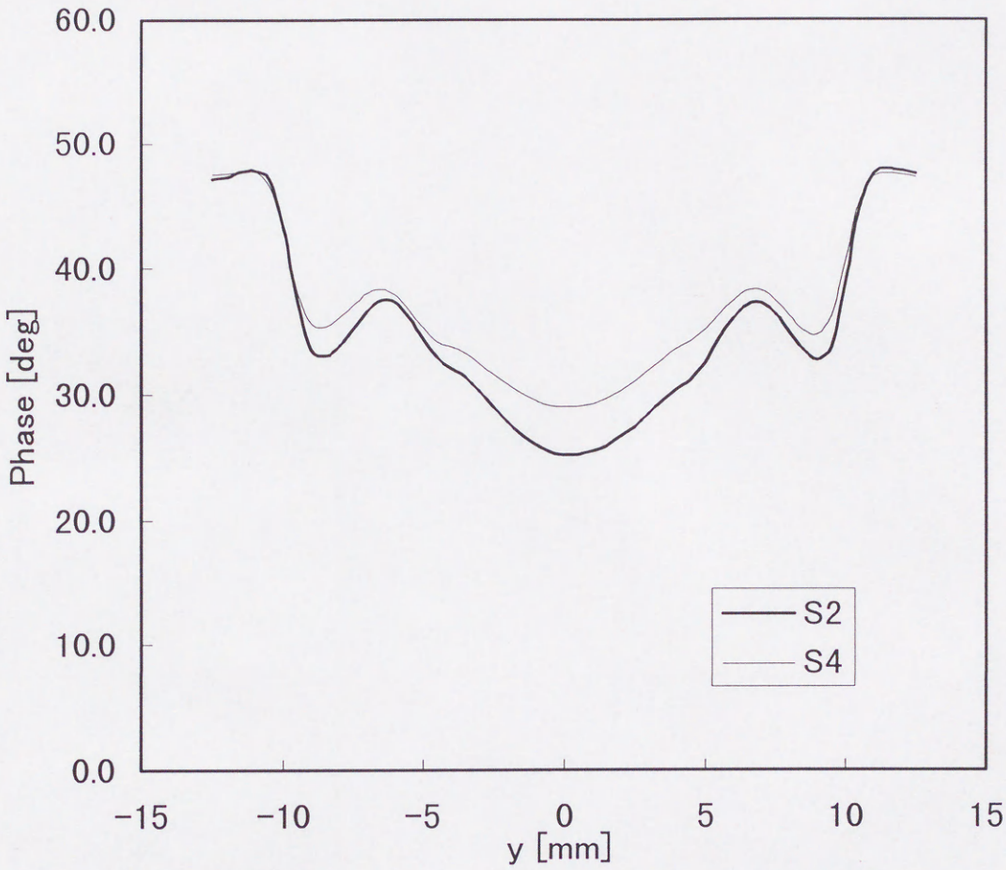

(b)

Fig. 4.3 Measured phase of effective reflection coefficient versus measurement position in the *y*-direction for series 3 samples: (b) comparison between S2 with and S4 without delamination

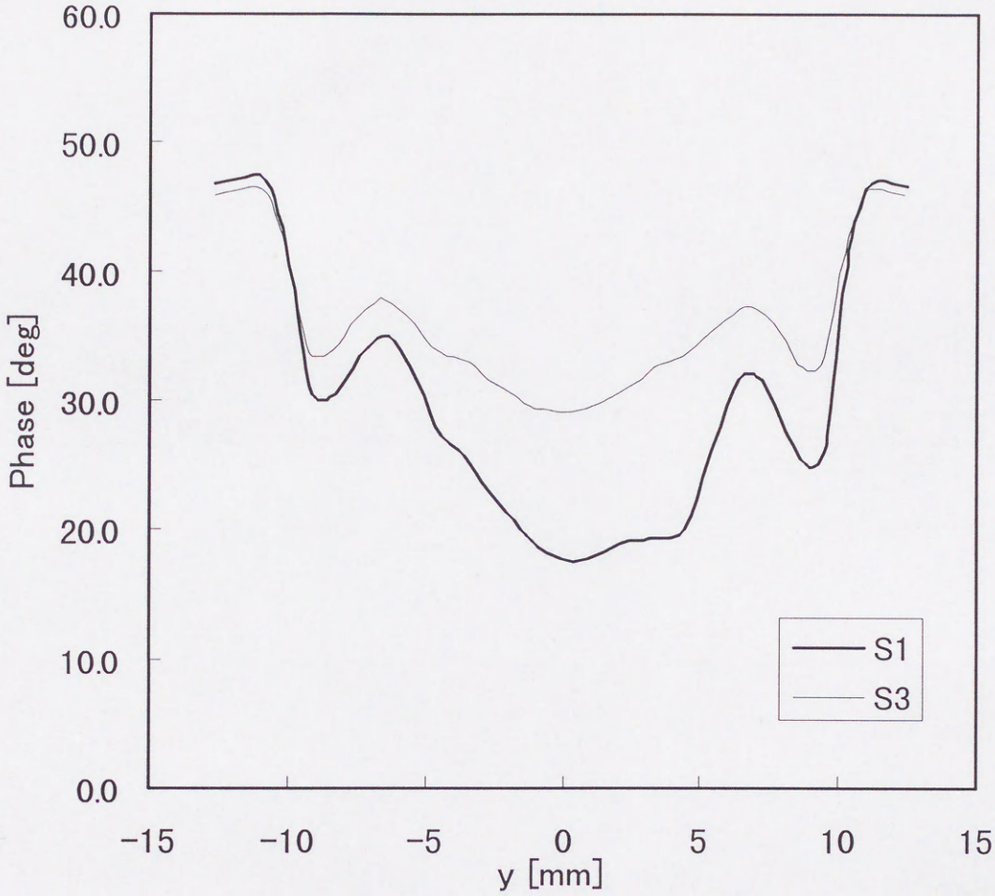

(a)

Fig. 4.4 Measured phase of effective reflection coefficient versus measurement position in the y-direction for series 4 samples: (a) comparison between S1 with and S3 without delamination

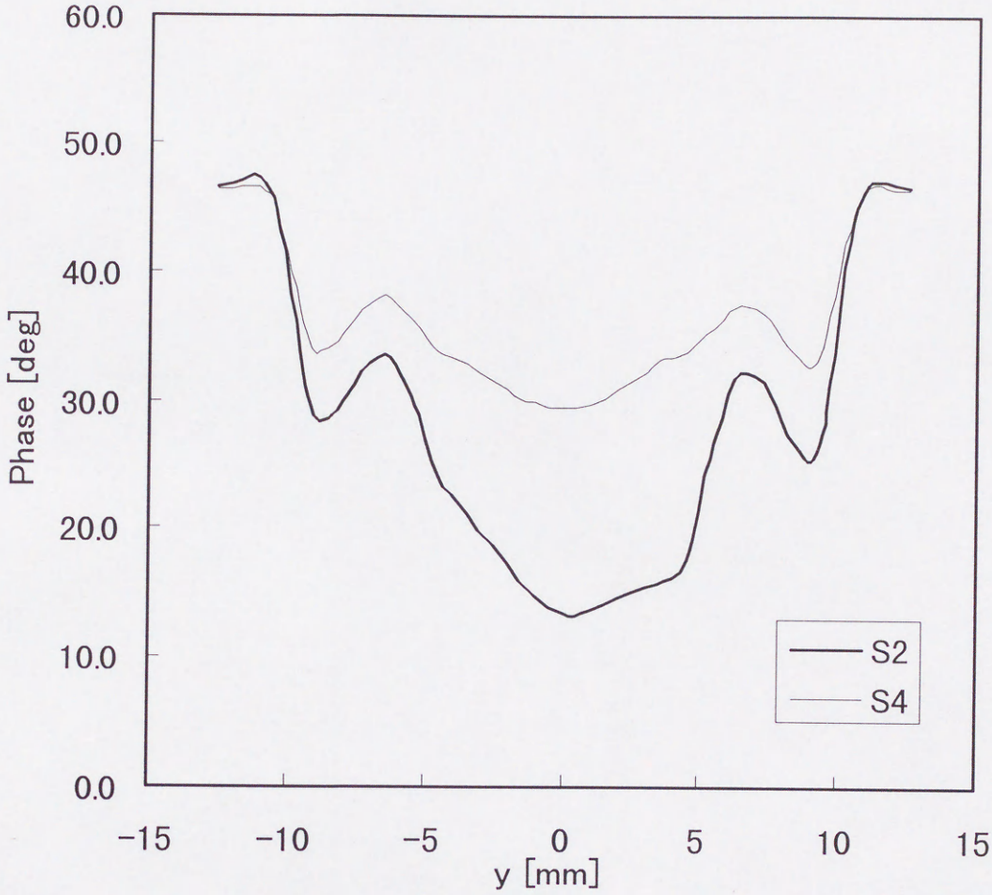

(b)

Fig. 4.4 Measured phase of effective reflection coefficient versus measurement position in the y-direction for series 4 samples: (b) comparison between S2 with and S4 without delamination

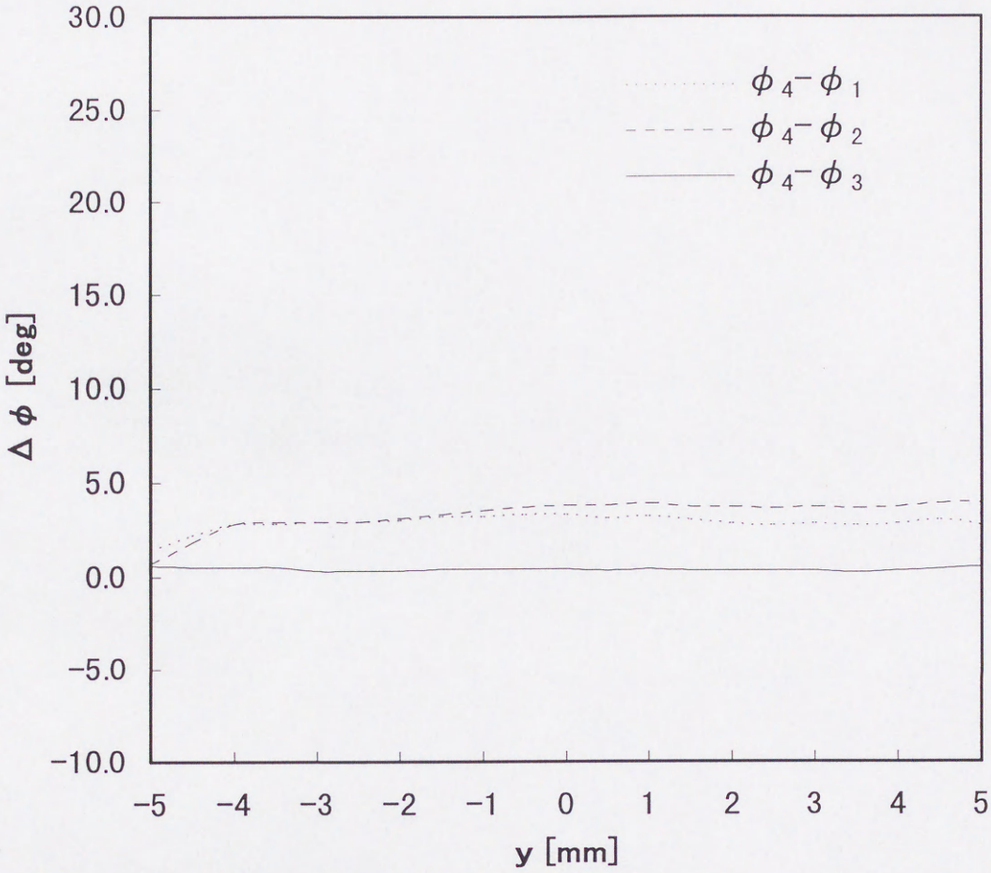

(a)

Fig. 4.5 Calculated phase difference versus measurement position for:
(a) series 1 samples

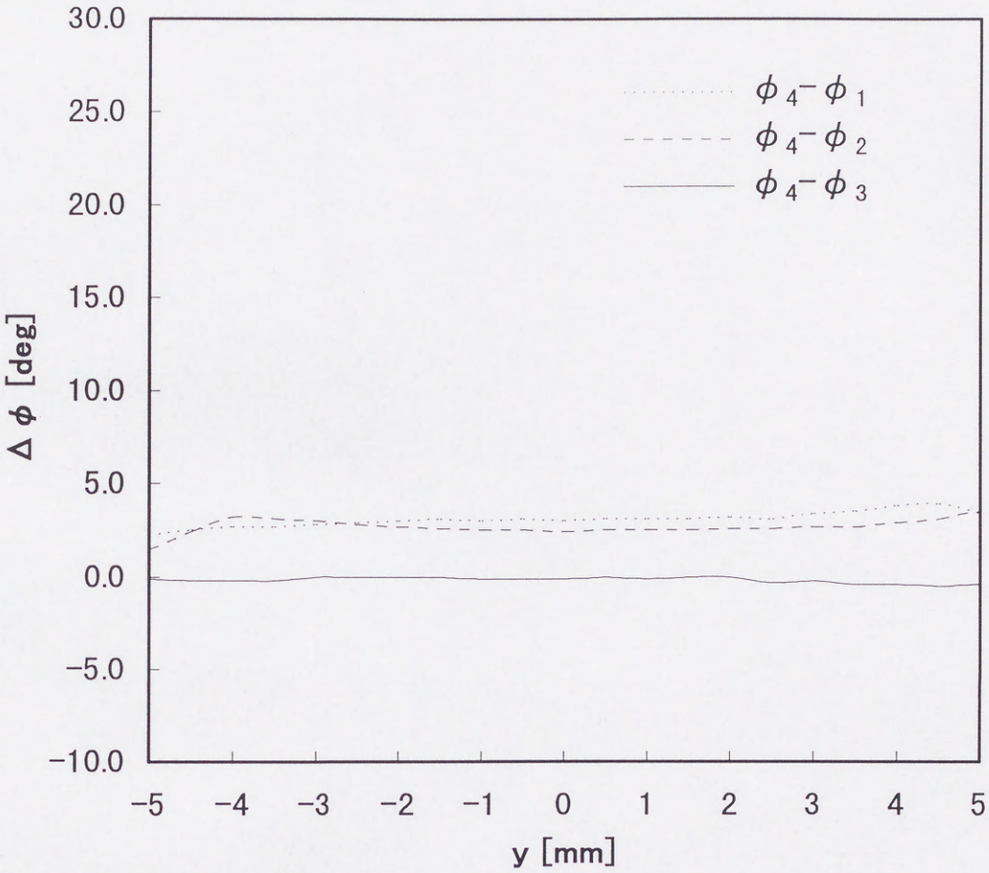

(b)

Fig. 4.5 Calculated phase difference versus measurement position for:
(b) series 2 samples

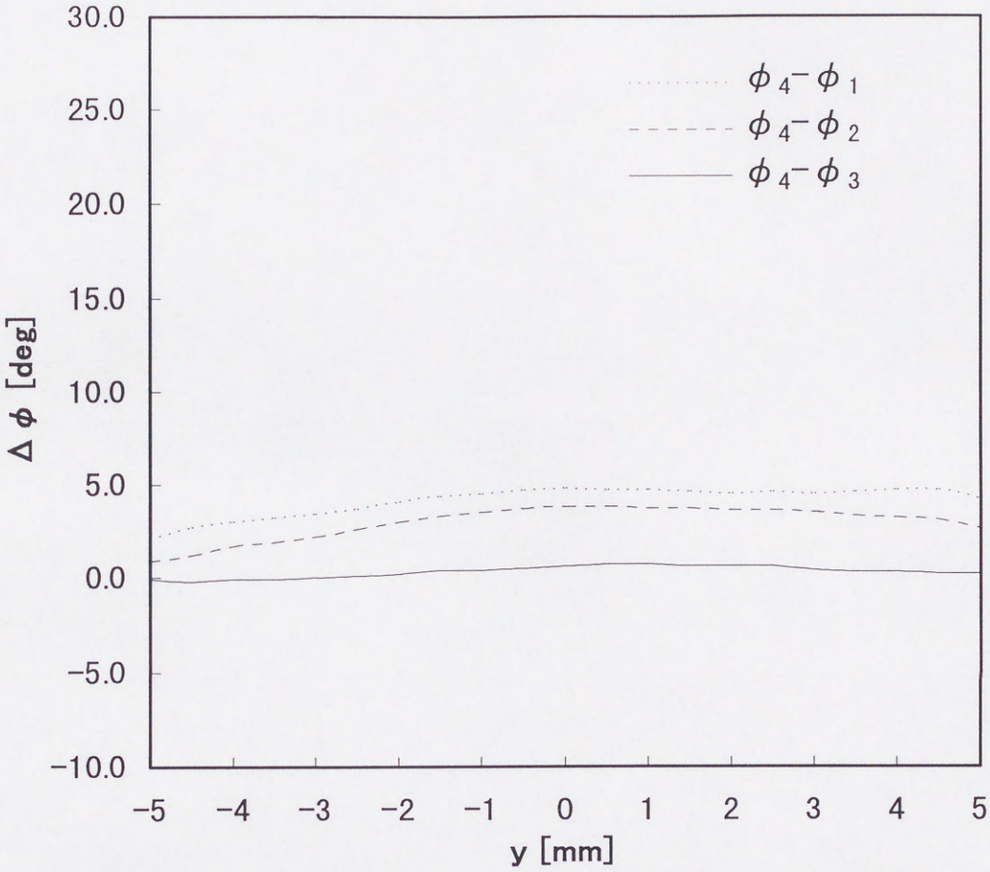

(c)

Fig. 4.5 Calculated phase difference versus measurement position for:
(c) series 3 samples

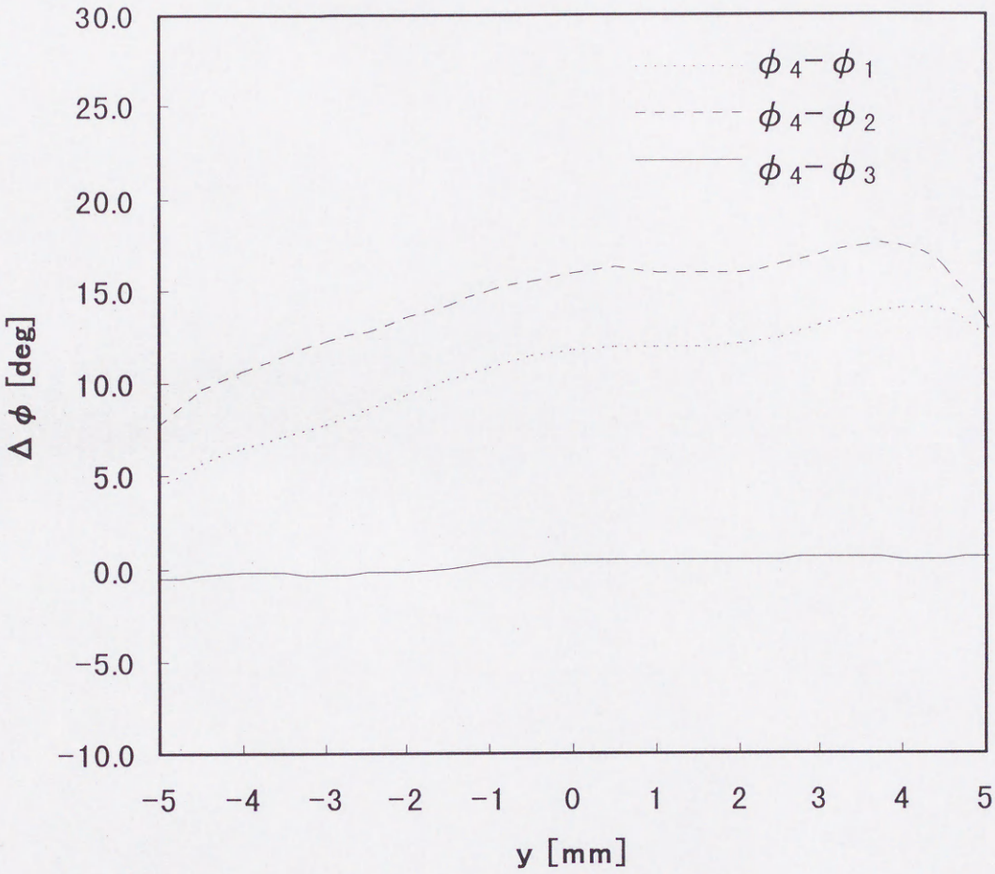

(d)

Fig. 4.5 Calculated phase difference versus measurement position for:
(d) series 4 samples

crack in the package. Same as series 1 samples, the relationship between phase differences of series 2 samples and the measurement position is shown in Fig. 4.5 (b), where the phase difference of Sample 2-S3 from the reference Sample 2-S4 is zero and curves $\phi_4 - \phi_1$ and $\phi_4 - \phi_2$ show delamination very clearly. The delamination level of series 2 samples is nearly same as that of series 1 samples, while it is a bit larger than the case of series 1 samples just at the edge of chip pad, which indicates the extended cracks are larger than those in series 1 samples. It is important to note that in the cases of series 1 and 2 samples, the SAT technique, which had been used to inspect these samples, was not able to detect the delaminations. Since the thickness of delamination is very thin there, the echoes from the surfaces of delamination and chip pad cannot be separated. On microwave inspection, phase measurement used is so sensitive to the varying distance in wave transmission direction that delaminations in these samples were presented significantly. Figure 4.5 (c) shows the phase differences measured for series 3 samples. The delamination level of series 3 samples was observed a little larger than the series 1 and 2 samples. The difference in measured delamination for Samples 3-S1 and 3-S2 illustrates the undulation of delamination becoming larger with the increase of delamination level. The results obtained for series 4 samples are shown in Fig. 4.5 (d), where the measured phase differences were significantly larger than the other series samples and the undulation of phase difference also became very evident. That is due to an existence of crack on the test area emanating from the larger level delamination. The measured results show the comprehensive effect of the delamination and crack interacting with microwave.

For finding the influence of the standoff distance, the experiment was carried out by changing standoff distance at the frequency of 20 GHz, where the sample was fixed under the center of the sensor. Figure 4.6 shows the relationship between measured phase of effective reflection coefficient and the standoff distance for Samples 3-S1 and 3-S3, with and without delamination respectively. The measured curves for 3-S1 and 3-S3 have a similar shape. According to increasing the standoff distance in its effective range, the phase difference shows less decrease. It means that the standoff distance does not affect the measurement sensitivity evidently, hence an optimum standoff distance is not required to be selected beforehand. It also shows when the standoff distance is larger than 0.5 mm, the phase difference become small, thus the measurement sensitivity is

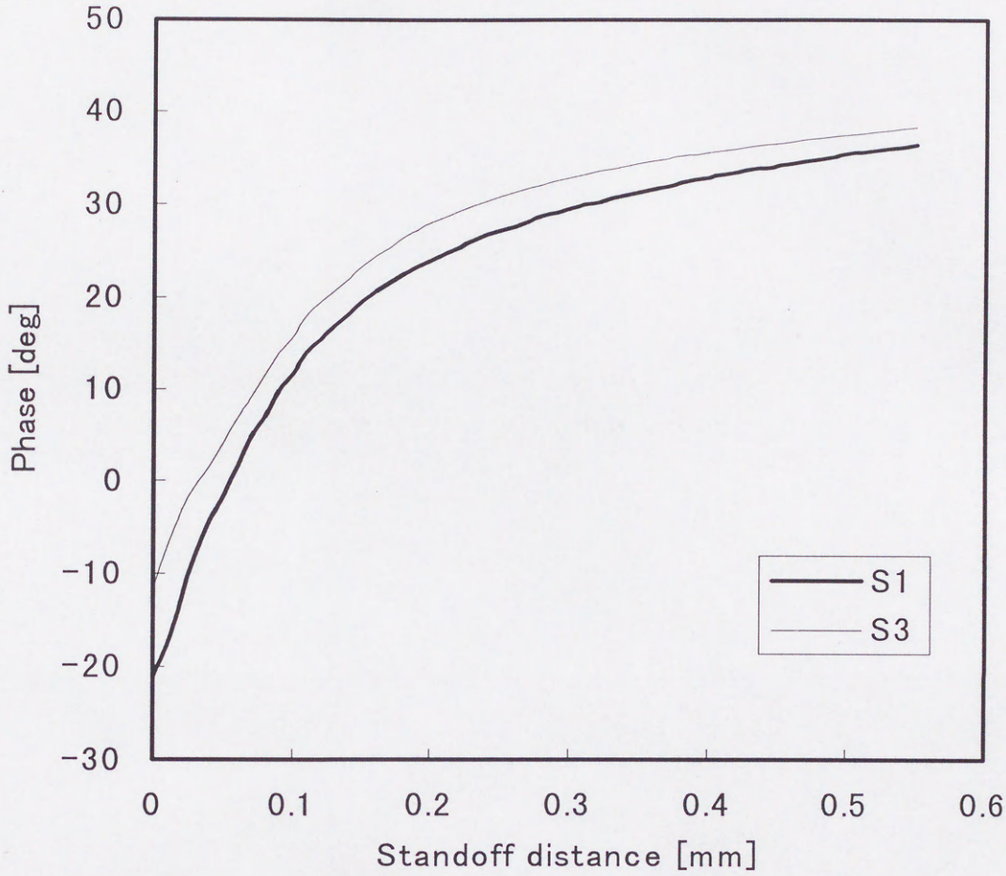

Fig. 4.6 Measured phase of effective reflection coefficient versus standoff distance for series 3 samples: S1 with and S3 without delamination

decreased. Same as the standoff distance, the influence of frequency was also measured for 3-S1 and 3-S3 with the standoff distance of 0.2 mm. As shown in Figs. 4.7 and 4.8, the measured phase for 3-S1 and 3-S3 changes linearly with the frequency in same slope. It indicates the measurement sensitivity is independent of the frequency in the range around 20GHz. Therefore, it is not necessary to select the operation frequency in advance.

4.5 CONCLUSIONS

Microwave inspection technique was confirmed to be a powerful tool to detect delamination in IC package. The open-ended coaxial line sensor was used to improve the spatial resolution. The phase of effective reflection coefficient at the coaxial line aperture in cases of package with and without delamination was measured as a characteristic signal to detect the delamination that made the measurement very sensitive. The phase difference of the sample from the reference eliminated the influence of the lack of spatial resolution effectively. The experimental results showed the delamination evidently at a relatively low microwave frequency. By measuring the delamination at the edge of chip pad, the extended crack in the plastic package was also estimated. The level of the delamination and crack affected by the quantity of the silica powder filled in the epoxy resin was observed clearly, that could be used to improve the design of IC package. The advantage of using the parameters without calibrating them in advance, makes the phase measurement convenient to realize automatic inspection. The phase measurement can be used for early detection of the defects in IC package and also for evaluation of other dielectric materials nondestructively.

REFERENCE

1 Ju, Y., Saka, M. and Abé, H., 'Microwave Nondestructive Detection of Delamination in IC Packages Utilizing Open-Ended Coaxial Line Sensor', *NDT & E International,* 1999, in press.

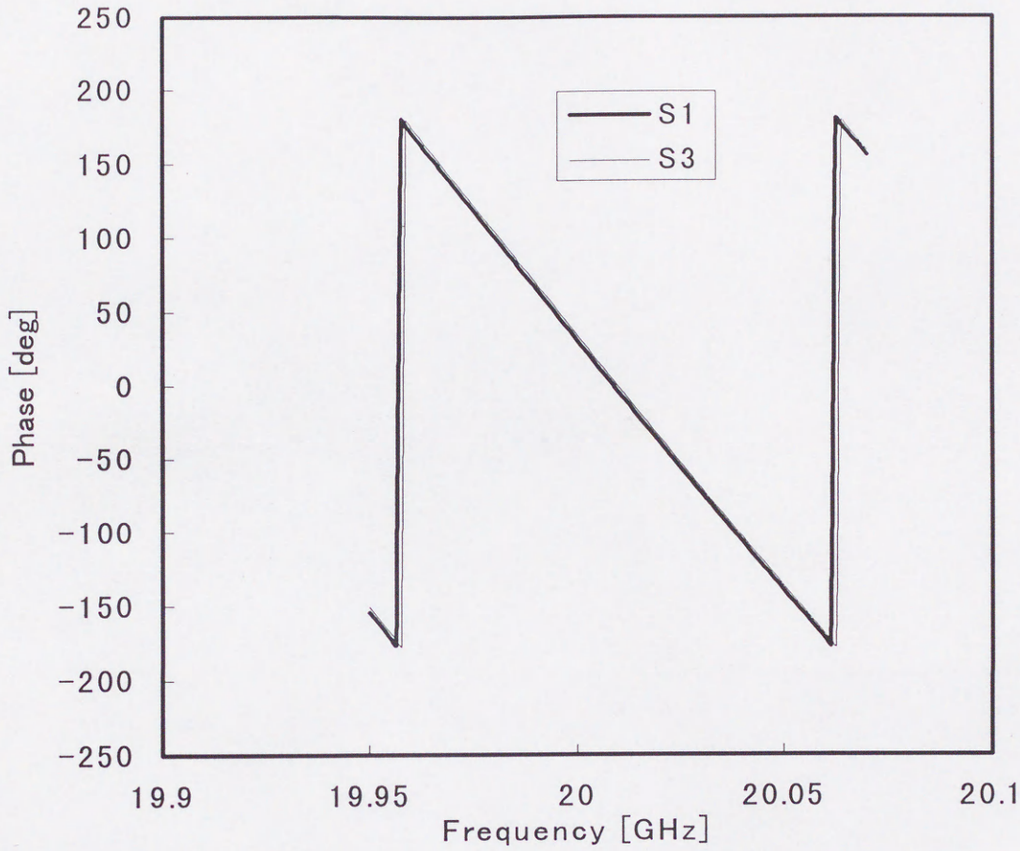

Fig. 4.7 Measured phase of effective reflection coefficient versus frequency for series 3 samples: S1 with and S3 without delamination

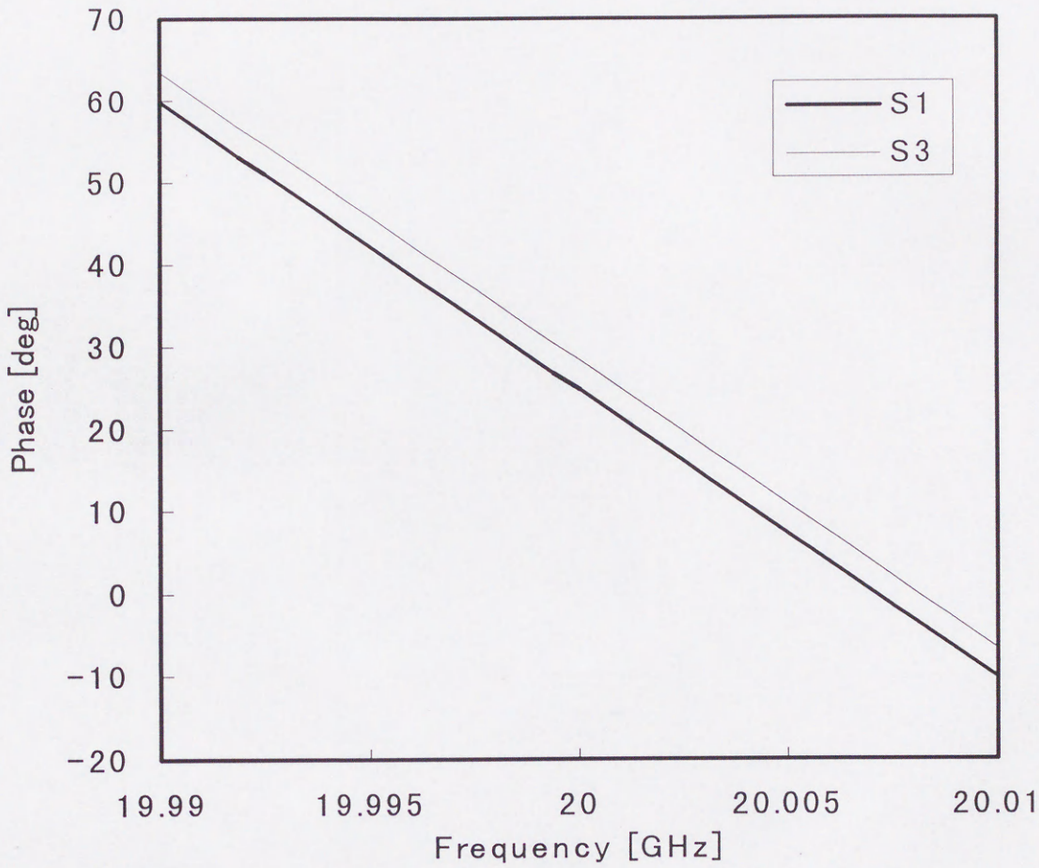

Fig. 4.8 Details of a part of graph in Fig. 4.7 measured with smaller scale of frequency

5

THEORETICAL CONSIDERATIONS

5.1 INTRODUCTION

The interaction of microwave with the IC package is a complex phenomenon. In order to evaluate the experimental results and optimize the conditions of the measurement (e.g., operation frequency and standoff distance; thickness and dielectric properties of packaging resin and delamination layer), it is important to understand the nature of this interaction. In this Chapter, the equation of effective reflection coefficient is derived from basic Maxwell's equations, based on the considered module of microwave interacting with IC package. The phase of effective reflection coefficient is calculated for evaluating delamination quantitatively. The theoretical analysis shows a good agreement with the experimental results.

5.2 THEORETICAL MODEL

Consider an incident signal, which is transmitted into a medium and reflects at the surface of the conducting plate in the medium. The ratio of the latter signal to the former gives the effective reflection coefficient of the medium. The phase difference between the effective reflection coefficient for a medium with a defect and one without a defect is related to the thickness and also the dielectric properties of the defect.

Assuming a time dependence $\exp(j\omega t)$ (which is omitted in the usual manner, where ω and t represent the angular frequency and time, respectively, and $j = \sqrt{-1}$),

and wave propagation along the z-axis, the electric and magnetic fields, $\vec{E}$ and $\vec{H}$, in a medium can be written as

$$\vec{E} = \vec{a}_\rho (E^+ e^{-\gamma z} + E^- e^{\gamma z}) \tag{5.1}$$

$$\vec{H} = \vec{a}_\phi (H^+ e^{-\gamma z} + H^- e^{\gamma z}) \tag{5.2}$$

and

$$\gamma = \alpha + j\beta \tag{5.3}$$

where E^+ and E^- denote the amplitude of the forward and backward traveling E-field, and H^+ and H^- denote that of the forward and backward traveling H-field. The symbols $\vec{a}_\rho$ and $\vec{a}_\phi$ are the unit vectors of polar coordinates. The quantity γ is the propagation constant in the medium, where α is the attenuation and β the phase constant, respectively, and are given by[1]

$$\alpha = \omega \sqrt{\frac{\mu\varepsilon}{2}\left[\sqrt{1+(\frac{\varepsilon''}{\varepsilon'})^2} - 1\right]} \tag{5.4}$$

$$\beta = \omega \sqrt{\frac{\mu\varepsilon}{2}\left[\sqrt{1+(\frac{\varepsilon''}{\varepsilon'})^2} + 1\right]} \tag{5.5}$$

The symbol μ is the permeability of the medium; it has same value as the permeability of free space, μ_0, when the medium is dielectric material. The symbol ε is the permittivity and generally a complex, $\varepsilon = \varepsilon' - j\varepsilon''$; where ε' is known as the dielectric constant and ε'' is the loss factor. For low loss material, ε'' is much smaller than ε'.

Assuming that the medium is source-free, Maxwell's equations can be written as

$$\nabla \times \vec{E} = -j\omega\mu\vec{H} \tag{5.6}$$

$$\nabla \times \vec{H} = -j\omega\varepsilon\vec{E} \tag{5.7}$$

With an $e^{-\gamma z}$ dependence, the above vector equations can be reduced to the following:

$$\vec{E} = \vec{a}_\rho (E^+ e^{-\gamma z} + E^- e^{\gamma z}) \tag{5.8}$$

$$\vec{H} = \vec{a}_\phi \frac{1}{\eta_e} (E^+ e^{-\gamma z} - E^- e^{\gamma z}) \tag{5.9}$$

where the complex intrinsic impedance of the medium, η_e, is given by

$$\eta_e = \frac{\eta}{\sqrt{1 - j\frac{\varepsilon''}{\varepsilon'}}} \tag{5.10}$$

The symbol η expresses the intrinsic impedance of a lossless medium:

$$\eta = \sqrt{\frac{\mu}{\varepsilon}} \tag{5.11}$$

The model of microwave interaction with IC package through the coaxial line sensor is shown in Fig 5.1. The medium for wave propagation in the coaxial line is denoted by using subscript *s*. The mediums in that the wave penetrates outside the coaxial line are expressed with subscript 0, 1 and 2, respectively, and the thickness of the corresponding medium is represented by d_0, d_1 and d_2. The back-wall of the package is faced to the aperture of coaxial line sensor, so the delamination layer is located between the aperture and chip pad. Referring the derivation by Zoughi and Bakhtiari[2], the effective reflection coefficient is calculated by deriving the forward and backward traveling electric and magnetic field components in each medium.

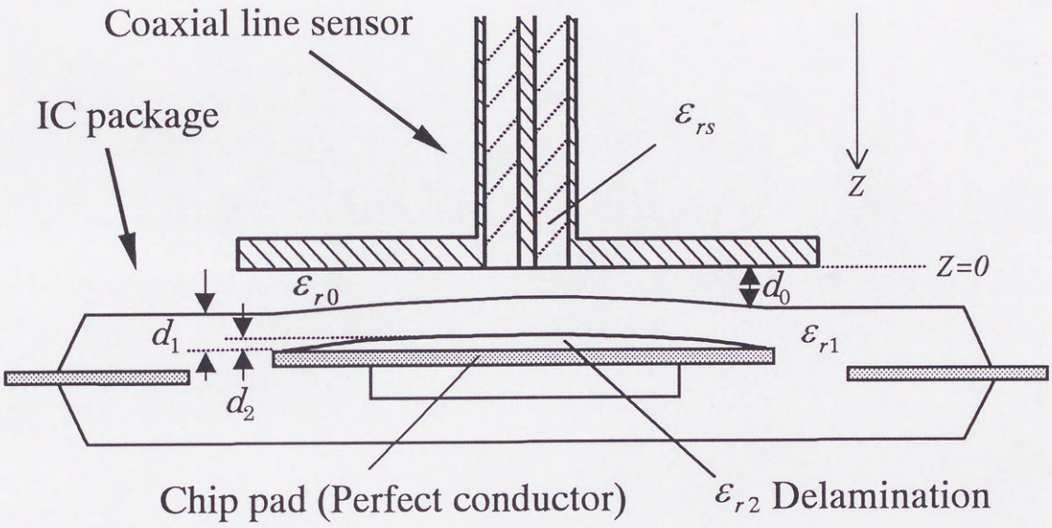

Fig. 5.1 Model of the interaction of microwave with IC package

Now the transverse field components in different mediums can be written as a function of position in the z-direction;

$$\vec{E}_n = \vec{a}_\rho (E_n^+ e^{-\gamma_n z} + E_n^- e^{\gamma_n z}) \tag{5.12}$$

$$\vec{H}_n = \vec{a}_\phi \frac{1}{\eta_{en}} (E_n^+ e^{-\gamma_n z} - E_n^- e^{\gamma_n z}) \tag{5.13}$$

where subscript n (= s, 0, 1, 2) represents different medium as shown in Fig. 5.1 and the origin of z is located at the aperture of coaxial line sensor.

At the surface of chip pad, $z = d_0 + d_1 + d_2$, boundary conditions force the tangential E-field on the surface of the perfect conductor to be zero. Thus

$$\vec{E}_2 = \vec{a}_\rho \{E_2^+ e^{-\gamma_2 (d_0+d_1+d_2)} + E_2^- e^{\gamma_2 (d_0+d_1+d_2)}\} = 0 \tag{5.14}$$

or

$$E_2^- = -E_2^+ e^{-2\gamma_2 (d_0+d_1+d_2)} \tag{5.15}$$

So the fields in the delamination medium can be written as

$$\vec{E}_2 = \vec{a}_\rho \{E_2^+ e^{-\gamma_2 z} - E_2^+ e^{\gamma_2 [z-2(d_0+d_1+d_2)]}\} \tag{5.16}$$

$$\vec{H}_2 = \vec{a}_\phi \frac{1}{\eta_{e2}} \{E_2^+ e^{-\gamma_2 z} + E_2^+ e^{\gamma_2 [z-2(d_0+d_1+d_2)]}\} \tag{5.17}$$

By applying the appropriate boundary conditions which require the corresponding tangential fields are continuous respectively at the interface of different mediums, Eqs. (5.12) and (5.13) are equated to Eqs. (5.16) and (5.17), respectively, when $z = d_0 + d_1$ and $n = 1$. By solving the simultaneous equations, we get

$$\frac{E_1^-}{E_1^+} e^{2\gamma_1(d_0+d_1)} = \frac{-1+\dfrac{\eta_{e2}}{\eta_{e1}}\tanh\gamma_2 d_2}{1+\dfrac{\eta_{e2}}{\eta_{e1}}\tanh\gamma_2 d_2} \tag{5.18}$$

or

$$E_1^- = E_1^+ A e^{-2\gamma_1(d_0+d_1)} \tag{5.19}$$

where

$$A = \frac{-1+\dfrac{\eta_{e2}}{\eta_{e1}}\tanh\gamma_2 d_2}{1+\dfrac{\eta_{e2}}{\eta_{e1}}\tanh\gamma_2 d_2} \tag{5.20}$$

Same as above derivation and applying the boundary conditions to $z = d_0$ and $z = 0$, respectively, the effective reflection coefficient can finally be written as

$$\tau = \frac{E_s^-}{E_s^+} = \frac{\dfrac{\eta_{e0}}{\eta_{es}} D - 1}{\dfrac{\eta_{e0}}{\eta_{es}} D + 1} \tag{5.21}$$

where

$$D = \frac{1+Ce^{-2\gamma_0 d_0}}{1-Ce^{-2\gamma_0 d_0}} \tag{5.22}$$

$$C = \frac{\dfrac{\eta_{e1}}{\eta_{e0}} B - 1}{\dfrac{\eta_{e1}}{\eta_{e0}} B + 1} \tag{5.23}$$

$$B = \frac{1+Ae^{-2\gamma_1 d_1}}{1-Ae^{-2\gamma_1 d_1}} \tag{5.24}$$

The dimensions of the coaxial line sensor and the operation frequency are selected to permit the propagation of the dominant TEM mode only. As a result, only this mode can be used to excite the sensor and carry out the measurement. In addition, as a sample

is put in the near field of the aperture, the scatter effect is neglected since it is sufficiently small to affect the measured phase of effective reflection coefficient. For low loss material, the loss factor is much smaller than the relative dielectric constant, therefore, only the dielectric constant is considered in order to simplify the calculation. When $\varepsilon'' \to 0$, we have $\alpha \to 0$, $\beta \to \omega\sqrt{\frac{\mu\varepsilon}{2}}$, and $\eta_e \to \eta$. Thus Eq. (5.21) can be written as

$$\tau = \frac{E_s^-}{E_s^+} = \frac{\frac{\eta_0}{\eta_s}D - 1}{\frac{\eta_0}{\eta_s}D + 1} \tag{5.25}$$

where

$$D = \frac{1 + Ce^{-2j\beta_0 d_0}}{1 - Ce^{-2j\beta_0 d_0}} \tag{5.26}$$

$$C = \frac{\frac{\eta_1}{\eta_0}B - 1}{\frac{\eta_1}{\eta_0}B + 1} \tag{5.27}$$

$$B = \frac{1 + Ae^{-2j\beta_1 d_1}}{1 - Ae^{-2j\beta_1 d_1}} \tag{5.28}$$

$$A = \frac{-1 + j\frac{\eta_2}{\eta_1}\tan\beta_2 d_2}{1 + j\frac{\eta_2}{\eta_1}\tan\beta_2 d_2} \tag{5.29}$$

The quantities β_n and η_n can be calculated from the corresponding relative dielectric constant, ε_{rn}:

$$\beta_n = \beta_0 \sqrt{\varepsilon_{rn}} \tag{5.30}$$

and

$$\eta_n = \frac{\eta_0}{\sqrt{\varepsilon_{rn}}} \tag{5.31}$$

where

$$\beta_0 = \frac{2\pi}{\lambda_0} \tag{5.32}$$

and

$$\eta_0 = \sqrt{\frac{\mu_0}{\varepsilon_0}} \tag{5.33}$$

The symbol λ_0 is the wavelength in free space, and μ_0 and ε_0 are the permeability and permittivity of free space, respectively.

Consequently, the phase of effective reflective coefficient, ϕ, can be calculated by

$$\phi = \tan^{-1}\left(\frac{\mathrm{Im}[\tau]}{\mathrm{Re}[\tau]}\right) \tag{5.34}$$

The phase difference, $\Delta\phi$, of a sample from the reference one can be calculated by

$$\Delta\phi = \phi_r - \phi_m \tag{5.35}$$

where subscripts *r* and *m* represent the cases of reference sample and the measurement sample, respectively.

5.3 EVALUATION

For evaluating the experimental results, the measured phase differences for series 3 samples described in Chapter 4 were used. The relative dielectric constant of the epoxy resin of series 3 samples was used as $\varepsilon_{r1} = 8.2$, and that of the delamination layer was

assumed to be the same as air ($\varepsilon_{r2} = 1$). The dielectric material filled in coaxial line sensor has a relative dielectric constant $\varepsilon_{rs} = 2.1$. In the calculation, working wavelength is 15 mm ($\lambda = v / f$; f = 20 GHz) and the standoff distance, d_0, is a function of the delamination thickness, d_2 (d_0=0.2-d_2; the constant 0.2 is the standoff distance for the case of without delamination); the resin thickness measured from package surface to chip pad is 0.7 mm (d_1=0.7 mm). The relationship between calculated phase difference and the thickness of delamination layer for series 3 samples is shown in Fig. 5.2. Using the calculated curve, the thickness of delamination can be estimated from the measured phase difference. The predicted thickness of delamination is shown in Table 5.1, where the phase difference undulating with the measurement position shown in Fig. 4.5 (c) is replaced by the intermediate value.

5.4 COMPARISON WITH EXPERIMENTAL RESULTS

In order to verify the experimental results and theoretical prediction, the value of delamination thickness predicted in Table 5.1 is compared with its actual value. Sample 3-S2 measured in Chapter 4 was cut along the x-direction at the center of the package after finishing the experiment; Figure 5.3 shows the actual delamination observed by microscope. The actual thickness of the delamination in Sample 3-S2 was approximately 31 μm, 1/500 of the working wavelength approximately. It is close to estimated value of 39.8 μm. One reason of their difference is on the undulation of the measured delamination. By substituting d_2=31 μm to Eqs. (5.34) and (5.35), the difference of phase for Sample 3-S2 from that for the reference Sample 3-S4 is calculated as 1.608 degree. The measurement results are compared with the calculation for Sample 3-S2 as shown in Fig. 5.4; measured phase difference is shown to be undulating around the theoretical value.

5.5 CONCLUSIONS

The basic principle of microwave interaction with IC package was clarified and the

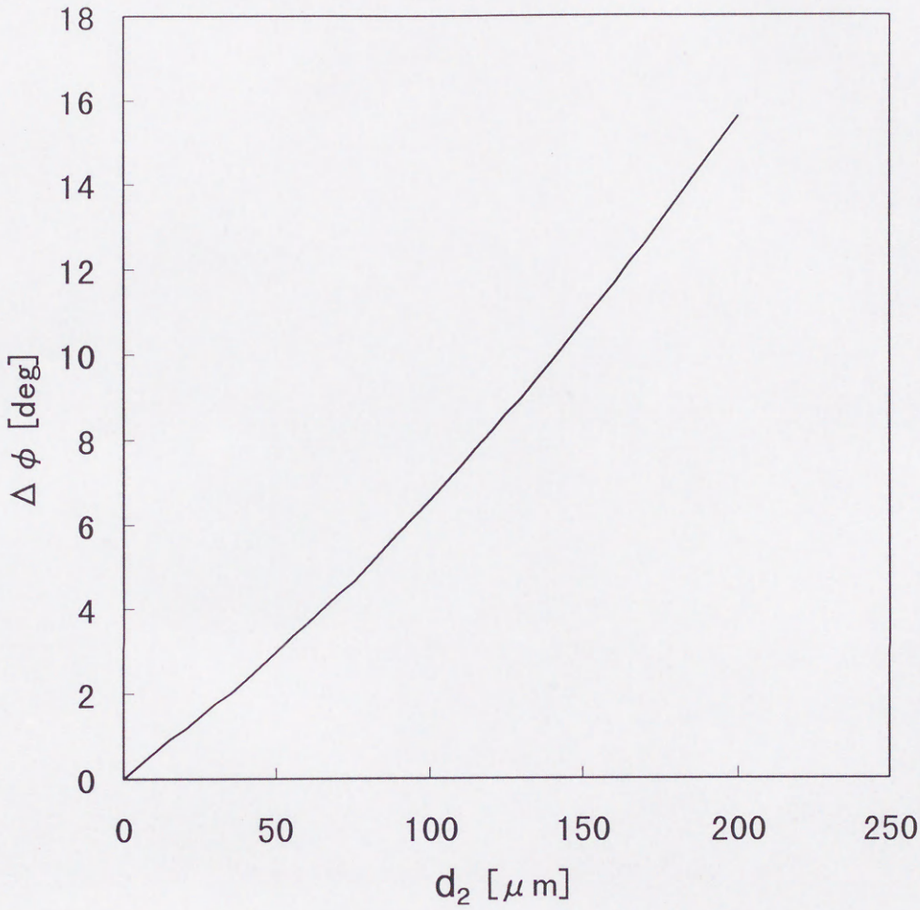

Fig. 5.2 Calculated phase difference versus thickness of delamination for series 3 samples

Table 5.1 Predicted delamination thickness

Sample	Measured Phase Difference from the Reference 3-S4 [deg]	Predicted Delamination Thickness μm
3-S1	3.45	56.9
3-S2	2.35	39.8
3-S3	0.25	4.6

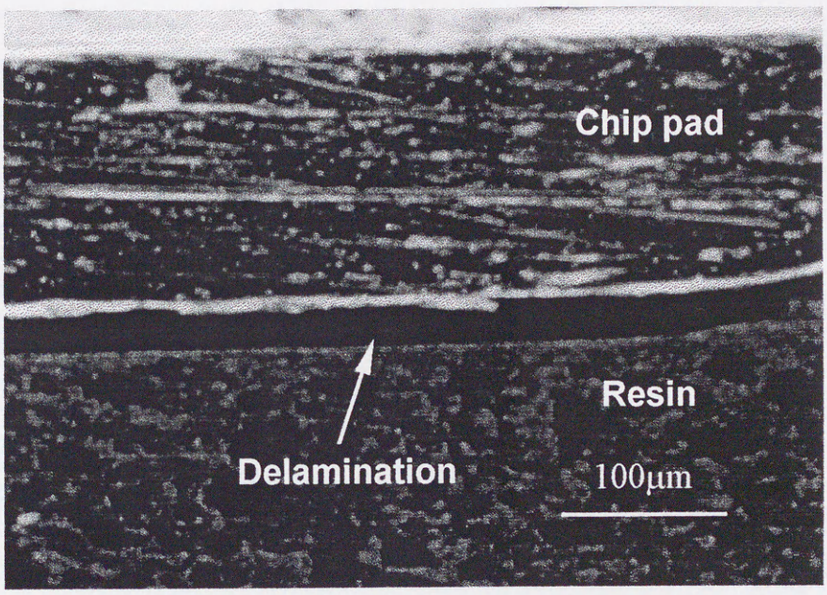

Fig. 5.3 Actual delamination in Sample 3-S2 observed by microscope

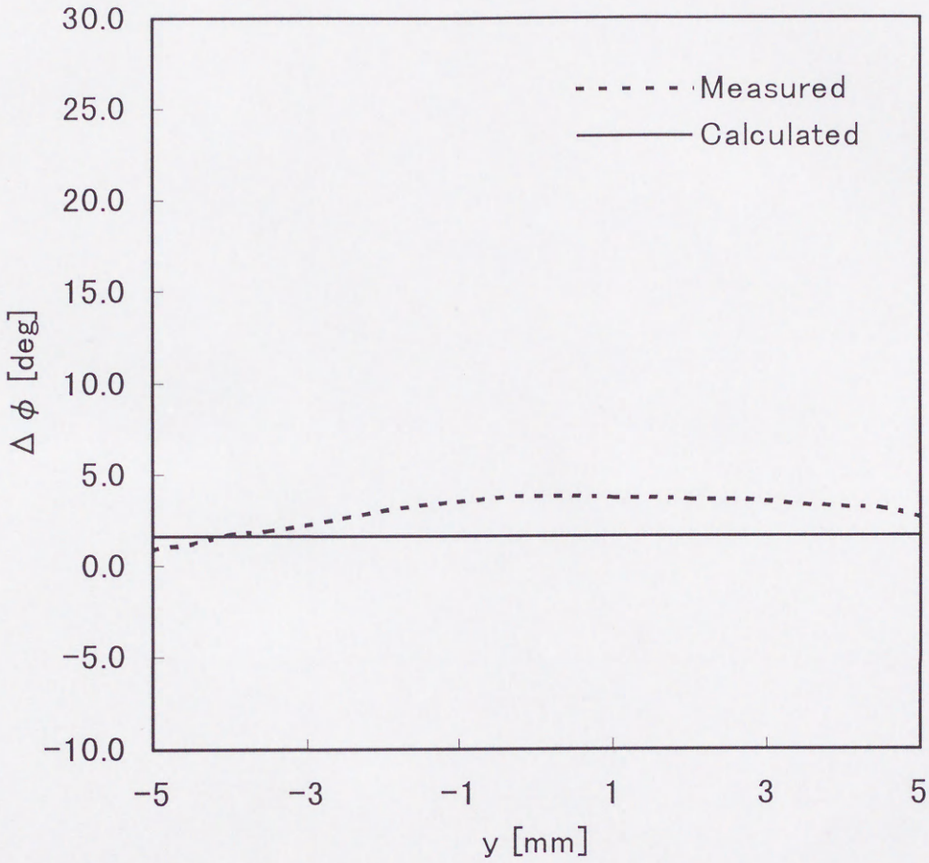

Fig. 5.4 Comparison of the measured result with calculation for Sample 3-S2

theoretical equations for calculating the phase of effective reflection coefficient was derived. It can be used to optimize and calibrate the experiment, and to replace the reference sample. The method of estimating the thickness of delamination from the experimental results was described. The good agreement of the experimental results with the calculation indicates that the present technique can be used for early detection and quantitative evaluation of the potential defects in IC package and other dielectric materials.

REFERENCES

1 Pozar, D. M., Microwave Engineering, ch. 4, 1990, Addison Wesley, New York.

2 Zoughi, R. and Bakhtiari, S., 'Microwave Nondestructive Detection and Evaluation of Disbonding and Delamination in Layered-Dielectric-Slabs', *IEEE Transactions on Instrumentation and Measurement*, Vol. 39, No. 6, 1990, pp. 1059-1063.

6

MICROWAVE IMAGING

6.1 INTRODUCTION

A novel microwave NDT technique utilizing open-ended coaxial line sensor has been used for the detection of delamination in IC package as described above. It was confirmed to be an effective tool for the integrity assessment of IC package. Nevertheless, modern NDT technique requires the inspection technique that is not only able to detect defects correctly but also observe defects directly. Imaging technique is a possible way to observe the shape and the size of the defects. Recently, microwave imaging has interested many researchers[1-2] because of its specific advantage to evaluate dielectric materials[4]. However, due to the divergent property, microwave cannot propagate along one direction, as similarly as x-ray, thereby the cross sectional resolution had been lower. For decreasing the effect of scatter thus for increasing the spatial resolution, the sensor aperture was designed in our study in small dimensions and the sample was put in the near field of the aperture, while the phase measurement was carried out. Microwave image was created by recording the phase of effective reflection coefficient continuously, when IC package was scanned. The measured package image showed the delamination in damaged package very clearly[5].

6.2 IMAGING SYSTEM AND SAMPLE DESCRIPTION

Microwave imaging is based on the interaction of electromagnetic wave with the IC

package. The coaxial line sensor acts as a source of microwave that transmits into the package, and also acts as the receiver of the signal reflected from the package. The phase of the effective reflection coefficient at the aperture of the coaxial line sensor, varying with the thickness and also dielectric constant of the delamination layer, is measured as a characteristic signal to create a two dimensional image. The configuration of the microwave imaging system is the same as that shown in Fig. 3.1; the actual microwave imaging system is shown in Fig. 6.1. The network analyzer (HP8510) was used to generate a continuous wave signal fed to the coaxial line sensor and measure the phase of effective reflection coefficient at the coaxial line aperture. While the sensor scans over the package, the phase information was continuously recorded corresponding to the measurement position. The computer was employed to generate an image using the data measured by the network analyzer and synchronize the stage translation in the x- and y-directions. Same sensor described in Chapter 3 was used in the experiment. The open-ended coaxial line sensor was faced to the back-wall of the package, so the delamination layer was located between the sensor aperture and the chip pad, as shown in Fig. 6.2. To conduct the experimental study, series 3 and 4 samples described in Chapter 4 (see Tables 4.1 and 4.2) were used.

6.3 MEASURED RESULTS AND DISCUSSION

A phase image was created by scanning a sample in the x- and y-directions. The scanned area was 20×25 mm and the pitch was 0.5 mm. The operation frequency was 20 GHz and the standoff distance between the sensor and the sample was 0.2 mm. Figure 6.3 shows the images of series 3 samples using the raw data without any image processing. In Fig. 6.3, (*a*) shows the images of Sample 3-S1 containing a delamination and Sample 3-S3 free from delamination, respectively. The yellow region in the image of 3-S1 indicates a delamination between the chip pad and the plastic package. In the image of 3-S3, package part is observed with green color completely, which means there is no delamination contained in the sample. The difference between the images of 3-S1 and 3-S3 illustrates the information of delamination; by comparing them, the delamination can be detected effectively. As shown in the figure, from the scale of

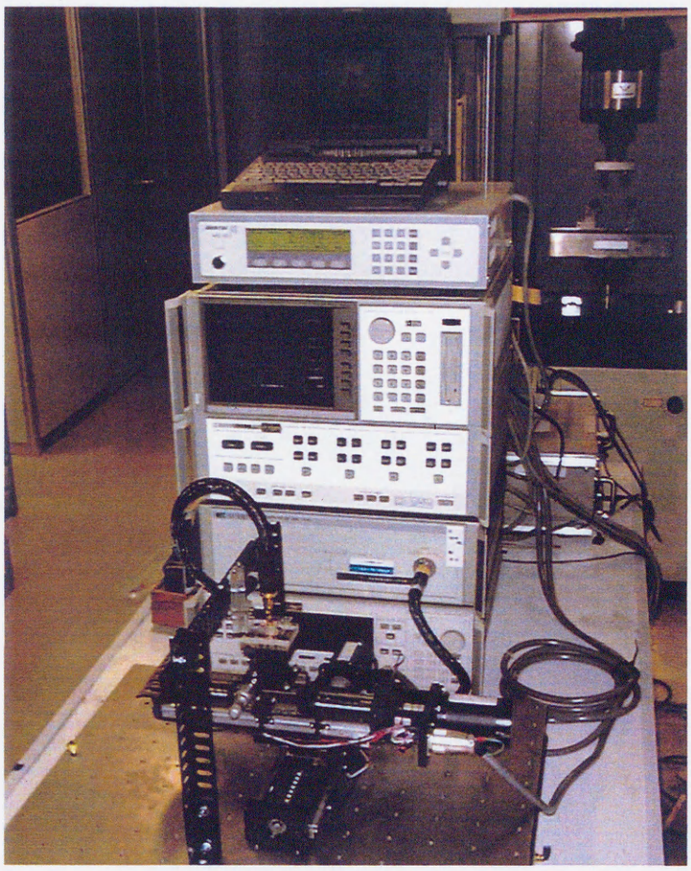

Fig. 6.1 Microwave imaging system

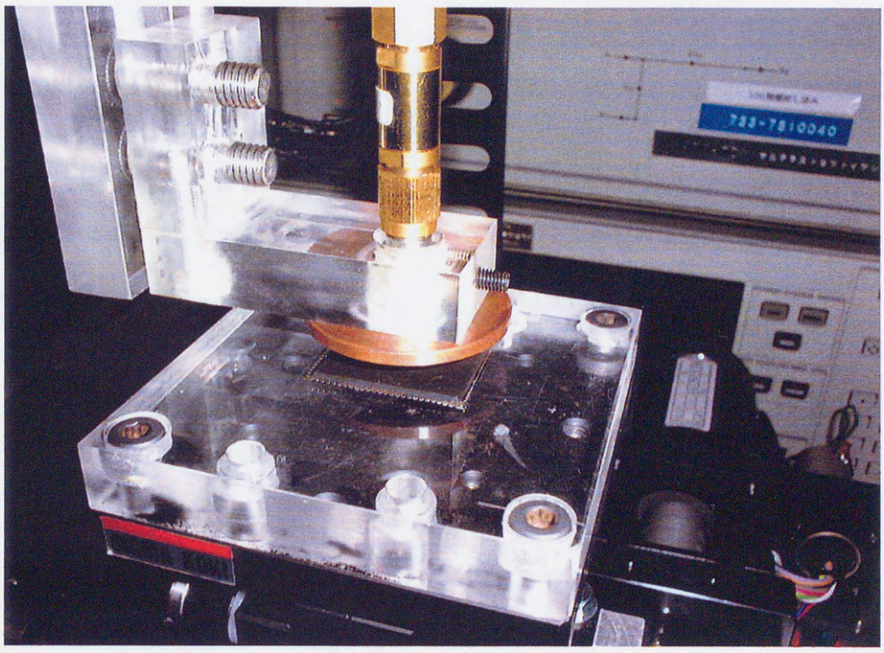

Fig. 6.2 Sensor and sample setup

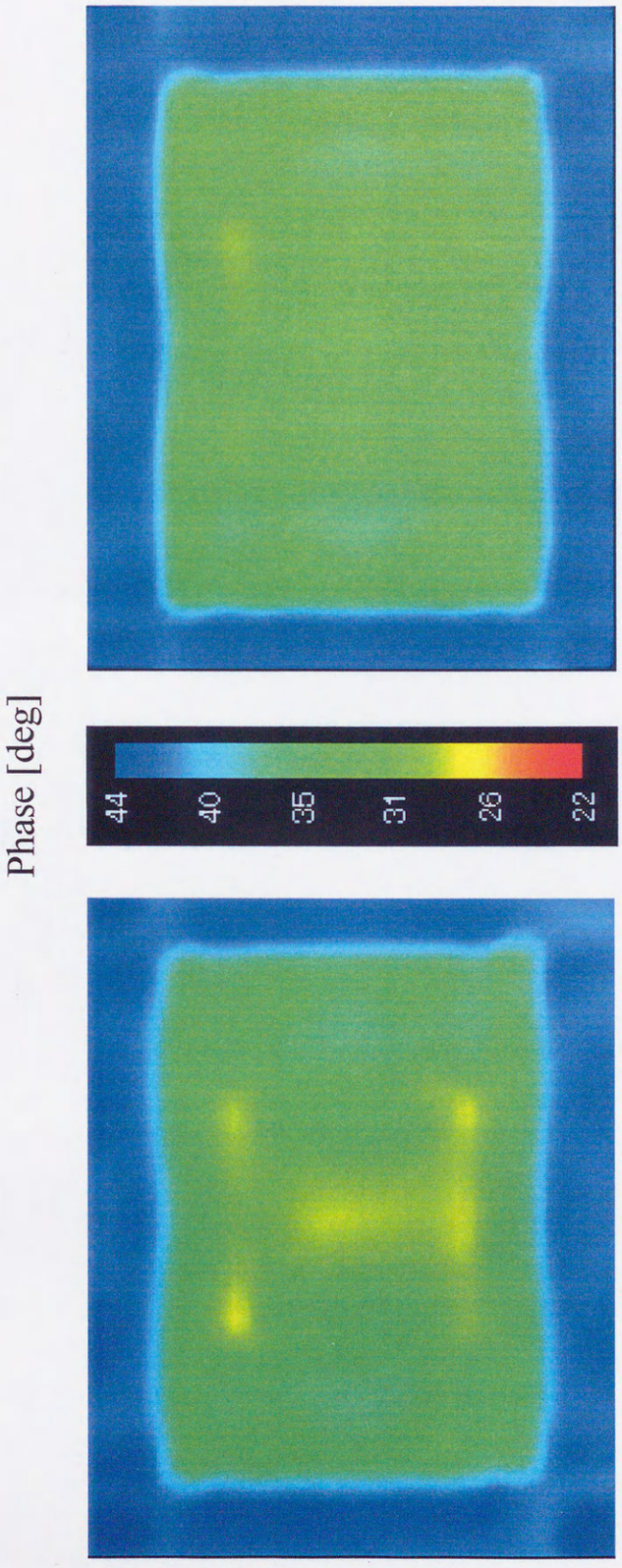

(a)

Fig. 6.3 Microwave image of series 3 samples, (a) Sample 3-S1 with and 3-S3 without delamination

phase, the threshold value of phase for distinguishing the delamination is observed to be about 28 degree which is, indeed, the phase value corresponding to the boundary of the green and yellow color. Another pair of Samples 3-S2 and 3-S4 was also measured as shown in Fig. 6.3 (*b*); the area of yellow in the package illustrates an existence of delamination in Sample 3-S2. Sample 3-S4 was observed nearly same as 3-S3 that shows a good reappearance of the experiment. For series 4 samples, images were shown in Fig. 6.4. In the images of 4-S1 and 4-S2, yellow regions are observed clearly larger than those in Fig. 6.3; it illustrates the delaminated areas in Samples 4-S1 and 4-S2 are larger than Samples 3-S1 and 3-S2. In addition, the red areas in the image of 4-S1 and 4-S2 show the thickness of delaminations is significantly large, thereby indicating extended cracks contained in those samples. It means the quantity of filled silica powder in epoxy resin will affect strongly the level of delamination. The green color throughout Samples 4-S3 and 4-S4 shows that they are free from the delamination. In the image of samples, the edge and the size of package were shown in good agreement with its actual shape and value. However, due to lack of spatial resolution, the observed area of delamination is smaller than its actual size. Higher resolution can be obtained by further increasing the operation frequency and decreasing the standoff distance. It is important to note that in the cases of Samples 3-S1 and 3-S2, the SAT technique that had been used to inspect these samples was not able to detect the delaminations; this is due to the fact that the thickness of delamination layer is very thin, and the echoes from the surfaces of delamination and chip pad cannot be separated. In the case of microwave imaging, since the phase measurement is used, which is very sensitive to variance of distance in the wave transmission direction, delaminations in those samples were presented significantly.

6.4 CONCLUSIONS

Microwave imaging was confirmed to be an effective tool to detect the delamination in IC package. By using the open-ended coaxial line sensor, the spatial resolution is improved. The image created by the phase of effective reflection coefficient shows the delamination clearly and also the area and the color of the corresponding region can be used to estimate the size of delamination. With the aid of the microwave imaging

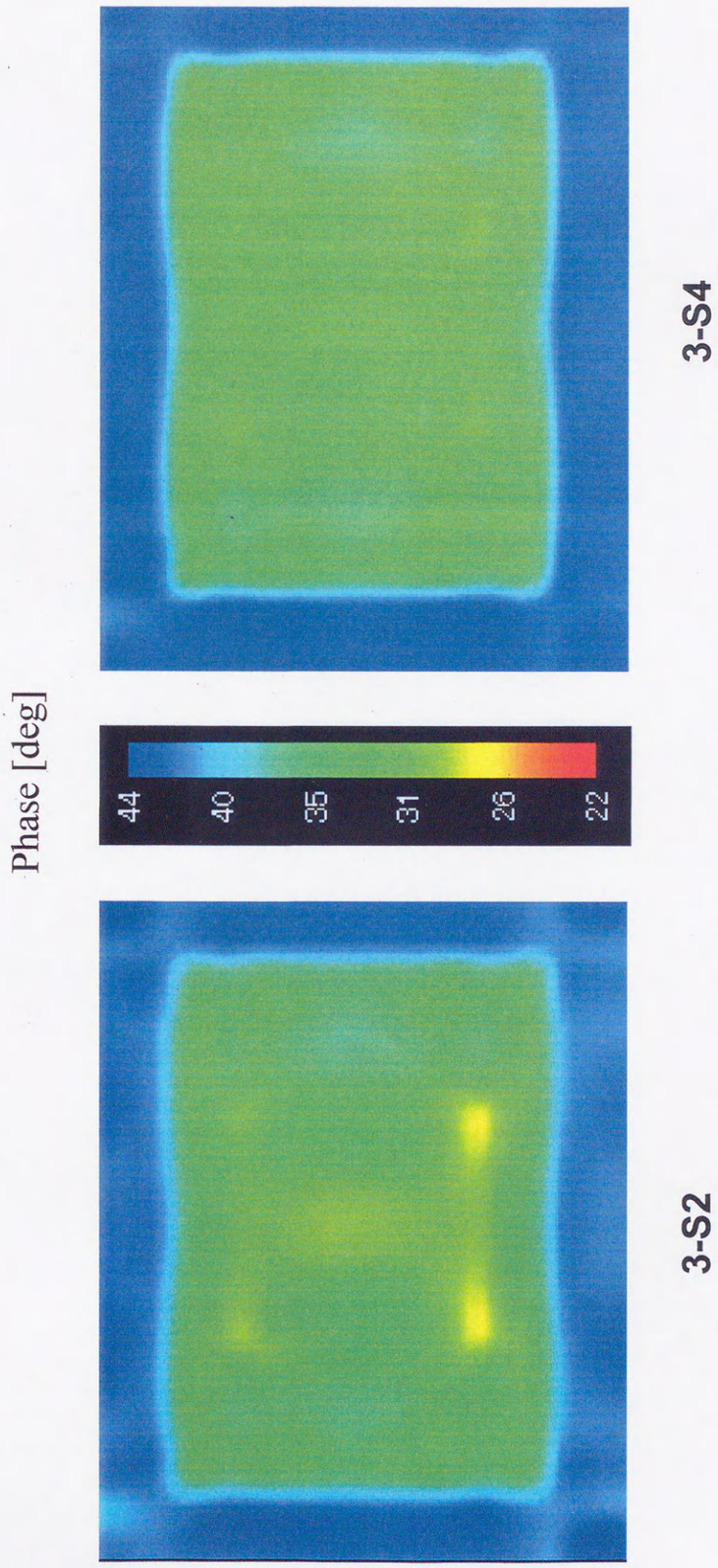

(b)

Fig. 6.3 Microwave image of series 3 samples, (b) Sample 3-S2 with and 3-S4 without delamination

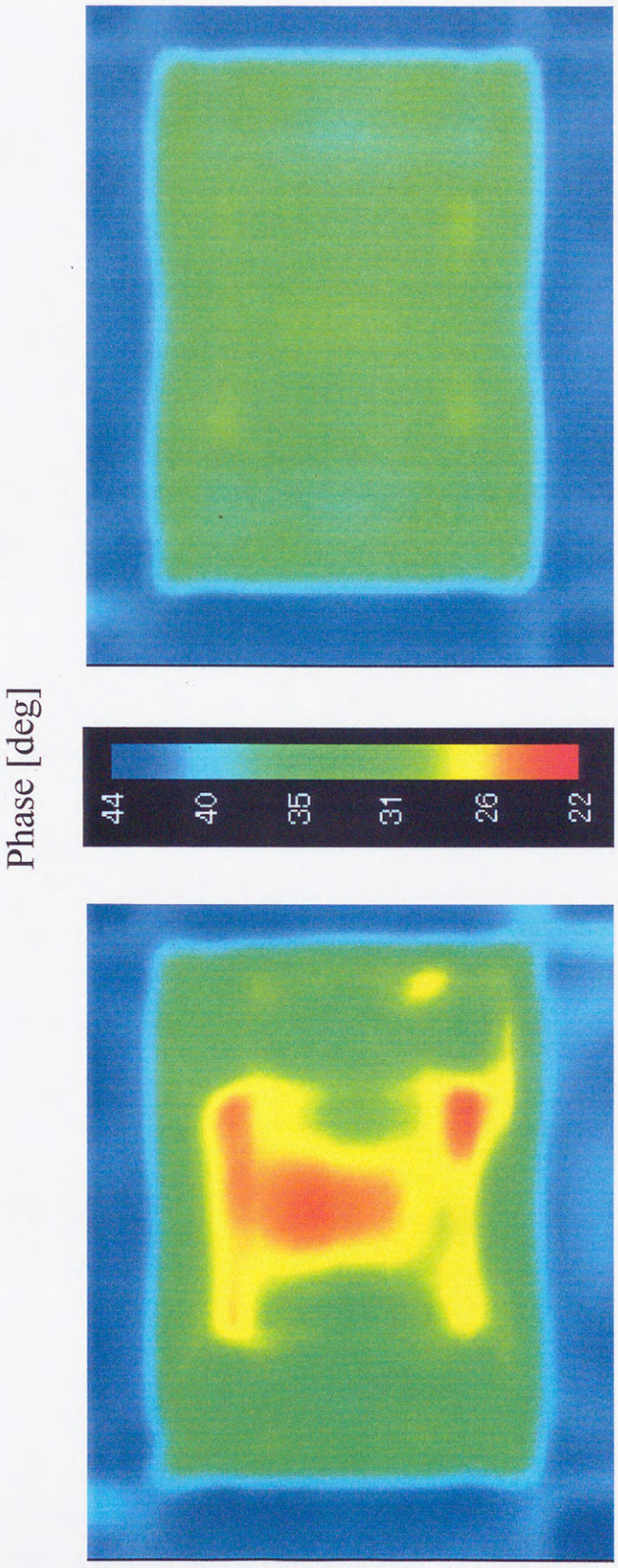

(a)

Fig. 6.4 Microwave image of series 4 samples, (a) Sample 4-S1 with and 4-S3 without delamination

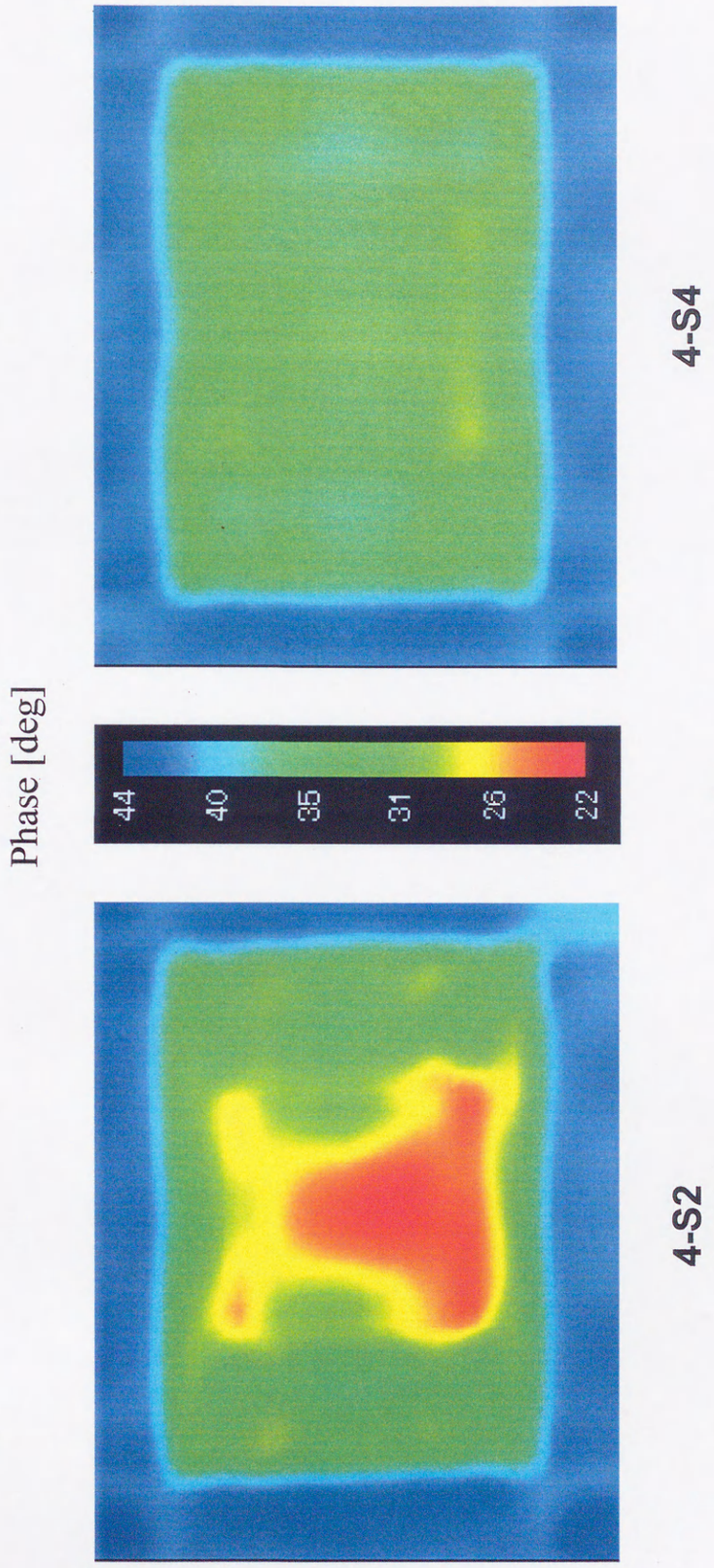

(b)

Fig. 6.4 Microwave image of series 4 samples, (b) Sample 4-S2 with and 4-S4 without delamination

technique, the full mechanism of delamination is expected to be observed in the soldering conditions, thereby the prediction of the condition of delamination and crack occurrence also becomes possible. Since delamination image can be obtained without optimizing the conditions of the measurement, such as operation frequency and standoff distance, microwave imaging technique can also be used for detecting earlier potential defects in IC package and assessing integrity of other polymeric materials automatically.

REFERENCES

1 Gopalsami, N., Bakhtiari, S., Dieckman, S. L., Raptis, A. C. and Lepper, M. J., 'Millimeter-Wave Imaging for Nondestructive Evaluation of Materials', *Materials Evaluation*, Vol. 52, No. 3, 1994, pp. 412-415.

2 Qaddoumi, N., Carriveau, G., Ganchev, S. and Zoughi, R., 'Microwave Imaging of Thick Composite with Defects', *Materials Evaluation*, Vol. 53, No. 5, 1995, pp. 926-929.

3 Diener, L., 'Microwave Near-Field Imaging with Open-Eeded Waveguide—Comparison with Other Techniques of Nondestructive Testing', *Research in Nondestructive Evaluation*, Vol. 7, No. 3, 1995, pp. 137-152.

4 Semenov, S. Y., Svenson, R. H., Boulyshev, A. E., Souvorov, A. E., Borisov, V. Y., Sizov, Y., Starostin, A. N., Dezern, K. R., Tatsis, G. P. and Baranov, V. Y., 'Microwave Tomography: Two-Dimensional System for Biological Imaging', *IEEE Transactions on Biomedical Engineering*, Vol. 43, No. 9, 1996, pp. 869-877.

5 Ju, Y., Saka, M. and Abé, H., 'Microwave Imaging for Nondestructive Inspection of Delamination in IC Packages by Open-Ended Coaxial Line Sensor', *Proc. of the Workshop on Mechanical Reliability of Polymeric Materials & Plastic Packages of IC Devices*, ASME/IEEE-CPMT/IMAPS, Paris, EEP-Vol. 25, 1998, pp. 265-270.

7

CONCLUSIONS

A new microwave NDT technique was developed for evaluation of delamination in IC packages. By using open-ended coaxial line sensor, spatial resolution was improved relative to the conventional microwave NDT techniques. Based on the specific properties of microwave that it penetrates deeply inside dielectric materials and reflects completely at metal surface, delamination in IC package was detected effectively. With the aid of this technique, the mechanism of the delamination can also be investigated. This advanced technique provides a new experimental method for integrity assessment of IC package, thereby supplying the capabilities to improve the design of packaging, as well as the reliability of IC package. Simultaneously, high sensitivity of this technique also offers a great possibility to evaluate other dielectric materials nondestructively. The results obtained are summarized as following:

(1) Open-ended coaxial line sensor was first used for microwave NDT and the spatial resolution was improved effectively. It was confirmed to be a powerful tool to detect small defects in dielectric materials. The magnitude of transmission coefficient is sensitive to the change in dielectric properties of materials. By using the first abrupt transition phenomenon, small defects can be detected effectively based on a difference of dielectric constant. When a sample is in contact with the sensor and defects are on the surface of the sample as the case of the present experiment, the requirement for resolution is not tight; thereby extremely low frequency is available. Measurement sensitivity is affected by the distance between the sensors. Increasing the distance, the sensitivity will be decreased. Transmission technique is suitable to detect the defects such as disbond,

delamination and void etc. in stratified dielectric materials.

(2) Delamination in IC package was first detected without using any coupling medium such as water. The delamination of thickness around 30 μm was detected by measuring the magnitude of effective reflection coefficient on the frequency of 48.50 GHz and the standoff distance of 0.24 mm. The spatial resolution of the open-ended coaxial line sensor is significantly high than that of conventional microwave NDT techniques. The coherent resonance phenomenon makes the measurement possessing very high sensitivity, thus it is suitable to detect the defects in small dimensions. The measurement sensitivity is significantly large at some special frequencies and lower at other frequencies and, it is also significantly large at a special standoff distance and lower at other standoff distances. Therefore, for optimizing the experiment, the selection of frequency and standoff distance is required. Also, for detecting delamination, a calibration using a known sample as the reference is required. In addition, since the measured magnitude is not linear with the thickness of delamination, automatic inspection and evaluation are difficult to be realized. Reflection technique can be used to detect defects on the metal surface, or in dielectric materials in the case of a metal substrate being placed behind the defects.

(3) Automatic inspection was realized. The phase of effective reflection coefficient is an extremely effective signal to detect delamination in IC package. Thin delamination that cannot be detected by the SAT technique was detected effectively. By analyzing delamination at the edge of chip pad, extended crack can be predicted. Since phase measurement is less affected by the scatter, relatively lower frequency can be used. Also the measurement sensitivity is not affected much by operation frequency and standoff distance, thereby selection of them in advance is not required. Because measured phase is linear with the thickness of delamination, automatic inspection and evaluation are easy to be realized. In addition, it is known that the level of delamination and crack is affected by the quantity of silica powder filled in packaging resin.

(4) New theoretical model was built up. With the aid of theoretical analysis, parameters related to the measurement such as operation frequency and standoff distance can be optimized and the reference sample can also be simulated. Based

on calculated relationship of phase difference with delamination thickness, the thickness of delamination can be estimated directly by measured phase difference. The experimental results agreed well with the calculation. The theoretical model has also an important significance to direct future research.

(5) New microwave imaging technique was developed. Image can be created by recording the measured phase during the sample was scanned. From obtained images, delamination in IC package can be observed clearly. The shape and the area of delamination can be observed directly and the thickness of delamination also can be evaluated by different colors. Thereby, the observation of the mechanism of delamination becomes possible.

ACKNOWLEDGEMENTS

The author would like to express his heartful gratitude to his supervisor, Professor M. Saka, for his invaluable and constructive guidance, warmhearted encouragement and well-meaning criticism.

The author would like to express his sincere thanks to Professor T. Shoji and Professor T. Takagi for their insightful suggestions and fruitful discussions.

The author would like to thank President H. Abé of Tohoku University, for his kind guidance.

Also the author would like to thank Associate Professor H. Soyama for his useful discussions.

The author would like to thank Mr. K. Oota of Sumitomo Bakelite Co., Ltd. for preparing the samples and Mr. M. Takeuchi of Sumitomo Bakelite Techno-research Co., Ltd. for his help to set up the measurement system. Finally the author wishes to acknowledge Mr. M. Mikami of Tohoku University for his help during the experiment.

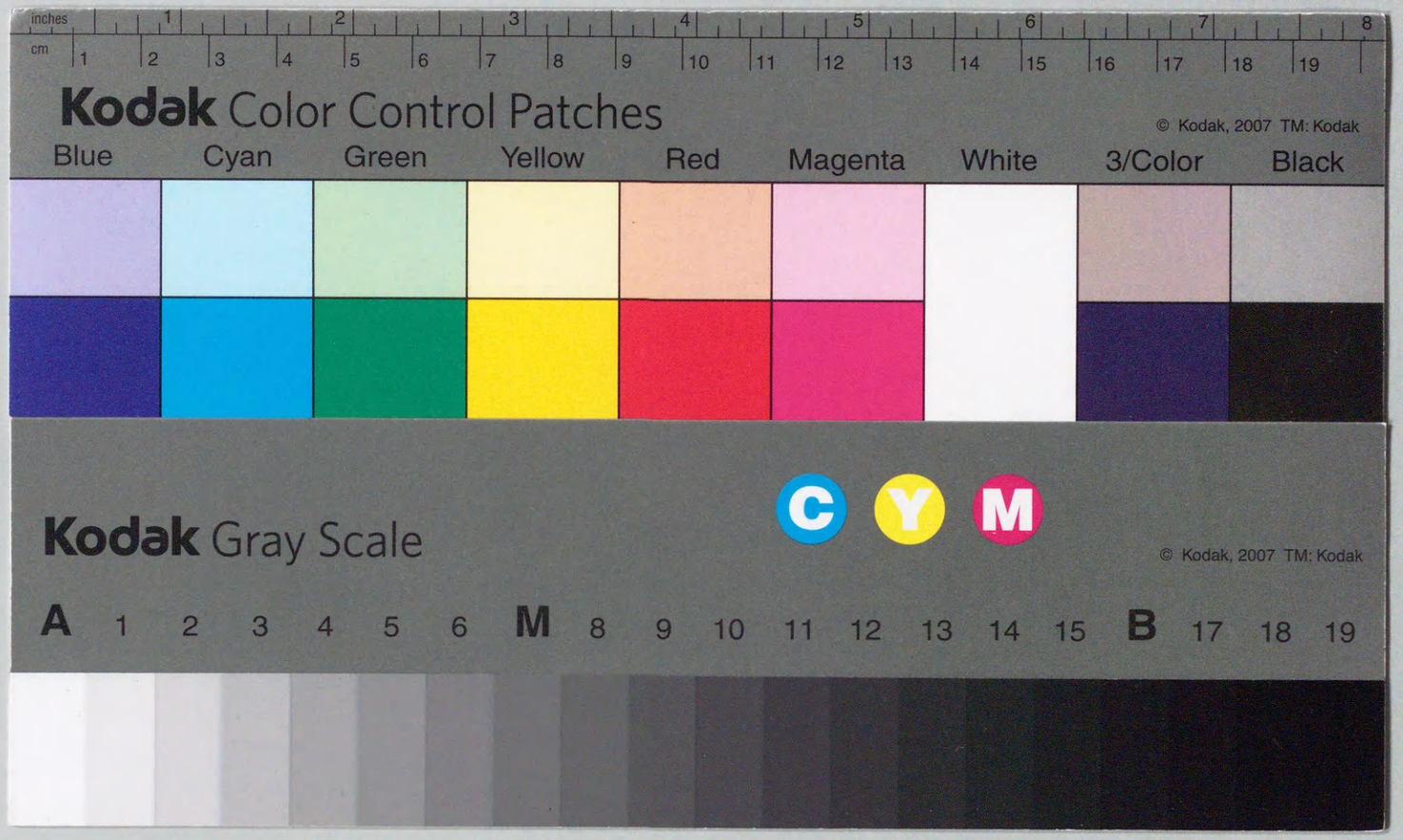
inches
cm
Kodak Color Control Patches
© Kodak, 2007 TM: Kodak
Blue
Cyan
Green
Yellow
Red
Magenta
White
3/Color
Black
Kodak Gray Scale
C
Y
M
© Kodak, 2007 TM: Kodak
A 1 2 3 4 5 6 M 8 9 10 11 12 13 14 15 B 17 18 19